EXPLORING AGE RELATED CHANGES IN CORTICAL BONE IN INDIVIDUALS OVER 50 USING RADIOGRAPHS

by

Jacob M. Cook B.A.

A thesis submitted to the Graduate Council of
Texas State University in partial fulfillment
of the requirements for the degree of
Master of Arts
with a Major in Anthropology
May 2019

Committee Members:

Nicholas Herrmann, Chair

Deborah Cunningham

Daniel Wescott

FAIR USE AND AUTHOR'S PERMISSION STATEMENT

Fair Use

Duplication Permission

ACKNOWLEDGEMENTS

I would like to acknowledge my committee for their help and guidance throughout this research: Dr. Nicholas Herrmann for his help with data processing and statistics, particularly the Procrustes analysis, Dr. Deborah Cunningham for radiography the femora, and Dr. Daniel Wescott for his input. I would also like to thank my cohort for their support as well as my dog Ned.

Finally, I would like to thank all those individuals who graciously donated their bodies to the Forensic Anthropology Center at Texas State. Without them this research would not be possible.

TABLE OF CONTENTS

Page

LIST OF TABLES

Table **Page**

LIST OF FIGURES

Figure **Page**

LIST OF ABBREVIATIONS

Abbreviation	Description
MV:BV	Medullary cavity volume to total bone volume ratio.
GPA	Generalized Procrustes Analysis
BMI	Body Mass Index
LOESS	Local estimated scatterplot smoothing
GSS	GPA sum of squares

ABSTRACT

Cortical bone loss is a general phenomenon in humans and has been found to be correlated with age. Changes in bone morphology are also known to occur throughout the adult aging process. In this study, I analyzed the relationship between the bone volume ratio (MV:BV) using linear measures of medullary cavity breadth and cortical bone thickness as a proxy at three areas of the shaft and changes in shaft shape with age in the left femora of 164 non-pathological individuals from the Donated Skeletal Collection at Texas State University. I found that the MV:BV is correlated with age (r=0.38) and that this relationship is stronger in females (r=0.49). I also found that there is site specific bone remodeling with consistent rates of cortical bone loss in the anterior and lateral sides and greater amounts of endosteal bone loss in the posterior and medial sides of the femoral diaphysis based on a Generalized Procrustes Analysis. Overall, the majority of variation in the MV:BV can be attributed to other factors. However, age does have a significant impact on the ratio and shaft shape in the femur. The findings of this study have the potential to be applied in both forensic and bioarchaeological settings for individual identification and paleo-demography respectively. Raw data of the measures taken and residuals from linear regression can be provided upon request.

I. INTRODUCTION

The ability to accurately estimate an individual's age is extremely important in both forensic and archaeological settings. As individuals age past skeletal maturity the accuracy of these estimations is significantly reduced. It is known that age estimation in older individuals is problematic and previously used techniques may be insufficient for accurate and reliable estimations (Cappella 2017). For this study, the term older has been quantified to include any individuals that are 50 or more years old at the time of death. I used measurements from digital radiographs of the femora of individuals 50 years and older to investigate changes in cortical bone throughout the aging process.

The goals of this study are: (1) to examine the extent of the relationship between the MB:BV (using proxy measures of medullary cavity area and cortical bone thickness at specific anatomical locations along the femoral diaphysis) with age and with sex in older individuals, (2) determine if this relationship is reliable enough to accurately estimate age using the MV:BV, and (3) explore any patterns of appositional growth throughout the aging process. I hypothesize that the MV:BV will be positively correlated with age, that this correlation will be sufficiently strong enough to predict age as well as some established methods, and that the correlation between the MV:BV and age will be slightly stronger in females than males (e.g. r=0.35 for females to r=0.30 for males). Regarding patterns of appositional growth, I hypothesize that there will be site specific areas of bone remodeling. I do not venture to guess where along the diaphysis these site-specific areas reside, only that there is site specific remodeling that can be attributed to age to some degree.

The MV:BV is a measure of the amount of total bone area that can be attributed to the medullary cavity space or cortical bone area at specific cross sections of the midshaft of the femur and can subsequently be used to trace the relationship between cortical bone thinning and age. In essence, the higher the ratio the thinner the cortical bone. In this study, I am using the medullary cavity breadth and total bone diameter ratio as a proxy for the MV:BV. Any further mention of the MV:BV will be in reference to these proxy measures. Appositional growth is the outward expansion of the subperiosteal cortical bone as individuals age (Cowin 2004). When used in conjunction with the MV:BV, the anatomical regions and patterns of appositional growth in these regions can accurately show changes in bone morphology as individuals age. The morphological changes in the diaphysis may be more extreme and/or directionally patterned at certain anatomical areas, or may be generalized, changing the entire midshaft in a somewhat uniform manner.

Potential relationships between the MV:BV and age and sex are analyzed using a variety of statistical methods. Tests of regression are used to measure the relationship between the MV:BV and age by sex, and a Generalized Procrustes Analysis (GPA) is used to track and analyze changes in shape. Prior to explaining the materials, methods, results, and conclusions of this study, it is important to understand how bone forms and remodels throughout an individual's life, what bones can tell us regarding forensic and archaeological contexts, and the benefits and drawbacks of other age estimation techniques.

Bones are made up of several different organic compounds, but the most important are calcium and collagen (Cowin 2004). They are formed out of specific ossification centers that determine their shapes and sizes (White, Black, & Folkens 2012).

Most long bones are completely formed and have finished fusing by the time an individual reaches 25 years old (White, Black, & Folkens 2012). Various factors impact the formation and growth of bone throughout an individual's life such as nutrition, physical activity, and certain pathologies (Cowin 2004). Once the bone is fully formed, processes of remodeling via osteoclasts and osteoblasts are the main determinants for bone characteristics (Cowin 2004; White, Black, & Folkens 2012). Bone remodeling processes are part of a bone structural adaptation. This structural adaptation assumes that a healthy individual's bones will adapt to chronic patterns of biomechanical loading and stresses; however, it has been found that these adaptations may not be uniform and may occur in site-specific areas of bones (Lovejoy et al. 2003).

As individuals age past ca. 34 years (Stein et al 1998), osteoclastic activity begins to exceed osteoblastic activity and long bones become thinner and less dense (Cowin 1983). This process can be seen on the endosteal surface of long bones through expansion of the medullary cavity with a subsequent thinning of cortical bone. This is caused by bone being resorbed (lost) at a higher rate on the endosteal surface than the rate it is deposited on the periosteal surface. Osteoporosis, or reductions in bone density, should not be confused with endosteal bone loss and periosteal bone deposition that is characteristic of appositional growth. Osteoporosis relates to an overall reduction of bone density through an increase in porosity and can visually be observed in the trabecular bone of the epiphyses (Cowin 2004). Some researchers have hypothesized that continuous appositional growth throughout the life span is a compensatory reaction to the weakening of bone from osteoporosis (Ruff & Hayes 1982, Cowin 1984). According to this hypothesis, periosteal bone deposition can compensate for bone weakening even

when rates of endosteal bone loss exceed those of said deposition. A small increase in subperiosteal area is enough to compensate for larger amount endosteal bone loss because the expansion of the diameter of the diaphysis increases the second moment of inertia (a measure of structural rigidity) (Ruff & Hayes 1982, Cowin 1984). This change has important implications in this study because it is well known that females are subject to more severe osteoporosis, especially post-menopause, than males. Therefore, as this study is looking exclusively at individuals over 50 years, the hypothesized compensatory response of appositional growth should be different for the sexes.

For the purposes of this study, I am working under the assumptions that: (1) the general processes of bone remodeling are consistent from individual to individual, (2) that site-specific bony responses can be identified, and (3) that when quantified and visualized these bony responses will be correlated with age. Any interruptions or irregularities in such processes must be accounted for and are addressed later in this thesis. For now, it is appropriate only to note that there are significant differences in bone size and density between the sexes, with men having overall larger and denser bones than women (White, Black, & Folkens 2012), and that biomechanical loading is the most influential external variable impacting the MV:BV and appositional growth (Cowin 2004).

Frost, Ferretti, & Jee (1998) proposed that bone strength and mass is positively correlated with muscle strength and that the forces applied on the bone by muscles are the most influential factor in bone mass and nonmechanical factors of bone. The inverse of this hypothesis is that reductions in activity level and patterns of loading will result in bone atrophy. This hypothesis has been supported by the findings of Tollison & Kriegel

(1990) and Weiping, Bauman, & Cardozo (2010) that a reduction or cessation of physical activity and loading results in bone loss in the inactive body regions.

Other demographic data such as socio-economic status and occupation were ignored in this study. However, there is potential for further investigation using this demographic data and multivariate analysis, particularly with the relationships between MV:BV and occupation and MV:BV and BMI, which likely covary.

Age estimation is a vital component in both forensic and archaeological analyses. Age is an important element of the biological profile and is usually one of the first biological attributes researchers attempt to estimate. An accurate biological profile is the most convincing argument for positive identifications of unknown individuals apart from DNA matches. The biological profile operates at an individual level, attempting to identify one individual among many. It is particularly useful in criminal investigations and mass disaster contexts because it can narrow down the number of potential missing persons. Accurate and precise age estimation is extremely helpful in further narrowing down the number of potential missing persons.

In archaeological settings, vital information can be obtained by accurately estimating aspects of the biological profile, specifically the age-at-death, for past populations. Reliable information on how long people were living, who was dying and at what ages, what types of skeletal traumas were occurring, and to some degree how they were dying enables researchers to reconstruct the demographics of past populations. For example, researchers can see whether women were living longer than men or, more rarely, the opposite, and what diseases or injuries they were subject to. Unfortunately,

with the age estimation methods available it is difficult to estimate age in individuals over ca. 50 years old at death.

The other aspects of the biological profile—sex, stature, and ancestry—are estimated using a variety of techniques that also use the femur as well as other skeletal elements. While sex is most often estimated using characteristics of the pelvis, or craniometrics when os coxae are not present, measurements of the femur, particularly maximum femoral head diameter, are often used as supporting data to reinforce estimations (Moore & DiGangi 2012).

Adult age estimation techniques are primarily based on joint wear and the analysis of these patterns of wear on different skeletal elements. The most well-known and widely applicable methods use the pubic symphysis and auricular surface (Suchey Brooks & Lovejoy). These method uses scores based on the appearance and topography of the pelvic surfaces to place individuals into age categories culminating in age categories of 50+ years. The age range covered by each category in the two methods necessarily becomes larger as the estimated age of the individual increases. This is because the characteristics of the pubic symphysis and auricular surface become increasingly obscured as individuals age. These methods are useful because the required skeletal elements are distinct and observable, and there are plaster casts and images available to aid in accurate assessment. However, these methods must be practiced with regularity to ensure accuracy, and the surfaces analyzed are subject to taphonomic forces that damage and obscure the characteristics observed.

Iscan, Loth, & Wright (1984;1985) use scores from the morphology of the sternal ends of the ribs, usually the fourth rib, to place individuals into age categories similar to

those in the Suchey-Brooks method (Iscan, Loth, & Wright 1984; Iscan, Loth, & Wright 1985). Some evidence for population specific scoring has emerged further reducing the accuracy of this method when applied to individuals with unknown ancestry (Geske 2013; Cerezo-Román, Espinoza 2014). This rib end scoring method is subject to some of the same limitations as the methods using pelvic indicators.

Another age estimation technique is histology, which is a more objective method than those previously discussed and can be quantified rather than relying on scores from morphological characteristics. Histology is the analysis of bone at a microscopic level that focuses on identifying the frequency and distribution of primary and secondary osteons and haversian canals (Moore & DiGangi 2012; White, Black, & Folkens 2012). It requires cutting a section of the bone, usually from either femora or ribs, and preparing it for analysis under a microscope (Moore & DiGangi 2012). Histology uses the number of osteons to estimate age and some studies have been able to accurately estimate age in older individuals (Crowder & Pfieffer 2010; Khan, Jamil, & Nor 2017).

For all three of these methods, pathologies, trauma, and taphonomic factors can obscure or obliterate the characteristics used in analysis. However, a pathological analysis can be tentatively used as a relative dating technique as some diseases and illnesses, such as osteoporosis or osteoarthritis, usually only present in older individuals. There are other less accurate and less reliable age estimation techniques that are not necessary to address here. There are, however, several studies on age estimation that have also used the femur or have used a similar method on other skeletal elements and will be examined in detail below.

It is beneficial to examine previous studies on age estimation that have used the femur or similar methods as those in this study in detail to frame my research questions and hypotheses, particularly that the MV:BV will be positively correlated with age and that this correlation will be stronger in females than males. As a brief reminder prior to the analysis of related studies, the goals of this study are to provide a method to better estimate the age of individuals over 50 years old using the MV:BV and to explore patterns of appositional growth along the midshaft of the femur using digital radiographs.

II. LITERATURE REVIEW

There are a variety of age estimation techniques that involve various elements of the skeleton. Because the femur is the largest bone in the body and preserves well in comparison to other skeletal elements in archaeological contexts there have been numerous studies involving a variety of femoral traits and measures. First, I will give an overview of the studies that are most relevant to my study. Then I will present the most influential factors other than age on femoral traits and measures.

Previous Studies

There are several studies that are necessary to mention and briefly assess prior to detailing this study in earnest. This literature review is by no means exhaustive; the articles below are what I consider the most relevant to this study regarding either methods or results. My analysis of the following articles will show the benefits and limitations of the relevant studies. The conclusions drawn by previous researchers are largely in congruence with one another.

Prior to discussing articles that used the femur, it is beneficial to briefly mention some studies that have also examined the relationship between age and cortical bone dimensions in non-weight-bearing bones. The second metacarpal, clavicle, and humerus are the main bones examined in these types of studies. The clavicle and humerus are often paired with the femur in order to assess potential differences between upper and lower limb bones and will be discussed later.

The earliest articles examining the second metacarpal are by Garn et al. (1968a & 1968b). These authors used radiographs to examine a large archaeological population (2799 individuals for both studies) and a contemporary population (113 individuals in the

second study) to analyze changes in bone size as individuals age. Age was estimated using previously established methods discussed earlier. The authors found that external width at midshaft of the second metacarpal increased with age. They suggest that this relationship may be higher in tall individuals because they are naturally larger. The authors also note that endosteal bone loss is precipitous after the age of 40 and that females have a higher net rate of bone remodeling. Other studies that used measures of the second metacarpal from both modern and archaeological samples produced similar results. In a longitudinal study using 754 individuals Garn et al. (1991) observed that the cortical bone area at a younger age strongly predicts the cortical bone area at an older age, Mays, SA (1996, 2006) found the increase in midshaft breadth and reduction of cortical bone is only statistically significant in females and there is a marked reduction in the cortical index (cortical area : total bone area) from 50 years on, Mays, SM (2015) found there is no secular change in the correlation of cortical bone reduction and age, and Umbelino et al. (2016) observed that cortical bone loss and appositional growth increase with age and that there are age and sex specific trajectories for this relationship that are related to bone fragility.

A study by Kaur & Jit (1990) focused exclusively on the comparison of cortical bone area to total bone area using measures from cross sectional cuts of the clavicle in a known age-at-death sample. The authors found that cortical area decreased after 40 years, that this decrease was greater in females, and that there were statistically significant differences between the sexes for all measures. Using these results, they separated their sample of 210 individuals into 10-year age cohorts culminating in a 60+ group.

Unfortunately, the researchers were unable to expand these age categories into the later decades.

The results from these studies on non-weight-bearing bones are in congruence with the findings from the following studies that focus almost exclusively on weight-bearing bones. However, in studies using non-weight-bearing bones it is necessary to address issues of use dominance asymmetry associated with handedness.

There are a variety of methods used to analyze endosteal bone loss and appositional growth in the femur. Radiographs and direct measurements from cross-sections cut from the diaphysis are the two most common. As there is sexual dimorphism in gross measures of the femur, that also varies by population, several of the following studies have separated their study samples by sex or only used one sex in their analyses. What follows is a loosely chronological review of studies focusing on endosteal bone loss and appositional growth in weight-bearing bones. I focus first on studies using radiographs then on those using measurements from cross sections cut from the diaphysis.

The first of several studies using radiographic imaging was conducted by Smith & Walker (1964). They examined radiographs of the femora of 2030 ambulatory women aged 45 to 90 years. The authors used a plastic ruler to measure subperiosteal width at the midshaft from antero-posterior (A-P) plane radiographs. They found that an increase in subperiosteal diameter is correlated with age, and that the rate of expansion increases with age. The authors hypothesized that this expansion may be a bony response to flexural stress produced by the anterior bowing of the femur. These findings should be looked at with caution because the authors used mean measurement values for their

statistical analysis which hides some of the individual variation and may skew the results. However, the results of Russo et al.'s (2005) study mirror what is seen in Smith & Walker's (1964) study. Using radiographs of the tibiae from living females, Russo et al. (2005) found that as age increased medullary area and total bone area increased and cortical area decreased. They also found that the increase in medullary area and decrease in cortical area are greater in females than males resulting in the conclusion that sexual dimorphism contributes to differences in bone fragility between the sexes.

Garn, Rohmann, & Wagner (1967) used radiographs to examine the correlation between the cortical thickness of the femoral diaphysis and age in several large and geographically diverse groups. The authors found that these variables are correlated with age but skewed by sex differences in bony responses to other factors. They also stated tere was less cortical bone loss in taller individuals than shorter individuals. This may be a result of either the sexually dimorphic nature of bone loss as males are often taller than females, or different responses to loading stresses between tall and short individuals, or some combination of both. Using longitudinal data, the authors also found that there is no significant relationship between calcium intake and cortical bone loss. This is particularly important because it implies that calcium intake is not one of the significant contributing factors to patterns of bone remodeling in older individuals.

Walker & Lovejoy (1985) included the clavicle and humerus along with the femur to estimate age-at-death from radiographs. They used 130 individuals of known age from the Hamann-Todd collection to explore the potential relationship between various changes in bone and age. They used a method of seriation to split the individuals into 8 age phases terminating in a 60 years plus group. Their results indicate that of the three

bones used in the study there is the highest amount of bone activity in the femur, that there is bone loss as individuals age, that this bone loss is site specific, that the effects of sexual dimorphism are mediated by significant bone loss in individuals of both sexes past the age of 40, and that the clavicle had the most consistent relationship with age when compared to anatomical age indicators. Of these conclusions, the most relevant for this study are that there are high rates of bone activity in the femoral diaphysis and that age associated bone loss is site specific to regions of the skeleton. If bone loss is site specific on a skeletal scale, it may be site specific on a single element scale.

A recent study by Curate & Cunha (2017) that examined patterns of cortical bone fragility in the femur using the Coimbra Identified Skeletal Collection illustrates the potential need for population specific studies examining changes in the MV:BV and appositional growth. Curate & Cunha's (2017) skeletal sample consisted of 98 individuals aged 21-89 years. The authors found that the patterns of fragility of the femur are different between the sexes, but this difference is not statistically significant. This finding is the opposite of what Russo et al. (2005) found for the tibia and may be due to differences in gross bone morphology, different reference samples, or a combination of these factors. Curate & Cunha (2017) found that for females there is a 13.6% loss of cortical bone, a 12.4% increase in appositional growth, and a 26% increase in midshaft width from the youngest age cohort to the oldest. For males there was a 5.4% loss, 7.2% increase, and a 12.6% increase respectively. The authors also note that these patterns are not strictly linear and rates of endosteal bone loss and appositional growth may vary throughout an individual's life. The results of Curate & Cunha's 2017 study are particularly important for this study. My research questions and hypotheses are guided

not only by the processes of bone remodeling throughout the life cycle, but also by the differences between the sexes seen in the Coimbra Identified Skeletal Collection.

An alternative method of obtaining measures of bone areas involves making transverse cuts of the femur either at midshaft or at specific lengths of the diaphysis. There are many studies using this method likely because it is replicable and eliminates some of the limitations of using 2-dimensional radiographs. These limitations will be addressed later. Many studies that use cross sections of the diaphysis from cut bone measure cortical, medullary, and total bone areas as well as moments of inertia. These measures are used to calculate the MV:BV and can be used to better understand changes in bone morphology and strength as individuals age. Van Gerven & Armelagos (1970) and Carlson, Armelagos, & Van Gerven (1976) conducted studies using caliper measurements of femoral cortical thickness on transverse cuts of the diaphysis at midshaft in a sample of individuals aged 20-55+. Similar to the findings of previous studies, these researchers concluded cortical bone loss is greater in females and that sex differences are present in measures of cortical thickness at the midshaft of the femur and that there is an increase in bone loss once individuals reach ca. 30 years. This bone loss is greater in females and, as the authors hypothesized, the resulting weakening of the bone may be compensated for by appositional growth.

One of the drawbacks of the 1970 and 1976 studies is that age groups were split into course age categories of variable length. These large groupings were necessary because the ages of many individuals had to be estimated using the macro-morphoscopic scoring methods mentioned earlier in the text. Unfortunately, the groupings do not allow for more precise examination of measures of cortical thickness at different ages. Pfeiffer

(1980) explicitly acknowledged the drawbacks of not knowing the precise age of individuals in her analysis of midshaft measures of humeri from an ossuary sample. She grouped the individuals into two categories (young & old) based on the presence of epiphyseal lines. Although her study used features of the humerus to age individuals, it is beneficial to acknowledge and understand that singular aging methods may be the only ones applicable in forensic and bioarchaeological contexts. Her results support the conclusions of other researchers that appositional growth is continuous throughout adulthood. The results also supported previous findings that there is significant dominance asymmetry in upper limb bones and that these bones are more sensitive to chronic patterns of physical activity.

Ruff & Hayes (1982) used five different cross sections cut from the femoral diaphysis and tibia in a prehistoric sample from the Pecos Pueblo archaeological collection. Unlike the previous studies, the researchers split their sample of 119 individuals into more precise age categories using 5-year age cohorts for individuals in their 20's and 30's, 10-year age cohorts from 40 to 60 years, and finally a 60 years plus cohort. Their findings indicate there is an increase in medullary area with a subsequent decrease in cortical area, there is an increase in subperiosteal area, and that these changes are larger in females than males. The authors concluded that these changes are responses to endosteal bone loss and biomechanical stress, which is consistent with the hypothesis that appositional growth, specifically the increase in subperiosteal area, compensates for the bone weakening caused by endosteal bone resorption and osteoporosis.

A later study by Stein et al. (1998) used cross sections cut from the midshaft of the femur in a sample with known ages and included adjustments for stature and body

mass. Their sample is significant because it not only has the known age-at-death for the individuals (21-92 years) but also is nearly evenly distributed by sex (51 females, 56 males). The researchers found that: females had higher levels of bone stress (compression, torsion, etc.) and lower cortical bone area at all ages, that bone size increases with stature and body mass, and that peak bone mass occurs around age 34 in their sample. While previous studies showed that there was a decrease in cortical bone area, this study quantified the loss – 10.5% loss from peak bone mass from ages 34 to 84. Unfortunately, the authors did not remark on the rate of bone loss as individuals age other than stating that post-menopausal females have accelerated rates. A study by Feik et al. (2000) had similar results. These researchers included analyses of the directionality of appositional growth and sex differences by age. They found that there is less appositional growth on the posterior margin with more bone resorption on the anterior endosteal surface, that the greatest sex differences are found in the middle years (40 to 60), and that the largest changes in medullary cavity and cortical bone areas occur in the transition from middle to old age (61+ years). They concluded that bone loss and appositional growth are continuous, but not uniform, throughout the aging process and have periods of greater or lesser remodeling activity depending on other factors. The Feik et al. (2000) study is the only study I found that included an analysis of site-specific bone loss and appositional growth. It is important because it uses a modern population and the results from Feik et al. (2000) can be compared to the results of this study. However, the coarse age ranges mask some of the variation that may be present.

Other studies on bone asymmetry, dimensions, and density lend some insight to what factors may be impacting the intensity and patterning of endosteal bone loss and

appositional growth. A few of these factors have been briefly discussed already, namely sex, body mass, and stature. These studies use dimensions, bone geometry, and measures taken from radiographs to analyze the impacts these factors have on bone morphology and the MV:BV.

Several studies, including Russo (1998), have examined femoral neck and shaft geometry to analyze any changes in these characteristics as individuals age and differences between the sexes. Zanetti et al. (2005) used radiographs of the femur to analyze bone geometry and its effects on stress distribution in bone. The authors employed an elastic solid theory and generated computer models to simulate different patterns of loading and stress on the femur and estimate changes in bone geometry in response to these stressors. They found that there are primary sites of stress distribution on the femur, namely the medial neck and posterior and anterior surfaces of the midshaft. The femoral neck and posterior surface of the shaft are under more compressive stress while the anterior surface of the shaft is under more tension stress. While this is based on a simulated model, it is still useful in further understanding patterns of appositional growth in these areas in response to different types of stress.

Karacaş, & Harma (2008) extended the scope of the studies on femoral geometry to include how the midshaft bows anteriorly. The authors found that femur length decreases with age in females but not males, indicating that there is more bowing in the femoral midshaft in females, which in turn alters patterns of loading and bony responses to changing patterns of stress. They attributed this difference in anterior bowing to a reduced efficiency of the compensatory mechanism (appositional growth) in females. These results provide evidence that there are sex differences in femoral shape that must

be considered when looking at patterns of bone remodeling throughout the aging process. However, these results must be looked with caution because there are a multitude of factors influencing bone morphology and changes in bone shape throughout the life cycle.

Taghizadeh et al. (2017) analyzed the relationships between bone shape, the TV:MV (total bone volume: medullary cavity volume, using trabecular bone), and bone mineral density. Using a principle components analysis, the authors found that the bone volume fraction is correlated with bone strength and that there is no correlation between the bone volume fraction and whole bone shape, which indicates that there is no relationship between trabecular bone structure and whole bone shape. However, there may be a relationship between the MV:BV (medullary volume: total bone) I am using and bone shape because it incorporates cortical bone into the equation.

There have been a multitude of studies examining bone density and a variety of other traits and factors. For the purposes of this paper I am only interested in density studies that are directly related to age differences in bone density of the femur. These changes in density are important because if appositional growth truly is a compensatory reaction to bone weakening, then it would be expected that appositional growth would increase with a reduction in density and that the MV:BV would also be positively correlated with bone density.

Atkinson & Weatherfell (1967) conducted one of the first studies on bone density using cross sections cut from the femoral diaphysis. They took several measures of bone density to analyze its relationship with age. The authors found that bone density decreased markedly after 50 years and that it was significantly lower on the posterior

aspect than other aspects of the diaphysis. This demonstrates that there is variable susceptibility to changes in bone density in different areas of the femur that may affect patterns of appositional growth.

Ruff & Hayes (1984) incorporated measures of bone geometry, mineral content, and cross-sectional geometry taken from sections of the diaphysis cut from the femur to analyze changes in comprehensive bone structure as individuals age. They found that the most significant changes in the bone involve geometry and are mainly volumetric, meaning that changes are predominantly occurring in the endosteal and subperiosteal regions. They also found that bone loss starts in earnest in the late 30's. According to the authors, differences between males and females and populations are due to sexually dimorphic differences in pelvis morphology and differences in biomechanical stresses produced by different cultural practices. This study is of particular importance because the volumetric changes are directly observable via changes in the MV:BV. Ruff & Hayes (1984) also incorporate potential origins of the sexual dimorphism seen in femoral measures.

Starting in the late 1990s, studies of bone density began to look past macroscopic changes in bone structure and mineralization to focus on smaller scale measures. Feik, Thomas, & Clement (1997) looked at age-related changes in the cortical porosity of the femoral midshaft. The authors used cross sections cut from the femoral diaphysis in a modern Australian known age-at-death sample to examine the cortical bone porosity at the endosteal and subperiosteal surfaces and well as the intra-cortical area. They found that cortical porosity increases with age, most notably at older ages, that the endosteal surface has the highest rates of porosity and becomes more trabecular like with age, and

that intra-cortical bone loss and porosity are due largely to medullary cavity expansion. These findings are consistent with what other researchers have found using the MV:BV.

Cooper et al. (2007) measured the three-dimensional structure of cortical porosity from cross sectional cuts from the midshaft of the femur in a known age-at-death sample. The authors examined the relationship of cortical porosity from a standardized region of interest with age, sex, and body size. They found that age was the only covariate that was statistically significant for all measures. Sex and body size were much less impactful, with sex having some covariation and body size having little to none. Females had greater overall cortical porosity particularly in individuals over 50 years. Although these findings are related to bone density, it is important to note that age was the most influential factor.

Finally, Curate et al. (2013) analyzed bone densitometry and its relationship to age in a documented skeletal collection. Using various measures of bone mineral density and overall bone density in the Ward's area on the neck of the femur, the authors were able to estimate age with an error of about 10 years. The Ward's area is a triangular area of low bone density in the neck of the femur that is the intersection of three sections of trabecular bone where different forces acting on the bone are equalized (Cardadeiro et al. 2010). Their method tended to overestimate age in young individuals and underestimate age in older individuals, which is typical of most age estimation methods.

It is important to understand previous studies to properly frame my research questions and hypotheses. As a reminder, I am investigating the relationship between the MB:BV and age as well as patterns of appositional growth throughout the aging process. I hypothesize that the MB:BV will be positively correlated with age, that this correlation

will be slightly higher in females, and that there are site-specific patterns of bone remodeling, specifically appositional growth, throughout the aging process. Previous studies also provide examples of what types of factors other than age may influence bone morphology.

Confounding Variables

There are numerous factors that can influence bone dimensions and characteristics. Sex is the most obvious and one of the most important factors and its impact on femoral shape, cortical bone area, and bone loss has been noted in the studies above. The two most influential remaining factors are biomechanics and nutrition. There are other factors that influence bone density, such as alcohol intake and smoking habits, however these have little to no effect on bone shape or the MV:BV (Hollenbach et al. 1993; Jin Kim et al. 2003; Hae-Dong et al. 2017).

Mays (2015) reviewed numerous studies to examine the effects of factors other than age on skeletal age indicators in adults. By comparing statistics from a variety of previous studies, he found that nearly 60% of variation in gross skeletal age markers can be attributed to factors other than age such as genetic, hormonal, nutritional, and biomechanical factors, and warns that there are widespread assumptions about the applicability of methods to multiple populations without proper comparative studies. In the present study, I am looking exclusively at age, but it is important to note that there are other variables that may have substantial effects on the MV:BV and appositional growth.

Biomechanics have a direct and often severe impact on bone, reshaping it rapidly in response to different types of stress or lack thereof. Cowin (1983) provides an in-depth analysis of bony responses to different types of mechanical stress and loading. As a

general rule, bone becomes thicker and denser as repeated chronic stress is applied – hypertrophy. In other words, increased levels of strenuous activity result in denser and thicker bones in the areas of the body associated with those activities. On the other hand, reduction or absence of stress results in thinner and less dense bones – atrophy. He concludes that there are two scales of remodeling processes (long and short term) that vary according to the pattern of stress. The long-term scales of remodeling are associated with changes in behavior, such as an increase in athletic activity over an extended period while the short-term scales of remodeling involve fracture or disease. The long-term remodeling is the primary concern in this study.

There is an assumed causal relationship between bone deposition and bone density with athletic exercise and/or manual labor. That as stress increases via exercise or labor there is increased bone deposition in areas under heaviest load and an increase in bone mineral density throughout the bone. In other words, bone becomes denser overall and physically thicker at areas under the highest levels of stress. Cowin (1983) supported his conclusions using acoustic velocity measures from ultrasounds of the tibiae of various levels of athletics ranging from professional athletes to 'non-athletic individuals'. The professional athletes had denser bones than non-athletic individuals, which reinforces the findings that there is a relationship between bone density and activity level.

Ruff and Hayes (1983) contributed to analyses on lower limb dimensions by examining responses to biomechanical stress using the same data as the Ruff & Hayes (1982) study. They found that the medial and lateral aspects are under compression and tension forces, respectively. That anterior-posterior bending/bowing increases distally and that this increase peaks in the distal third of the femoral diaphysis where shearing

stresses are maximized. This can be used in conjunction with the findings of Feik et al. (2000) that there is less appositional growth on the posterior surface, higher rates of endosteal bone resorption on the anterior surface of the femur, and that the femur becomes more circular as individuals age. The increase in anterior bending/bowing would put the anterior surface under higher rates of tensional stress and the posterior surface under higher rates of compressive stress. Therefore, similar patterns of bone remodeling may be found on the anterior and lateral surfaces and the posterior and medial surfaces. However, there are other stresses (shearing and torsion) that are acting on these surfaces as well.

Ruff (1984) expanded on the findings of Ruff & Hayes (1983) by using more contemporary samples and incorporating second moments of inertia into analyses of bone strength. He found that medullary area is not correlated with bone length, cortical area is weakly to moderately correlated with bone length, and that the second moment of inertia has a higher correlation with length than cortical area. This indicates that there is a relationship between bone length and bone strength, which is in accordance with previous findings that diaphyseal breadth is greater in taller individuals (Feik et al. 2000; Garn, Rohmann, & Wagner 1967). It also shows that the MV:BV has a weak correlation with bone length, and by extension stature.

Nutrition is the other predominant factor in bone shape and density. It is well known that nutritional deficiencies, such as scurvy and rickets, can cause dramatic changes in bone geometry, morphology, and mineral content. Garn et al. (1964) examined protein-calorie-malnutrition using radiographs from clinical samples of Guatemalan children. They found that there is no delayed ossification in malnourished

children and that the smaller bone dimensions may be due to actual bone loss rather than stunted growth. Garn, Solomon, & Friedl (1981) used radiographs to trace any relationship between calcium intake and cortical bone area in elderly individuals. These authors found that there is little to no relationship between calcium intake and cortical bone area. The combination of these two studies indicates that bone development and patterns of remodeling are associated with more nutritional factors than overall calorie intake or specific mineral intake. In children, effects on bone via malnutrition may be accounted for later in life through periods of improved nutrition and catch-up growth. In adults, specifically the elderly, reduced calorie or mineral intake has a much less dramatic effect on bone shape and size but has a significant impact on bone density and strength. However, appositional growth as compensation for bone weakening can only account for weakness brought on by normal bone remodeling. Malnourishment further weakens the bone and may result in fractures.

The results of previous studies generally agree. The researchers in all these studies have found that the MV:BV is positively correlated with age. The results are fairly similar in terms of levels of correlation with most studies showing a weak to moderate positive correlation. There is a consensus among these studies that bone remodeling is site specific, but not on where the highest rates of bone remodeling are occurring. The results also indicate that age and biomechanical forces are the two most influential factors on the MV:BV and patterns of appositional growth.

It is important to remember that some of these studies were conducted using archaeological material from a wide range of time periods (prehistoric to medieval). We need to realize that there may be some secular change in femur morphology, that the

average age-at-death is higher in a modern population, and that activity patterns of modern individuals can be drastically different from individuals from these archaeological populations. It must also be noted that age cohorts for these samples were quite large and age-at-death was estimated using macro-morphoscopic methods.

In the studies using known age-at-death samples they were still unable to reliably and accurately predict age-at-death in older individuals using the measures gathered either from cross sections cut from the diaphysis or those gathered from radiographs. The materials and methods presented below will hopefully provide an accurate and replicable method for estimating age-at-death in individuals over 50 years.

III. MATERIALS & METHODS

Materials

The femora used in this study are a sample from the documented human skeletal collection at Texas State University curated by the Forensic Anthropology Center at Texas State (FACTS). The number of processed and curated individuals in the donated collection as of March 2018 is 322 adult individuals (50+ years). There are 189 males and 133 females. Of these individuals, one individual is self-identified (or was identified by family members) as Asian/Unknown, 12 as Black, 12 as Hispanic, and 297 as White. Intake paperwork that details the individual's age, stature, body mass, socio-economic status, and pathologies accompanies each donation. Cadaveric stature and body mass are available for most individuals in the FACTS donated skeletal collection database and intake paperwork. While there are 322 adult individuals to choose from, not all donations could be used in this study due to a variety of factors explained below.

After applying my exclusionary protocols (see below), 164 individuals remained for analysis. There are 106 males and 58 females in the sample of mostly white ancestry. There are only 6 individuals who self-identified as black (4 males and 2 females) and only 7 individuals who self-identified as Hispanic (4 males and 3 females) leaving 151 individuals who self-identified as white (98 males and 53 females).

I selected the left femora of these 164 individuals because, after excluding individuals for various reasons, radiographing both femora would have been redundant. This redundancy is due to the nature of bipedal movement. Even

though there are slight variations in size between right and left femora, bipedalism disperses biomechanical forces equally between the two legs regardless of which leg is larger or could be considered dominant.

Methods

Exclusionary Protocols

The 164 femora were chosen because they all had reported ages a death at 50 years or older, were relatively free of pathologies (there was no immediately observable effect on the morphology of the bone that would impact the MV:BV), did not have a knee or hip replacement, did not have any evidence of healed or healing fractures for either femur, and were complete and available during the radiography period. Pathologies that affect the morphology of the femur obscure what can be considered normal bone remodeling in this study. Osteoporosis is nearly impossible to see with the naked eye and was not included in the exclusionary protocols. However, bone density did have an impact on the measures taken. The endosteal margins of cortical bone were obscured in several of the images, making it difficult to pinpoint exactly where the cortical bone ended (Figure 1). The density of the bone at this area and the foam fixtures used to hold the femora may be contributing to this issue. A solution to this issue is presented later.

Figure 1. Digital radiograph of a femur at 20% length from the distal end. Note how the endosteal border of the cortical bone is difficult to observe.

Knee and hip replacements change the dimensions of the bone, particularly hip replacements, and how individuals move which can result in asymmetrical bone remodeling post-surgery. Hip and femoral fractures also directly change the morphology and remodeling patterns of the bone. Tibial and fibular fractures can also indirectly affect the morphology of the femur through short-term changes in body mass distribution and activity level. For these reasons, individuals with fractures of the lower leg were removed from the available sample pool.

The bones were x-rayed over a two-week period at the end of July 2018 and beginning of August 2018.

Measurements

Prior to taking the x-rays, I measured each femur for maximum femur length, according to the DCP 2.0 (Langley et al. 2016), to attach plastic beads averaging 5.964mm in diameter (based on a random sample of 30 beads) in the

sagittal and lateral planes at 20%, 50%, and 75% of bone length from the distal end (Figure 2). The beads were carefully removed after radiographs were taken.

Figure 2. Left femur with beads marking 20%, 50%, and 75% length from the distal end for A-P & M-L radiography.

I used digital calipers to measure the anterior-posterior and medio-lateral diameters at midshaft for each femur as well as maximum femoral head diameter, also according to the DCP 2.0 (Langley et al. 2016). I took the midshaft measures to ensure that the images used for analysis are scaled correctly and to calculate a standard error between measurements taken by hand and measurements taken from the images.

Radiography

I then placed each femur in one of two 20 cm by 20 cm foam block fixtures that held the bone upright and stable during radiography (Figures 3 & 4). I constructed two fixtures because there is a significant amount of femur size variability in the donated collection. One fixture was used for the small/medium femora and another for the larger femora. A large femur was any femur that had an epicondylar breadth that exceeded the size of the hole for the small/medium fixture (ca. 90 mm). I packed smaller pieces of foam into the hole to keep the bone in a fixed position during radiography. I inserted and glued a plastic peg (ca. 5 mm in diameter) at the center of the bottom of the foam fixture to keep the fixture and femur in proper alignment during radiography.

Figure 3. Femur in foam fixture with smaller pieces of foam to reduce movement of the bone during radiography.

Figure 4. Femur and foam fixture in antero-posterior radiography position in North Star Imaging X5000 system.

Digital radiography was conducted on the North Star Imaging X5000 system located in the Grady Early Forensic Anthropology Laboratory by Dr. Deborah Cunningham. Optimal exposure levels were found by an initial pilot study that produced images of sufficient quality for analysis. The femora were scanned in the antero-posterior position first and the medio-lateral position second. I placed the fixtures in the scanner with the anterior surface directly facing the filament (Figure 4). Dr. Cunningham used a 90-degree rotation program to rotate the femora so that there was a standard location for the medio-lateral scans. A Wallis filter was applied to the images using efX-View software to increase contrast and aid in identifying the extent of the cortical bone on the endosteal surface before the images were exported (Figure 5). A Wallis filter utilizes local adaptive contrast enhancement to increase the contrast between light and dark tones in an image and is more applicable in this study than other filters because it can increase contrast on both ends of the brightness spectrum instead of either increasing only light or dark tones (MicroImages Inc.). The radiographs and filtering produced 8 mb images that were then exported and analyzed on a personal computer using ImageJ (Schneider, Rasband, & Eliceiri 2012; Schindelin et al. 2012).

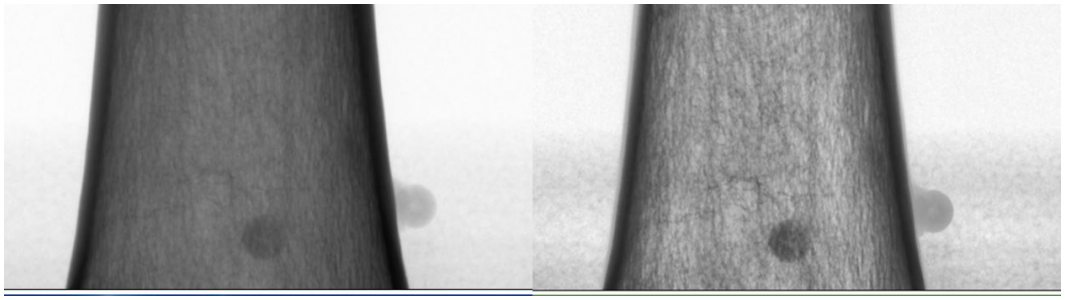

Figure 5. Digital radiograph of a femur at 20% total length from the distal end. Left: no filter, right: Wallis Filter applied.

Image Processing

I used the open source program ImageJ (Schneider, Rasband, & Eliceiri 2012; Schindelin et al. 2012) to do most of the image processing. I set the scale manually in each image using the 5.964 mm beads at midshaft. For femora over 500 mm the fixture had to be moved from its standard position to capture the extent of the midshaft needed for analysis, thus changing the magnification of the images and subsequently the scale. Once the scale had been properly set, I used the line tool to measure the amount of total bone area at the 20%, 50%, and 75% points that was accounted for by the cortical bone and medullary cavity respectively (Figures 6 & 7). The ROI manager application in ImageJ saved the measures of the lines which could then be exported into an excel spreadsheet. These values were used to calculate the MV:BV in excel. The raw data is available upon request.

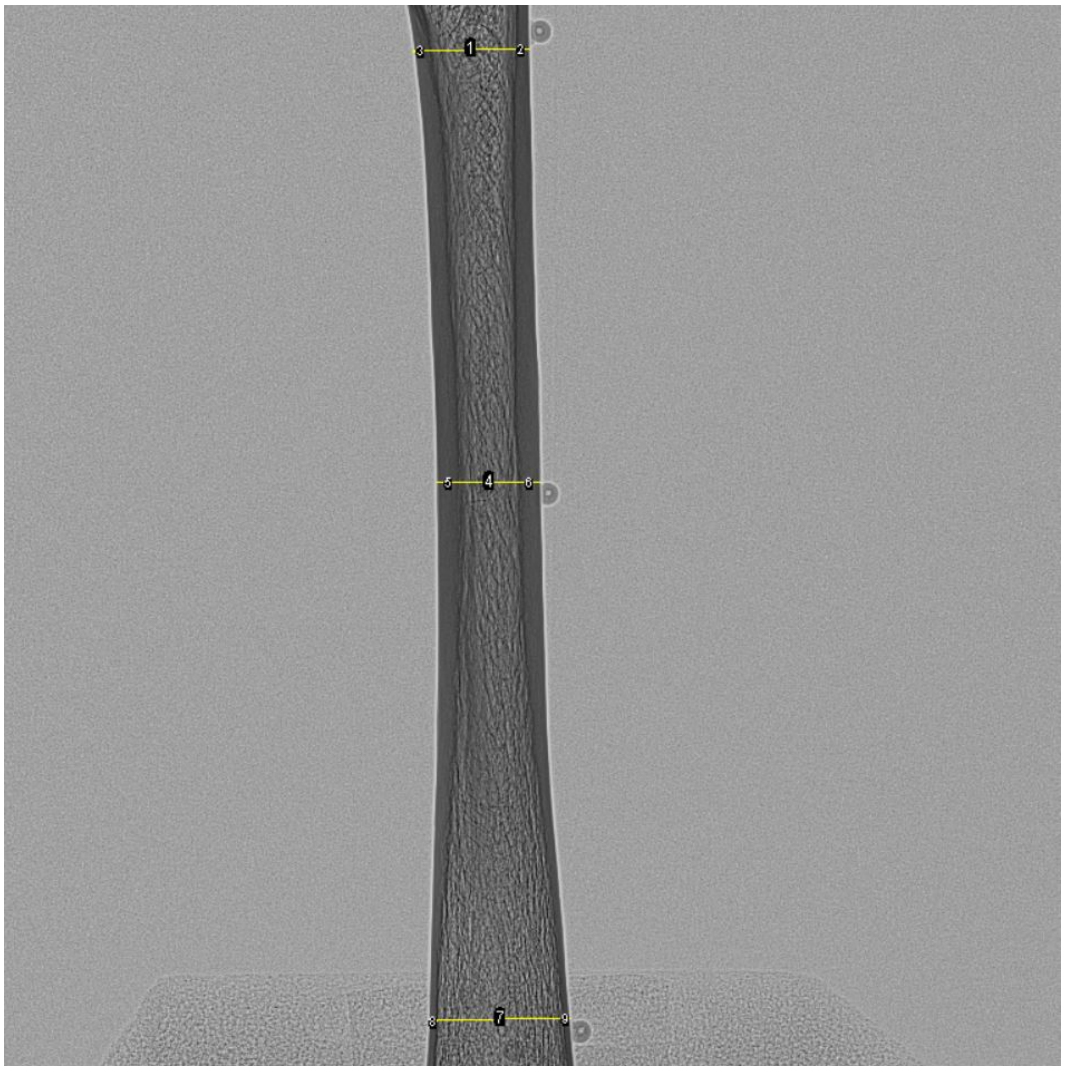

Figure 6. A-P Radiograph of the femur of D02-2010 with digitized lines measuring cortical bone area and total bone area at 20%, 50%, and 75% total length from the distal end.

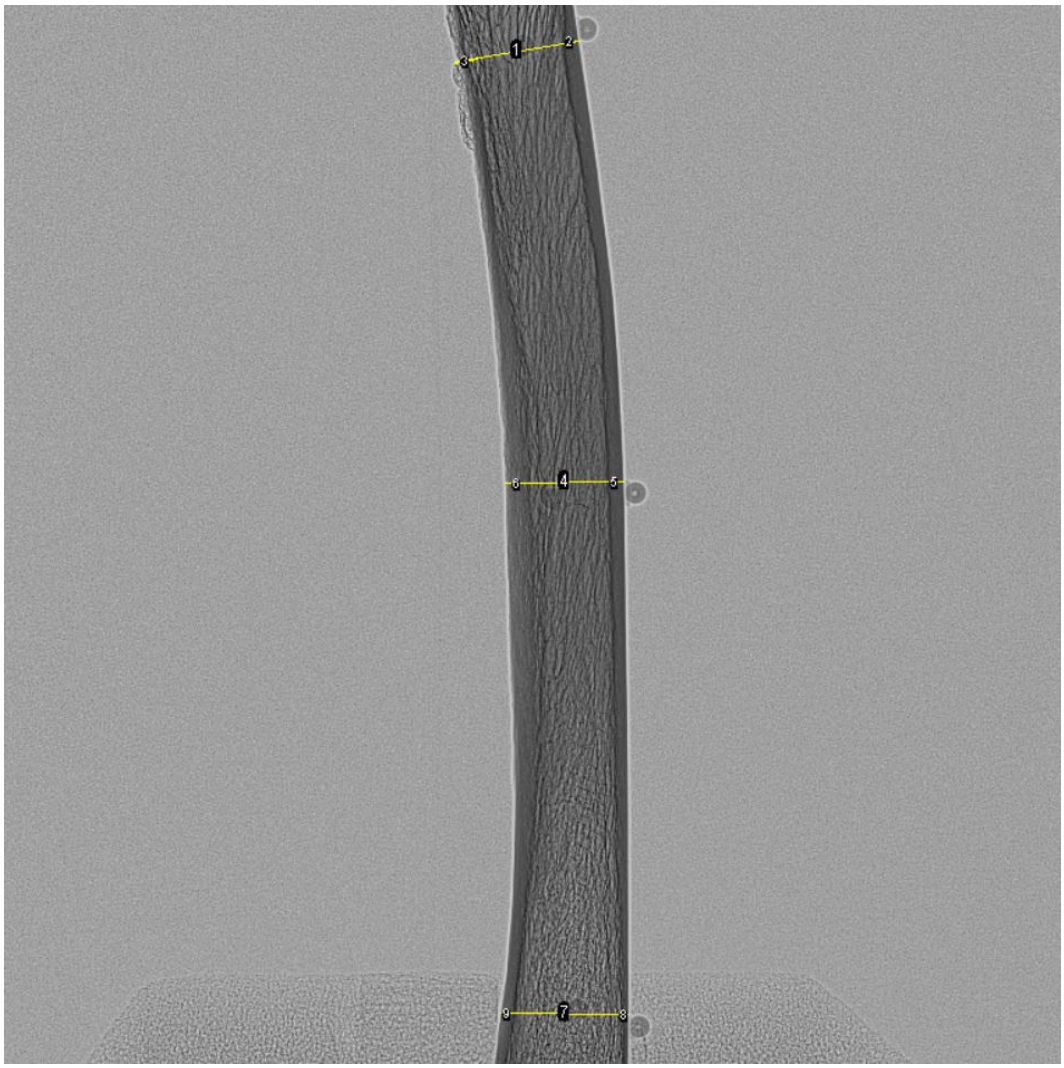

Figure 7. M-L Radiograph of the femur of D02-2010 with digitized lines measuring cortical bone area and total bone area at 20%, 50%, and 75% of total length from the distal end.

I also digitized lines along the interior and exterior margins of the cortical bone for each femoral shaft in the antero-posterior and medio-lateral views using ImageJ in order to conduct a Generalized Procrustes Analysis (GPA) to visually assess the relationship between patterns of bone remodeling and age and measure changes in diaphyseal shape with age (Figure 8). Using the ROI manager, the coordinates of these lines were recorded and subsequently exported into a text file. I then imported the coordinates into ArcGIS version 10.6 (ESRI 2017). I ran the create lines function in ArcGIS to transform these points into polylines. Then I

ran an generate equidistant points along a polyline function to produce 11 equidistant pseudo-landmarks along the interior and exterior margins of the cortical bone of each femoral shaft. These equidistant coordinates were then exported into a spreadsheet and used to conduct a GPA by 10-year age cohorts. I then used a combination of the statistical programs JMP Pro 14 (JMP®, Version 14) and R (R Core Team 2013) to run tests of distribution, various regressions, and a GPA.

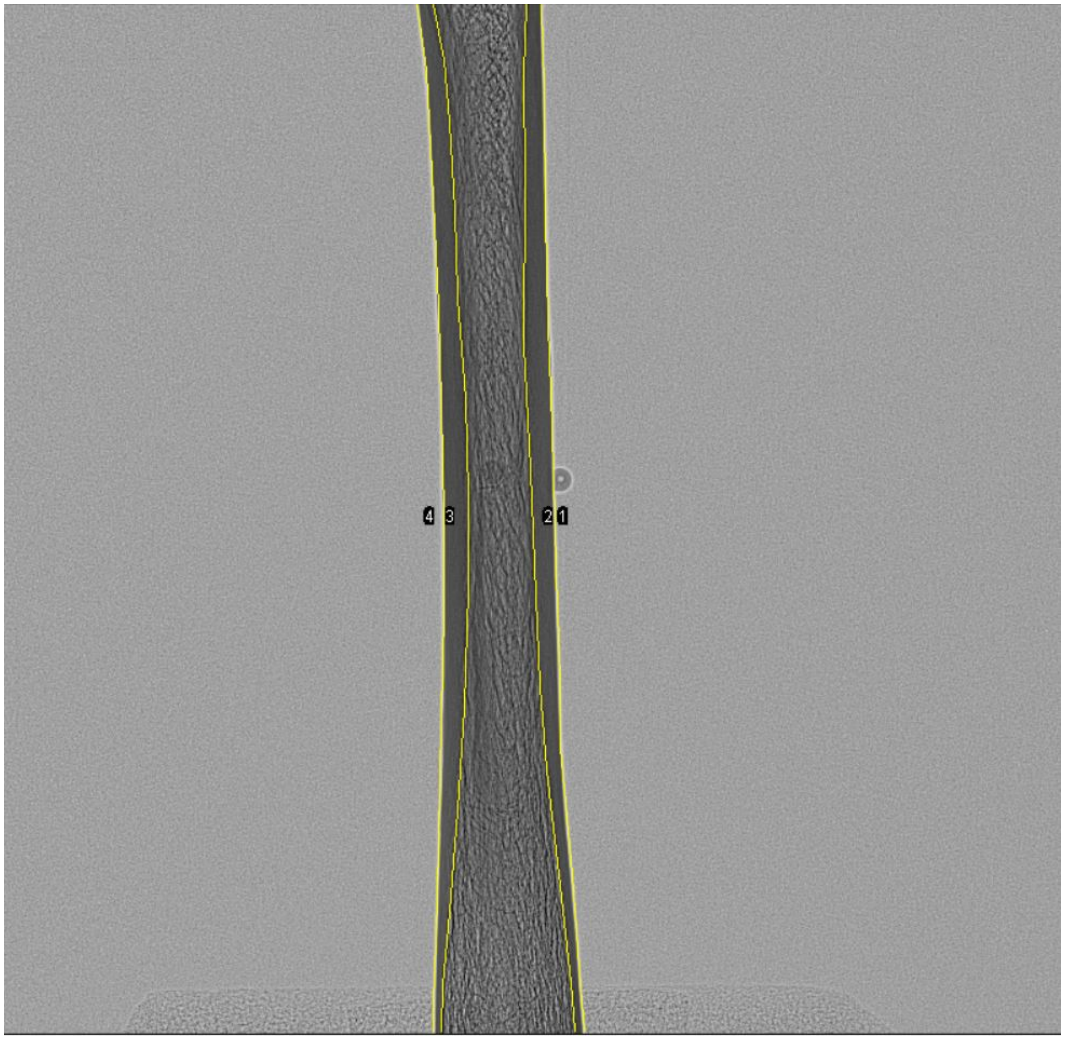

Figure 8. A-P Radiograph of the femur of D02-2010 with digitized lines along the margins of cortical bone used for the Generalized Procrustes Analysis.

Statistical Tests & Procrustes Analysis

All distribution and regression statistics were run using JMP Pro 14 statistical software (JMP®, Version 14). The generalized Procrustes analysis was run using the shapes() package (Dryden 2018) in the open source program R (R Core Team 2013) and visualized using RStudio (RStudio 1.1.463, 2016). Prior to running any interpretative statistics, I ran a Shapiro-Wilke's goodness of fit test and other tests of distribution (skewness and kurtosis) to determine whether the sample followed a normal distribution. Then I linear regressions to assess the relationship between the MV:BV and age-at-death for all measures separately, the averaged measures, and the summed measures. Finally, I ran a LOESS (local estimated scatterplot smoothing) regression using the default parameters for the entire sample and for each sex and fit a line through the dataset to follow the degree of correlation by age cohort.

A LOESS regression is a non-parametric regression model that creates a line of best fit throughout the dataset by fitting a polynomial through localized subsets of the data that are automatically determined by the LOESS regression model according to a k nearest neighbor analysis (i.e. a weighted-least-squares polynomial regression) (Cleveland 1979; Cleveland & Devlin 1988; Fox & Weisberg 2018). It is a less restrictive model of regression than a linear model. The line of best fit algorithm for a LOESS regression is applied to each point in the dataset to create a polynomial line through the entire dataset (Cleveland 1979; Cleveland & Devlin 1988; Fox & Weisberg 2018). The resulting polynomial line represents the degree of correlation between the two variables in the dataset at any

given point. Following the linear regressions, I calculated prediction intervals using the residuals and regression equations for each measure in each age cohort to assess the accuracy of the linear regression equations and examine the bias of the sample.

A GPA arbitrarily selects a form based on landmark coordinate data, in this case pseudo-landmark, that is used to compare the shape of each individual in the dataset (Gower 1975; Goodall 1991; Dijksterhuis & Gower 1992). The GPA also generates a mean shape of the dataset (Gower 1975; Goodall 1991; Dijksterhuis & Gower 1992), which I used as a consensus form to compare the shape of the femoral shaft by age cohort. Some of the femora had to be excluded because of digitizing error, which reduced the number of individuals for the Procrustes analysis to 160 in the A-P view and 162 in the M-L view. The GPA controls for size and looks exclusively at shape which eliminates any variation based on size and allows us to see the specific areas of medullary cavity expansion, cortical bone loss, and appositional growth.

IV. RESULTS

Hypothesis & Research Questions

A brief reminder of the hypotheses and research questions will help frame what is seen in these results. I hypothesize that there will be a positive correlation between the MV:BV (medullary cavity area : total bone area) and age, with endosteal bone loss exceeding the rate of periosteal bone deposition, that the levels of correlation will be different between males and females (specifically that the correlations will be slightly higher for females), that rates of endosteal bone loss exceed rates of periosteal bone deposition, that there is site specific cortical bone loss, and that there are peak periods of cortical bone loss throughout the aging process.

Tests for Normalcy, Linear Regression, & Prediction Intervals

Distribution, Shapiro-Wilke's, Skew, & Kurtosis

Out of a sample of 164 individuals, there are 109 males and 55 females. The average age-at-death is ca. 68 years old and does not differ significantly for males and females (Table 1). The Shapiro-Wilke's goodness of fit test showed that the age distribution of the total sample does not follow a normal distribution ($p=0.0003$). However, linear regression can still be used to assess the correlations between various measures and age-at-death, albeit with caution, considering that my hypothesis assumes that there is a linear relationship between the MV:BV and age and because I am also using a non-parametric LOESS regression to assess this relationship. The total sample has negative kurtosis and a leftward skew toward the younger age ranges considered (50-79). When separated by sex, the female

subsample has a moderate negative kurtosis and shows a comparatively significant leftward skewing. The male subsample has greater negative kurtosis but less overall skewing than the female subsample (Table 1).

Table 1. Sample Distribution Statistics.

Sample	N	Mean	Min (yrs)	Max (yrs)	Std Dev	Skew	Kurtosis
All	164	68.28659	50	97	11.24778	0.416597	-0.62335
Female	55	69.36364	53	97	12.17217	0.551200	-0.60735
Male	109	67.74312	50	93	10.76896	0.288812	-0.77307

Linear Regression & LOESS Regression

Linear regression with and without outliers was performed on the entire sample and separately for each sex for each of the measures taken as well as averaged and summed measures. There were several MV:BV measures that showed different levels of correlation between the A-P and M-L planes and there was virtually no difference in the levels of correlation and p values between averaged and summed measures regardless of whether the outliers were included (Tables 2 & 3).

Table 2. Correlations and Linear Regression Equations for All Measures with and without outliers for Females. Red indicates p value greater than 0.05. Correlations over 0.40 in bold.

Measure	Outliers	Correlation	Linear Regression Equation
Avg Ratio 75%	Y	**0.42746**	Age Yrs= 25.866314 + 70.635291 x Avg Ratio 75%
Avg Ratio 75%	N	**0.41190**	
AP Ratio 75%	Y	0.38975	Age Yrs= 23.436985 + 71.534251 x A-P Ratio 75%
ML Ratio 75%	Y	0.38054	Age Yrs= 38.424722 + 52.660889 x M-L Ratio 75%
AP Ratio 75%	N	0.38975	
ML Ratio 75%	N	0.38054	
Sum Ratios 75%	Y	**0.42746**	Age Yrs= 25.866314 + 35.317646 x Sum Ratios 75%
Sum Ratios 75%	N	**0.42746**	
Avg Ratio Mid	Y	**0.50549**	Age Yrs= 32.778611 + 62.658759 x Avg Ratio Mid
Avg Ratio Mid	N	**0.49788**	
AP Ratio Mid	Y	**0.51902**	Age Yrs= 32.739804 + 59.202551 x A-P Ratio Mid
ML Ratio Mid	Y	**0.42591**	Age Yrs= 41.066145 + 51.952215 x M-L Ratio Mid
AP Ratio Mid	N	**0.51902**	
ML Ratio Mid	N	**0.42591**	
Sum Ratios Mid	Y	**0.50549**	Age Yrs= 32.778611 + 31.32938 x Sum Ratios Mid
Sum Ratios Mid	N	**0.50549**	
Avg Ratio 20%	Y	0.33307	Age Yrs= -28.32959 + 114.33359 x Avg Ratio 20%
Avg Ratio 20%	N	0.32420	
AP Ratio 20%	Y	0.38576	Age Yrs= -57.99642 + 151.31212 x A-P Ratio 20%
ML Ratio 20%	Y	0.20562	Age Yrs= -0.395732 + 80.273044 x M-L Ratio 20%
AP Ratio 20%	N	0.38576	
ML Ratio 20%	N	0.20562	
Sum Ratios 20%	Y	0.33307	Age Yrs= -28.32959 + 57.166797 x Sum Ratios 20%
Sum Ratios 20%	N	0.33307	
Avg Ratio All	Y	**0.49589**	Age Yrs= 3.2048842 + 96.622714 x Avg Ratio All
Avg Ratio All	N	**0.48308**	
Sum Ratios All	Y	**0.49589**	Age Yrs= 3.2048841 + 16.103786 x Sum Ratios All
Sum Ratios All	N	**0.49588**	

Table 3. Correlations and Linear Regression Equations for All Measures with and without outliers for males. Red indicates p value greater than 0.05.

Measure	Outliers	Correlation	Linear Regression Equation
Avg Ratio 75%	Y	0.23338	Age Yrs= 41.546506 + 43.907882 x Avg Ratio 75%
Avg Ratio 75%	N	0.23610	
AP Ratio 75%	Y	0.10197	Age Yrs= 55.789519 + 18.964019 x A-P Ratio 75%
ML Ratio 75%	Y	0.31333	Age Yrs= 39.375757 + 49.59627 x M-L Ratio 75%
AP Ratio 75%	N	0.10197	
ML Ratio 75%	N	0.31333	
Sum Ratios 75%	Y	0.23610	Age Yrs= 41.303728 + 22.052772 x Sum Ratios 75%
Sum Ratios 75%	N	0.23610	
Avg Ratio Mid	Y	0.30434	Age Yrs= 39.941397 + 52.587312 x Avg Ratio Mid
Avg Ratio Mid	N	0.32087	
AP Ratio Mid	Y	0.22342	Age Yrs= 48.570665 + 34.373541 x A-P Ratio Mid
ML Ratio Mid	Y	0.36055	Age Yrs= 38.705715 + 57.323527 x M-L Ratio Mid
AP Ratio Mid	N	0.22342	
ML Ratio Mid	N	0.36055	
Sum Ratios Mid	Y	0.32087	Age Yrs= 38.319692 + 27.678486 x Sum Ratios Mid
Sum Ratios Mid	N	0.32087	
Avg Ratio 20%	Y	0.12444	Age Yrs= 32.083071 + 42.058684 x Avg Ratio 20%
Avg Ratio 20%	N	0.23968	
AP Ratio 20%	Y	0.22537	Age Yrs= 6.1291862 + 73.671234 x A-P Ratio 20%
ML Ratio 20%	Y	0.19224	Age Yrs= 0.0321477 + 78.172237 x M-L Ratio 20%
AP Ratio 20%	N	0.22537	
ML Ratio 20%	N	0.19224	
Sum Ratios 20%	Y	0.23968	Age Yrs= -16.37422 + 49.429614 x Sum Ratios 20%
Sum Ratios 20%	N	0.23968	
Avg Ratio All	Y	0.28845	Age Yrs=19.025546 + 74.070079 x Avg Ratio All
Avg Ratio All	N	0.32158	
Sum Ratios All	Y	0.32158	Age Yrs= 12.476372 + 13.956147 x Sum Ratios All
Sum Ratios All	N	0.32158	

Initial tests using the entire sample and averaged measures showed correlations between 0.21 & 0.39 with the average ratio at 20% length being the least correlated with age and a combination of all three measures showing the highest correlation (Table 4). The lowest correlation for females between MV:BV and age using combined measures (0.333) was higher than any of the correlations in the male group (0.304) (Table 4).

Table 4. Correlations for combined A-P and M-L measures. Correlations over 0.35 in bold.

Sample	Measure	Correlation	Covariance	P-value	R^2
Combined	Avg Ratio 20%	0.210025	0.078309	0.0069	0.044110
	Avg Ratio Mid	**0.393567**	0.355557	<0.0001	0.154895
	Avg Ratio 75%	0.320249	0.229264	<0.0001	0.102560
	Avg Ratio All	**0.383825**	0.221043	<0.0001	0.147321
N=164					
Females	Avg Ratio 20%	0.333067	0.143756	0.013	0.110934
	Avg Ratio Mid	**0.505488**	0.604192	<0.0001	0.255518
	Avg Ratio 75%	**0.427463**	0.383276	0.0011	0.182725
	Avg Ratio All	**0.495890**	0.377075	0.0001	0.245907
N=55					
Males	Avg Ratio 20%	0.124435	0.042695	0.1973	0.015484
	Avg Ratio Mid	0.304336	0.204255	0.0013	0.092620
	Avg Ratio 75%	0.233384	0.143862	0.0146	0.054468
	Avg Ratio All	0.288450	0.130271	0.0024	0.083204
N=109					

There are some measures that are significantly different when analyzed separately, particularly between the A-P & M-L measures in males. At 75% total length the M-L measures have triple the level of correlation (0.101 to 0.313) with age, at midshaft this difference in correlation is reduced but still significant, and at 20% total length the M-L measures still have higher levels of correlation, but this difference is negligible. For females, the levels of correlation are significantly higher than for males for all measures. The differences between levels of correlation for the A-P and M-L measures for females is smaller than for males. There is however still a significant difference in some of the measures. Apart from the measures at 75% total length, the A-P measures in females have higher correlations (ca. 0.1 at midshaft and ca. 0.2 at 20% total length). In summation, the correlation with age is greater in the M-L measures in males and in the A-P measures in females. All the plotted regression lines with confidence intervals had

flatter slopes for males than females. Measures with the highest differences in correlation between the sexes were plotted with 95% confidence intervals and can be seen in Figures 9-13. Plotted regressions by sex for all individual measures, averaged measures, and summed measures can be found in Appendix A. The accompanying residuals for all tests of linear regression are available upon request.

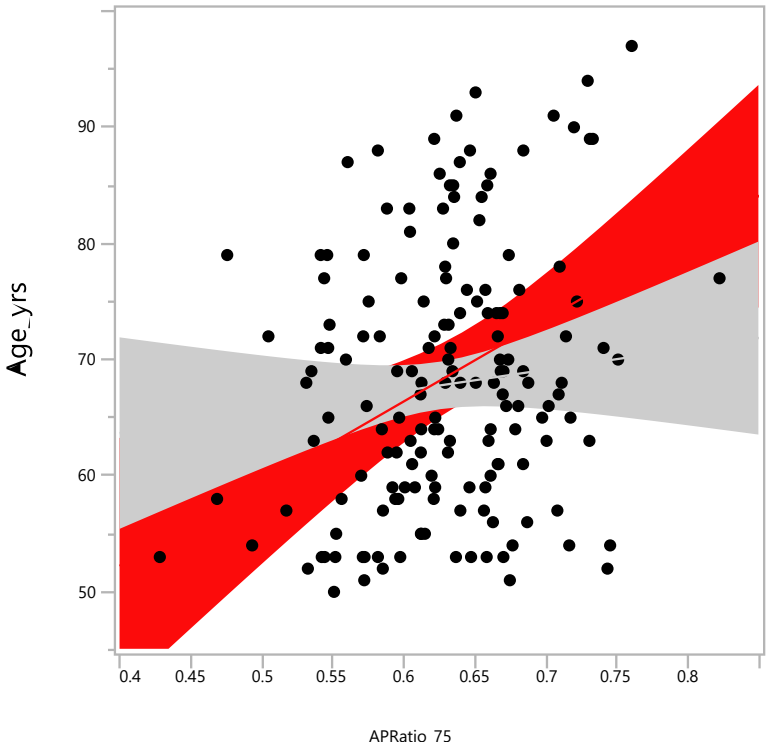

Figure 9. A-P MV:BV at 75% length from the distal end liner regression plot. Shaded areas repesent the 95% Confidence Interval. Red: females, gray: males. These shaded areas and colors are consistent for all linear regression plots.

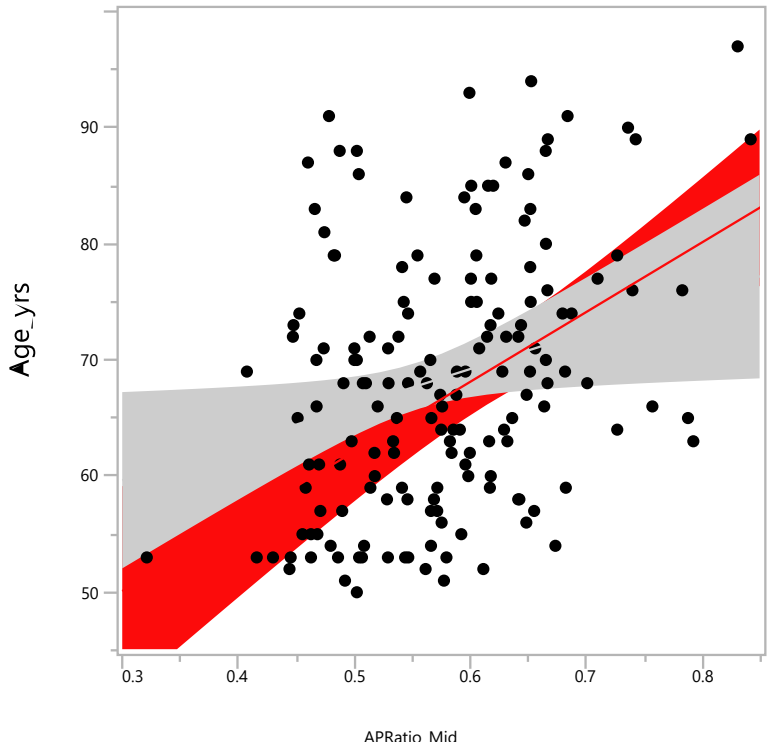

Figure 10. A-P MV:BV at 50% length from the distal end linear regression plot.

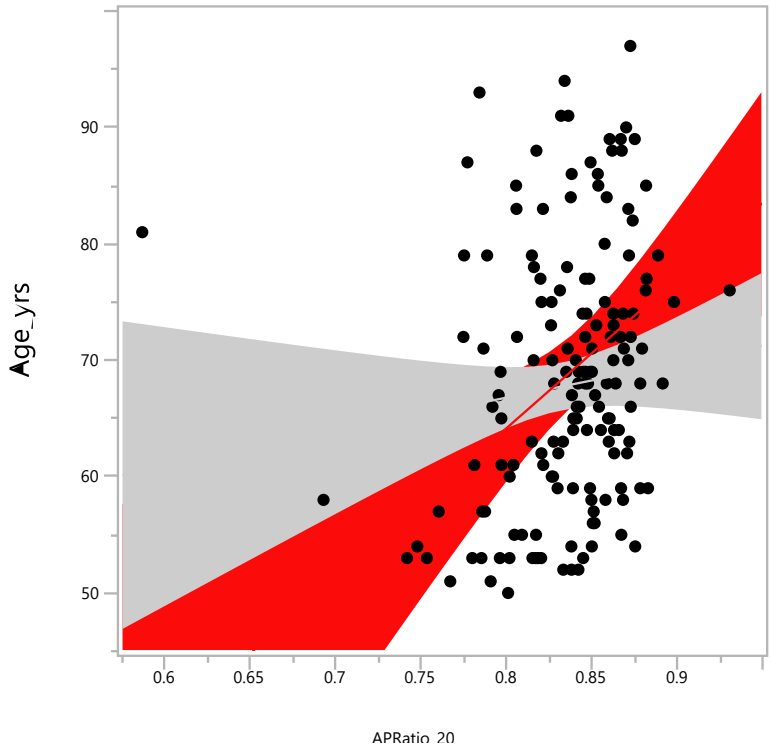

Figure 11. A-P MV:BV at 20% length from the distal end linear regression plot.

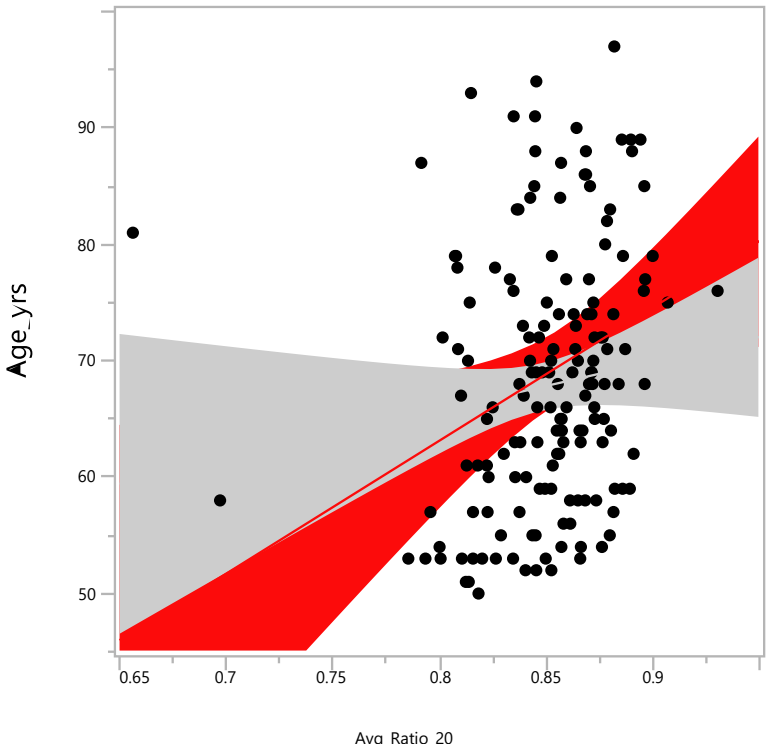

Figure 12. Averaged MV:BV at 20% length from the distal end linear regression plot.

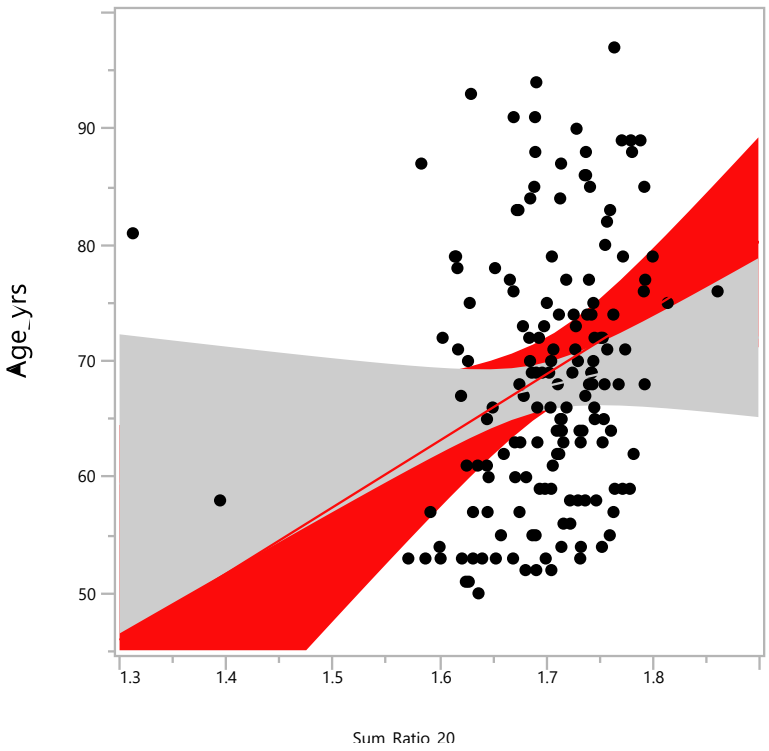

Figure 13. Summed MV:BV at 20% length from the distal end linear regression plot.

The LOESS (local estimated scatterplot smoothing) regressions for the entire sample show that the correlation between the MV:BV and age is variable throughout the aging process. The A-P measures at midshaft have the highest levels of correlation in both sexes (>0.304) and the measures in both planes at 75% and 20% have low levels of correlation (0.101-0.239). When averaged, the MV:BV measures obscure some the variation seen at specific cross sections of the diaphysis. LOESS regressions for measures that show a non-linear relationship between MV:BV and age can be found in Figures 14-17. When separated by sex, females show a much more consistent relationship between the MV:BV and age and this relationship approaches linearity for each of the measures individually. However, there are still some undulations in the line of best fit that show that there is not a strictly linear relationship (Figure 18). Males show a much less consistent relationship between the MV:BV and age. The line of best fit indicates that the MV:BV is actually negatively correlated with age to some degree, which is the opposite of what was predicted, and that there are peak periods of increase in the MV:BV from ca. 75 years and upward. (Figure 19). LOESS regression can be sensitive to outliers in the sample (Cleveland & Devlin 1988; Fox & Weisberg 2018). To control for this, I eliminated two individuals with ratios far outside the rest of the sample. One was an 81-year-old Hispanic male the other a 58-year-old White female. The removal of these individuals did not significantly impact the statistical results of the LOESS regression but did affect how the line of best fit was plotted for MV:BV values below 0.55. The results of the LOESS regressions mirror the differences seen in the linear regressions for females and males. The MV:BV ratio at midshaft for females in the A-P view has a line of best fit that is much more linear than this measure in the M-L view. This makes sense given the

level of correlation between the MV:BV and age is greater in the A-P measure than the M-L measure. The same trend is seen when comparing the A-P and M-L LOESS regressions for females at 20% total length. The LOESS regressions for males are all flatter than those for females, and follow the pattern seen in the linear regressions with the M-L measures showing more linear lines of best fit.

Bivariate Fit of Age_yrs By MLRatio_Mid Sex=F

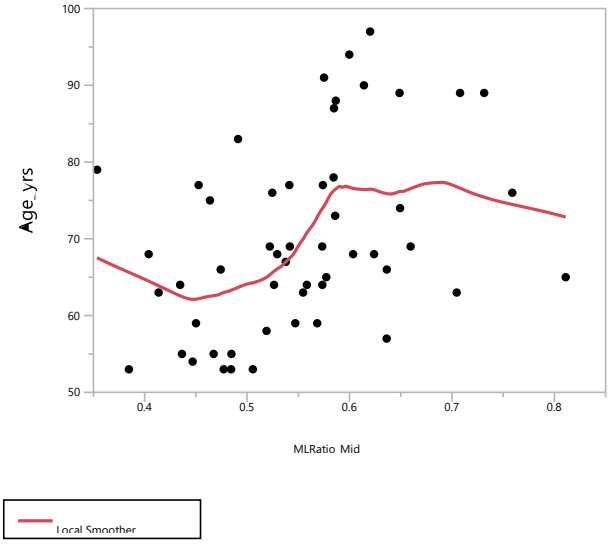

Figure 14. LOESS regression for M-L MV:BV at 50% length from the distal end. Females.

Bivariate Fit of Age_yrs By MLRatio_20 Sex=F

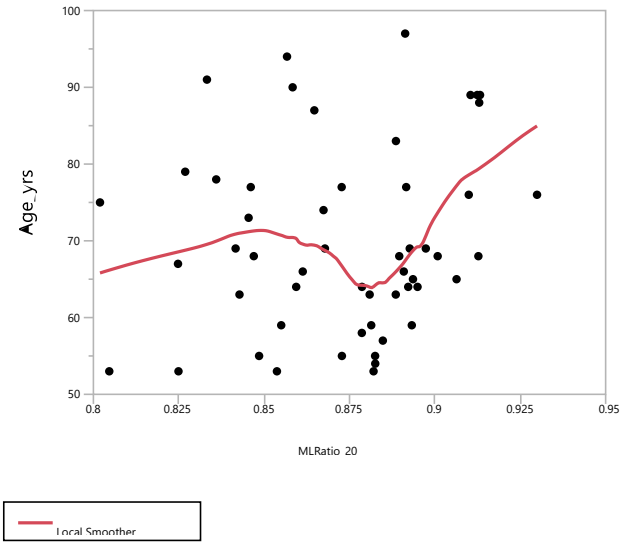

Figure 15. LOESS regression of M-L MV:BV at 20% length from the distal end. Females.

Bivariate Fit of Age_yrs By Sum_Ratio_Mid Sex=F

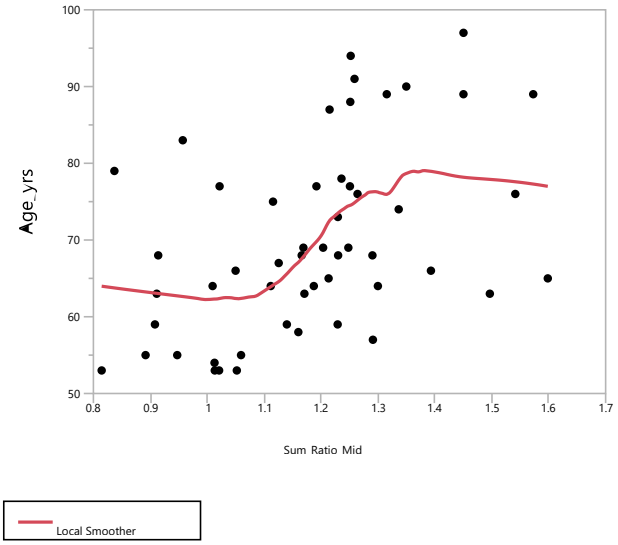

Figure 16. LOESS regression of summed MV:BV at 50% length from the distal end. Females.

Fit Group Sex=M

Bivariate Fit of Age_yrs By APRatio_75 Sex=M

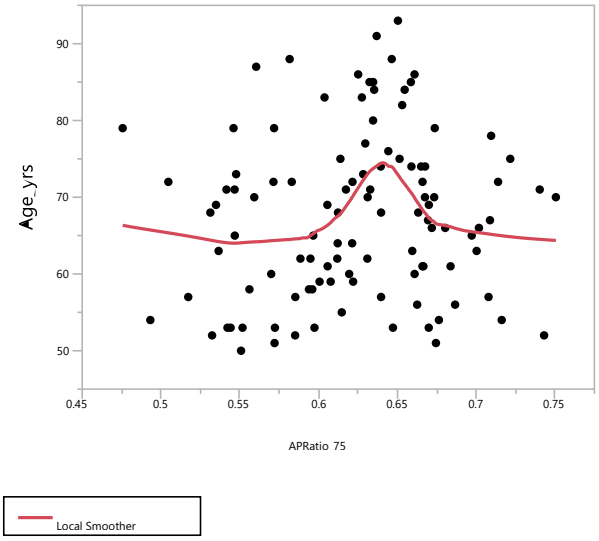

Figure 17. LOESS regression of A-P MV:BV at 75% length from the distal end. Males.

Bivariate Fit of Age-years By Avg-Ratio-All Sex=F

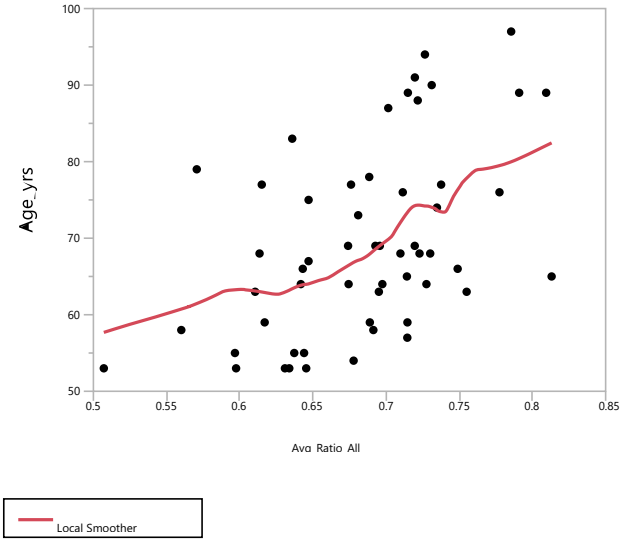

Figure 18. LOESS Regression of all measures averaged. Females.

Bivariate Fit of Age-years By Avg-Ratio-All Sex=M

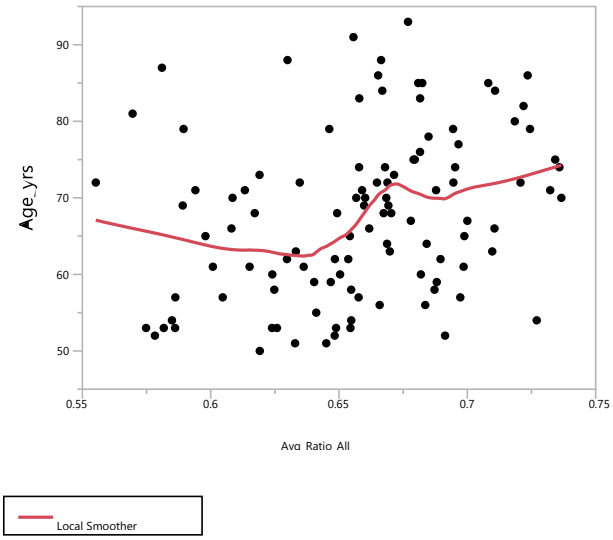

Figure 19. LOESS Regression of all measures averaged. Males.

Prediction Intervals

The predictions intervals generated by the sex separated linear regression analyses on averaged measures showed an average error of less than 10 years for the entire sample (Table 5). The plotted prediction intervals for all averaged measures can be found in Figures 20 & 21. The range of predicted ages for all measures is 45-90 years. The range of predicted ages is smaller for females than males. Prediction intervals were not generated for individual measures but will be in future analyses of this data. When broken down by age cohort, errors ranged from less than 5 years for the age cohorts nearest the mean to upwards of 20 years for the 90+ years age cohort (Table 6). Age is overestimated in the age cohorts below the mean and underestimated in the age cohorts above it. The results of the separate analyses mirrored that of the combined sex sample with the age cohorts grouped around the mean having a smaller error than the older age cohorts (Tables 7 & 8).

Table 5. Prediction Intervals and average error for the entire sample and by sex.

Sample	Measure	Avg Lower 95%	Avg Upper 95%	Range	Absolute Error
Combined	Avg Ratio 20%	46.083753	90.489417	44.405663	9.045001
	Avg Ratio Mid	47.325148	89.248022	41.922873	8.461945
	Avg Ratio 75%	46.693456	89.879714	43.186258	8.817822
	Avg Ratio All	47.207577	89.365593	42.158016	8.529645
N=164					
Females	Avg Ratio 20%	45.714464	93.012808	47.298344	9.613506
	Avg Ratio Mid	47.71894	91.008332	43.289391	8.428561
	Avg Ratio 75%	46.685336	92.041936	45.35660	9.161881
	Avg Ratio All	47.579713	91.147559	43.567845	8.657780
N=55					
Males	Avg Ratio 20%	46.270092	89.216146	42.946053	8.758140
	Avg Ratio Mid	47.126446	88.359792	41.233346	8.478790
	Avg Ratio 75%	46.697553	88.788685	42.091132	8.644213
	Avg Ratio All	47.019802	88.466436	41.446634	8.464989
N=109					

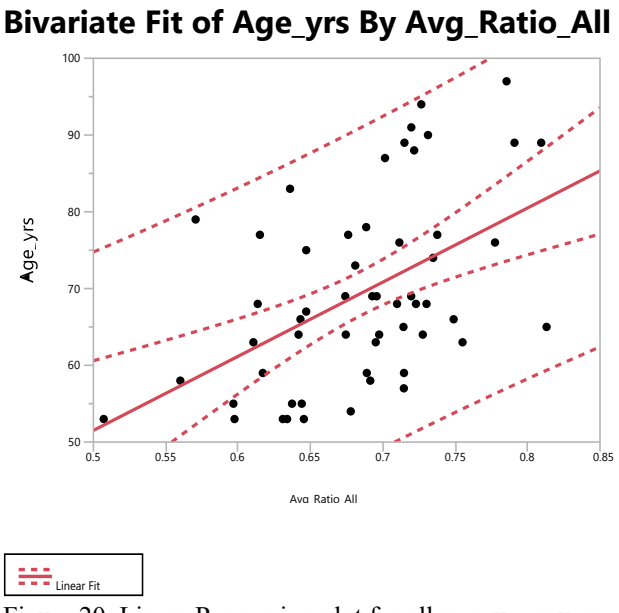

Figure 20. Linear Regression plot for all measures averaged for females. Curved dotted line: 95% Confidence Interval. Straight dotted line: 95% Prediction Interval.

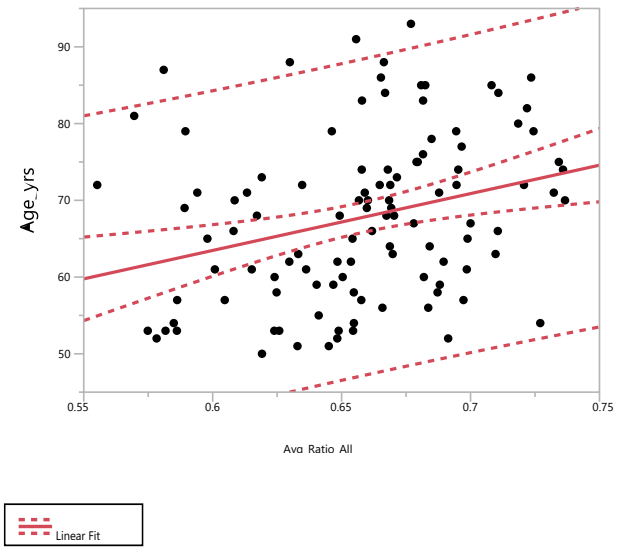

Figure 21. Linear Regression plot for all measures averaged for males. Curved dotted line: 95% Confidence Interval. Straight dotted line: 95% Prediction Interval.

Table 6. Prediction Intervals for each age cohort. Combined sex sample.

Age Cohort	Measure	Avg Lower 95%	Avg Upper 95%	Range	Error
50-59	Avg Ratio 20%	44.928914	89.489791	44.560877	12.487727
	Avg Ratio Mid	44.711007	86.682038	41.971030	10.687790
	Avg Ratio 75%	45.099391	88.332908	43.233517	11.693423
	Avg Ratio All	44.741743	86.968721	42.226977	10.899607
N=44					
60-69	Avg Ratio 20%	46.516493	90.992912	44.476419	4.002739
	Avg Ratio Mid	47.666402	89.641203	41.974801	4.756218
	Avg Ratio 75%	46.970608	90.247640	43.277032	4.361377
	Avg Ratio All	47.632299	89.818729	42.18643	4.648595
N=51					
70-79	Avg Ratio 20%	46.457383	90.427606	43.970222	-5.676552
	Avg Ratio Mid	48.051651	89.783122	41.73147	-5.201660
	Avg Ratio 75%	46.706517	89.640193	42.933676	-5.945692
	Avg Ratio All	47.771387	89.742424	41.971036	-5.362142
N=42					
80-89	Avg Ratio 20%	46.752756	91.183971	44.431214	-16.364969
	Avg Ratio Mid	49.455250	91.352966	41.897716	-14.929224
	Avg Ratio 75%	48.054396	91.082779	43.028383	-15.764745
	Avg Ratio All	49.063568	91.196979	42.13341	-15.203059
N=21					
90+	Avg Ratio 20%	45.917372	91.542027	45.624654	-23.936966
	Avg Ratio Mid	51.053982	93.610191	42.556209	-20.334580
	Avg Ratio 75%	51.172739	95.561505	44.388765	-19.299544
	Avg Ratio All	51.237584	94.043334	42.805750	-20.026207
N=6					
Average Age	68.286				

Table 7. Prediction Intervals for each age cohort. Females.

Age Cohort	Measure	Avg Lower 95%	Avg Upper 95%	Range	Error
50-59	Avg Ratio 20%	42.875666	90.604661	47.728995	11.140163
	Avg Ratio Mid	42.767849	86.172343	43.404493	8.870096
	Avg Ratio 75%	43.704978	89.126217	45.421239	10.815598
	Avg Ratio All	42.908642	86.621431	43.712788	9.165036
N=15					
60-69	Avg Ratio 20%	46.808314	93.854636	47.046321	4.231475
	Avg Ratio Mid	48.709021	91.902831	43.193809	4.205926
	Avg Ratio 75%	47.558952	92.763224	45.204271	4.061088
	Avg Ratio All	48.766167	92.202314	43.436147	4.38424
N=20					
70-79	Avg Ratio 20%	46.436164	90.433216	43.997052	-5.66287
	Avg Ratio Mid	48.032191	89.77917	41.746978	-5.19188
	Avg Ratio 75%	46.695601	89.654347	42.958746	-5.922586
	Avg Ratio All	47.749512	89.736694	41.987182	-5.354457
N=10					
80-89	Avg Ratio 20%	48.989564	96.204558	47.214993	-14.90294
	Avg Ratio Mid	51.585707	95.028533	43.442825	-14.19288
	Avg Ratio 75%	49.539579	95.077511	45.537931	-15.19145
	Avg Ratio All	51.787807	95.500769	95.500769	-13.85571
N=6					
90+	Avg Ratio 20%	46.101195	93.106434	47.005239	-23.39618
	Avg Ratio Mid	52.758027	95.991752	43.233725	-18.62511
	Avg Ratio 75%	52.631623	98.227553	45.595929	-17.57041
	Avg Ratio All	52.988769	96.557326	43.568556	-18.22695
N=4					
Average Age	69.363				

Table 8. Prediction Intervals for each age cohort. Males.

Age Cohort	Measure	Avg Lower 95%	Avg Upper 95%	Range	Error
50-59	Avg Ratio 20%	45.990939	88.913135	42.922195	12.727899
	Avg Ratio Mid	45.716089	86.945673	41.229584	11.606743
	Avg Ratio 75%	45.82064	87.922576	42.101936	12.14747
	Avg Ratio All	45.689899	87.148354	41.458454	11.694989
N=29					
60-69	Avg Ratio 20%	46.328221	89.146639	42.818417	3.598671
	Avg Ratio Mid	46.993744	88.182088	41.188344	4.556814
	Avg Ratio 75%	46.591032	88.624683	42.033651	4.025829
	Avg Ratio All	46.900771	88.280932	41.38016	4.243014
N=31					
70-79	Avg Ratio 20%	46.704938	89.627209	42.922271	-5.302675
	Avg Ratio Mid	47.808505	89.069151	41.260646	-5.029921
	Avg Ratio 75%	47.14056	89.316082	42.175522	-5.240428
	Avg Ratio All	47.848403	89.333367	41.484963	-4.877864
N=32					
80-89	Avg Ratio 20%	45.858033	89.175736	43.317702	-16.949781
	Avg Ratio Mid	48.603067	89.88274	41.279672	-15.223763
	Avg Ratio 75%	47.460323	89.484887	42.024564	-15.994061
	Avg Ratio All	47.973873	89.475463	41.50159	-15.741998
N=15					
90+	Avg Ratio 20%	45.549728	88.413212	42.863484	-25.018529
	Avg Ratio Mid	47.645892	88.847068	41.201177	-23.753519
	Avg Ratio 75%	48.254972	90.229409	41.974436	-22.757809
	Avg Ratio All	47.735213	89.015351	41.280137	-23.624717
N=2					
Average Age	67.743				

Procrustes Analysis

Overall, the Procrustes analysis showed low levels of variation in mean shape in the entire sample, when divided by sex, when divided by age cohort, and when mean shapes of each cohort were compared and plotted (Tables 9 & 10). The low rho scores paired with the sum of squares scores (GSS) indicate that there is little to no deviation from the mean shape in any of the analyses. The age cohort with the highest rho score and GSS in the A-P view (70-79 years) is visually distinct from the other age cohorts in the plotted comparisons. The 70-79 years age cohort also has the highest rho score in the analyses of the cohorts in the M-L view. However, the rho score for the 70-79 years cohort in the M-L view is much closer to the other age cohorts than that for the A-P view (Table 10). The GSS (i.e. a quantified amount of Euclidean distance from the selected form for all points in the dataset) for each sample are heavily influenced by the number of individuals included and the number of landmarks used (Gower 1975; Goodall 1991; Dijksterhuis & Gower 1992). To partially circumvent this issue and directly compare levels of variation between sexes and age cohorts, the GSS values are standardized by dividing the score by the number of individuals in that particular sample.

The highest GSS value is found is in the A-P plane for the 70-79 years age cohort for males. This indicates that the cohort has the largest amount of variation from the mean shape in terms of Euclidean distance. The lowest GSS values are in the 90+ years age cohorts for both sexes, but this is a product of sample size (4 for females, 2 for males). The GSS values for the other subsamples show consistent trends as age increases.

Centroid sizes can also be used to analyze changes in bone shape. I calculated the average centroid size for the combined sex sample and for females and males separately.

One would logically expect centroid sizes to increase as the diameter of the diaphysis increases. However, centroid sizes decrease with age in the A-P plane and show no trend of increase or decrease in the M-L plane in females and show no trends of increase or decrease with age in either the A-P or M-L planes in males (Table10).

Table 9. Procrustes Analysis by age cohort. Combined sex sample.

	Sample	N	rmsrho	rmsd1	GSS	Stand. GSS	% Var PC
A-P							
	All	160	0.02164676	0.02163393	1067813.000	6673.831	60%
	50-59	42	0.01866830	0.01866686	211411.200	5033.600	69%
	60-69	51	0.01898694	0.01898434	263666.500	5169.931	63%
	70-79	41	0.02693449	0.02690163	441250.500	10762.207	73%
	80-89	20	0.01899059	0.01898890	102477.500	5123.875	70%
	90+	6	0.01853922	0.01853771	27357.180	4559.530	89%
	Mean Shape	5	0.00573916	0.00573911	2342.146	468.429	93%
M-L							
	All	162	0.01749374	0.01749241	718855.800	4437.381	56%
	50-59	44	0.01698381	0.01698267	182990.200	4158.868	60%
	60-69	51	0.01684181	0.01684047	209352.800	4104.957	53%
	70-79	42	0.01756902	0.01756780	192280.600	4578.110	58%
	80-89	19	0.01672634	0.01672511	76654.180	4034.431	66%
	90+	6	0.01477547	0.01477475	17376.760	2896.127	79%
	Mean Shape	5	0.00637019	0.00637009	2897.198	579.440	96%

Table 10. Procrustes Analysis by age cohort. Separated by sex.

View/Sex	Age Cohort	N	rmsrho	GSS	Stand. GSS	% Var PC	Centroid Size
AP/Females	50-59	14	0.02	73525.60	5251.83	73.57	3750.91
	60-69	23	0.02	126426.80	5496.82	71.92	3695.03
	70-79	10	0.02	51519.25	5151.93	63.41	3688.47
	80-89	6	0.02	19746.89	3291.15	85.50	3590.01
	90+	4	0.01	10902.93	2725.73	96.80	3599.02
AP/Males	50-59	28	0.02	131806.20	4707.36	69.51	3863.94
	60-69	28	0.02	113351.50	4048.27	54.84	3853.96
	70-79	31	0.03	383358.40	12366.40	78.78	3903.20
	80-89	14	0.02	74546.31	5324.74	79.47	3836.61
	90+	2	0.02	10828.70	5414.35	100.00	3711.74
ML/Females	50-59	15	0.02	68914.97	4594.33	71.96	3675.60
	60-69	19	0.02	70903.98	3731.79	57.39	3618.12
	70-79	10	0.01	26970.15	2697.02	79.45	3682.91
	80-89	5	0.02	25725.58	5145.12	87.70	3558.23
	90+	4	0.01	8242.80	2060.70	88.50	3587.74
ML/Males	50-59	29	0.02	108324.80	3735.34	57.81	3853.18
	60-69	32	0.02	129479.90	4046.25	56.58	3906.70
	70-79	32	0.02	155673.60	4864.80	61.96	3897.80
	80-89	14	0.01	44334.08	3166.72	64.31	3872.25
	90+	2	0.01	2727.86	1363.93	100.00	3734.63

The mean shapes for the combined sex sample visually capture the areas of highest variation between sexes and age cohorts when presented graphically. It is important to note that these are the mean shapes for each age cohort and are obscuring some the variation at the individual level. The proximal and distal ends of the diaphysis in all GPAs show slight variations in shape but have consistent cortical bone thicknesses throughout age. All GPAs also showed a general expansion of the medullary cavity with age and that most of the variation in cortical bone area can be found near and just distal to the midshaft. This medullary expansion with age was greater in females.

Most of the variation in the anterior-posterior plane in females can be seen along the lateral side of the femur. There is visual pattern of medullary cavity expansion as individuals age and there is a greater amount of cortical bone thinning on the lateral side

of the femur. This thinning primarily occurs between 30% and 60% of total bone length (Figure 20). There is also a small increase in the diameter of the femur through the age cohorts up to 80-89 years. The 90+ years age cohort has a smaller diameter.

Most of the variation in the medio-lateral plane can be seen in the same area of the diaphysis (30-60% length) (Figure 20). There is a visually significant difference in cortical bone area between the anterior and posterior sides of the femur. The anterior side has thinner cortical bone overall and shows a consistent pattern of thinning with age, while the posterior side has thicker cortical bone that thins from 50-79 years then becomes a consistent thickness from 80-90+ years. There may be a small increase in anterior bowing of the shaft through age, but it is difficult to see if there is a consistent pattern.

In females there is a visually significant reduction in cortical bone area along the diaphysis. This reduction is consistent throughout the aging process along the anterior and lateral sides of the bone. The reduction is greatest along the posterior side of the bone followed by the medial side. The reduction in cortical bone area along these sides occurs primarily from 50-79 years. After 80 years the reductions in cortical bone become uniform.

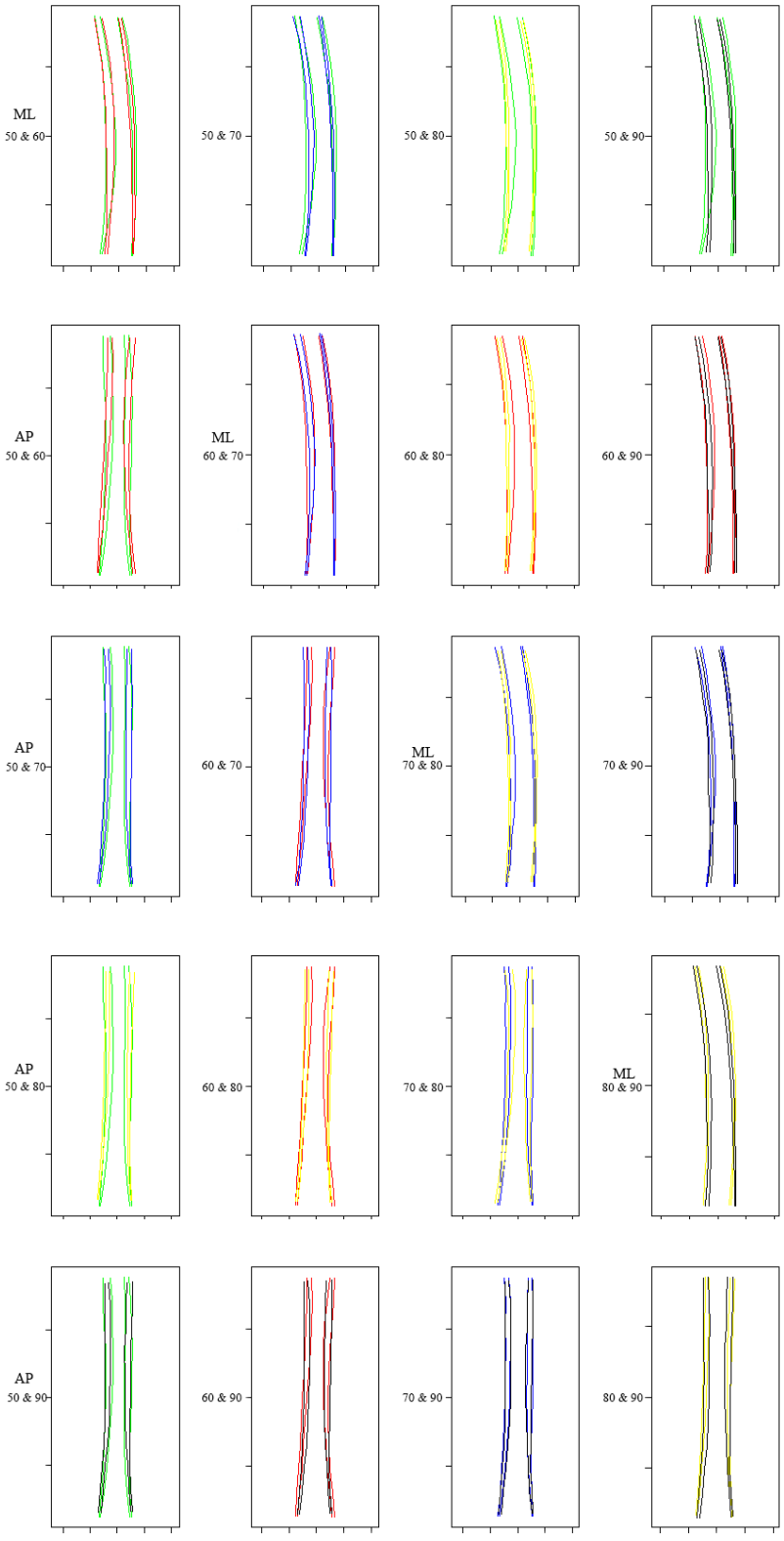

Figure 22. Plot matrix age cohort comparisons. Females. Green: 50-59 years, red: 60-69 years, blue: 70-79 years, yellow: 80-89 years, black: 90+ years. These colors are the same for both plot matrices.

The A-P GPA for males showed similar trends as those seen in the A-P GPA for females. There is a slight but consistent pattern of cortical bone thinning along the lateral side of the bone with age. The medial side of the bone thins from 50-79 years, then actually becomes thicker from 80-89 years before thinning again in the 90+ years ag cohort. These changes in cortical bone area occur primarily between 30% and 60% length from the distal end of the bone (Figure 21).

The M-L GPA for males was visually distinct from the M-L GPA for females. In the male sample, there is still a consistent pattern of anterior cortical bone thinning with age but there is a remarkably lower amount of cortical bone thinning along the posterior side. There are small if any changes in cortical bone area along the posterior side with age. Cortical bone area along the posterior side is also visually greater than that along the anterior side (Figure 21). As in females, there may be some anterior bowing of the shaft with age.

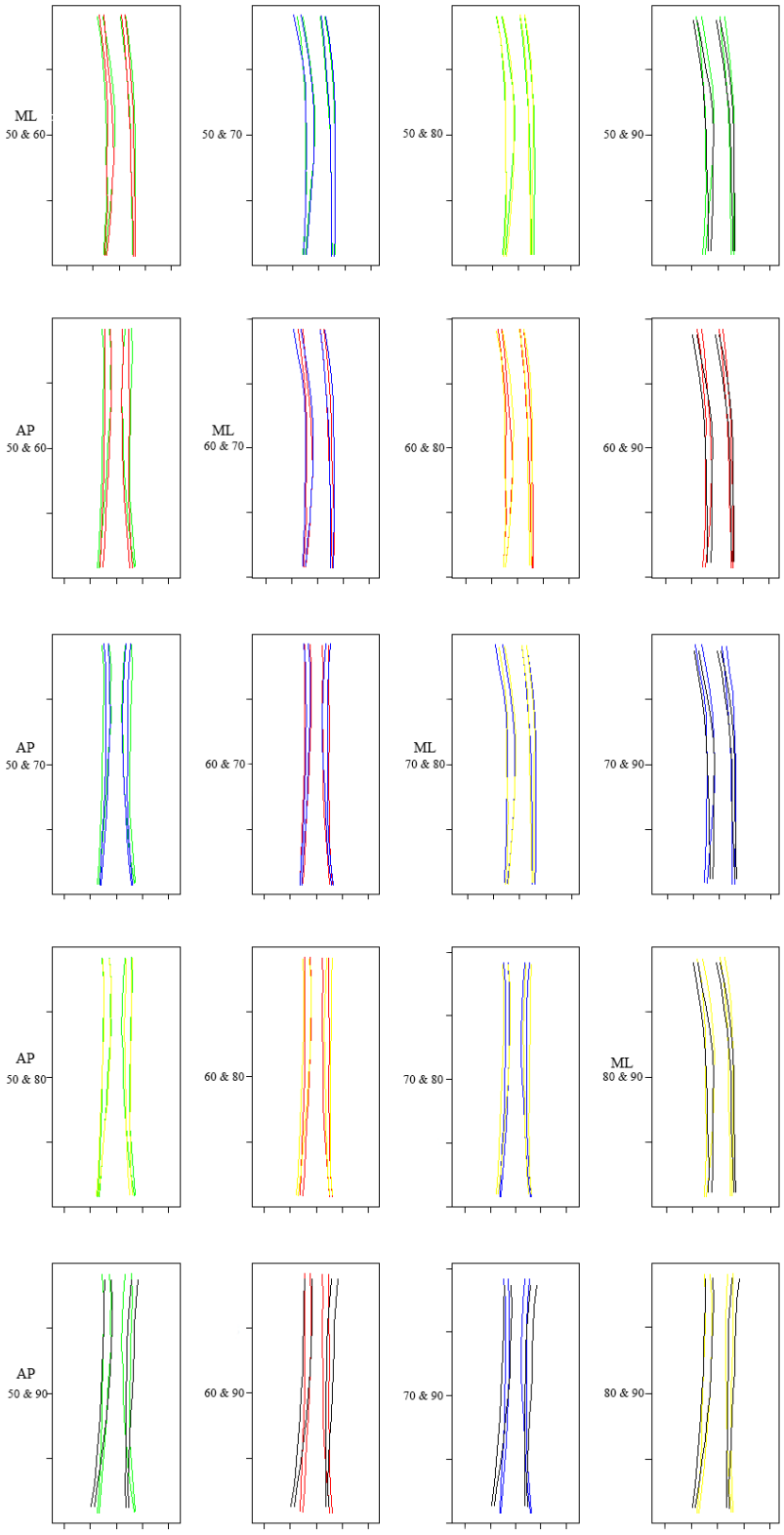

Figure 23. Plot matrix age cohort comparison. Males.

V. DISCUSSION

Limitations

The results of this study must be looked at with a degree of caution. Although, there are significant findings, they may be limited in their application. Foremost among the limitations of this study is the distribution of the sample. Males outnumber females nearly 2 to 1 (109 males, 55 females). However, by separating by sex this limitation is circumvented. The individuals in this sample primarily self-identified as White. A consequence of this is that the results of this study are essentially population specific. There is also an uneven distribution of individuals among the age cohorts. The 80-89 years and 90+ years age cohorts have substantially fewer individuals that the other cohorts. This issue is exacerbated in the Generalized Procrustes Analysis (GPA) because the number of individuals in each age cohort is further reduced due to separation by sex.

The small values for distances from the mean shape show that the variation in overall shape between femora in this sample is low and in all analysis over 50% of the variation was accounted for by the first two principle components. Procrustes results for the later age cohorts should be approached with relative caution because of their respective subsample sizes (5 & 14 for females and males respectively – M-L view, 6 & 14 – A-P view) for the 80 to 89 years age cohort and 2 & 6 for the 90+ years cohort. The small subsample sizes may not be capturing the extent of variation seen at these ages and the mean shapes produced are the product of handful of individuals that may have different bone morphology than the majority of the actual population in those age cohorts.

There are two limitations related to radiography. The first limitation is that biplanar radiographs can only capture the variation seen in the A-P and M-L planes and

variation in different planes is inherently obscured or lost. No bone cross section is perfectly circular, with most conforming to an ovoid shape (White, Black, Folkens 2012). The second is that the endosteal border of the cortical bone at 20% length from the distal end is difficult to observe. The density of the bone at this area may be lower and the shape of the diaphysis at this area also changes. The diaphysis of the femur becomes less ovoid and the posterior side flattens. The foam fixture could be causing some degree of scatter, which would affect the resolution of the radiograph around this area. On a small number of femora the foam fixture actually extended to cover the beads at 20% length.

Discussion

The results of the study generally support the hypotheses presented in the introduction. The MV:BV is correlated with age and this correlation is stronger in females than in males. I originally proposed that females would have a slightly stronger correlation than males, but the results of the linear regressions show that this relationship is in fact significantly stronger in females than males. I also proposed that bone remodeling is not uniform throughout the aging process and that there may be site-specific areas of bone remodeling. The results of the linear regressions and GPAs show that there are in fact areas of the femoral diaphysis that undergo greater levels of bone remodeling than others, particularly around midshaft.

The results of the linear regression tests for correlation are consistent with what previous researchers have found (Smith & Walker 1964; Garn, Rohmann, & Wagner 1967; Garn, Rohmann & Ascoli 1968; Van Gerven & Armelagos 1970; Carlson, Armelagos, & Van Gerven 1976; Martin & Atkinson 1977; Ruff & Hayes 1983; Mays 1996; Feik at al. 2000; Curate & Cunha 2017; Umbelino et al. 2019). There is a weak to

moderate correlation with age and the MV:BV in both the anterior-posterior and medio-lateral planes.

The prediction intervals and average error are also consistent with other methods of age estimation. The average error of around 10 years for the entire sample is comparable to other age estimation methods using the pubic symphysis, auricular surface, and rib ends (Iscan, Loth, & Wright 1984; Iscan, Loth, & Wright 1985; Lovejoy et al. 1985; Martille et al. 2007; Moore & DiGangi 2012). However, these age estimation methods usually terminate in an age cohort of 50 or 60+ years. The results of this study indicate that it may be possible to more precisely estimate the age of individuals in these terminal age cohorts. I argue that the results of this study can be used to accurately estimate the age of individuals up to 80 years old at death. However, the generated prediction intervals range from the lower limits to the upper limits of the sample (45-98 years) and there is still a substantially large amount of error in the 80-89 years and 90+ years age cohorts. The prediction intervals are necessarily large because they must incorporate values that are within two standard deviations. Additionally, part of the large prediction intervals and the increase in error range for individuals at the upper range of the sample may be due to the small relative sample sizes of the 80-89 (21) and 90+ (6) groups and/or the centering of the sample around the mean age of 68 years.

The GPAs generated interesting results. In general, they were consistent with previous studies showing a reduction in cortical bone throughout the diaphysis with the highest amount of variation occurring near the midshaft (Garn et al. 1968; Carlson, Armelagos, & Van Gerven 1976; Ruff & Hayes 1983; Feik et al. 2000; Lerebours et al. 2016).

The weak to moderate correlation seen throughout the linear regressions is stronger in females, is strongest near the midshaft, and weakest at 20% of total bone length from the distal end for the combined sample and both sexes separately. There are peak periods of bone loss indicated by the increase in the MV:BV relative to the increase in age from ca. 65 to 80 years as suggested by the fitted polynomial line in the LOESS regressions for averaged measures and the mean shapes and centroid sizes in the GPAs. Females showed a more consistent relationship between the MV:BV and age than males, and this relationship approached linearity. This indicates that males are experiencing bone loss at different rates and likely in different ways than females. The mean shapes generated by the GPAs are helpful in determining where along the diaphysis these changes are occurring. The linear regressions indicate that the relationship between the MV:BV and age is strongest around midshaft in both sexes and less reliable near the epiphyses. The GPAs show us that bone loss is occurring primarily around the midshaft in the posterior side in females and the medial side in males.

The differences in the correlations with age between males and females can be tied to sexual dimorphism. As previous studies have shown, taller individuals have thicker cortical bone and lose less cortical bone than shorter individuals (Garn, Rohmann, & Wagner 1967; Garn et al. 1968a & 1968b; Stein et l. 1998). Males are in general taller and more robust than females and therefore should have higher relative cortical bone thickness and lose less bone as they age. It is also known that post-menopausal females suffer from higher rates of osteoporosis than older males. While this usually only affects bone density, some studies have shown that this reduction in density is somewhat compensated for by increased resorption of the endosteal surface and deposition on the

subperiosteal surface of the bone (Cowin 1983; Cowin 2004). As this sample is looking exclusively at individuals over 50 years, it is likely that post-menopausal osteoporotic activity is contributing to some of the differences seen between males and females. Cultural norms regarding levels of physical activity for males and females may also be affecting the MV:BV ratio and shape of the femur.

The LOESS regression for averaged measures shows there is a roughly non-linear relationship between MV:BV and age until after ca. 70 years. It may not be a coincidence that the ratio increases the most during this life stage in males because it is consistent with the average age of retirement (66 years old) in the United States (Newport 2018). Males are likely retiring from their jobs and partaking in a less physically rigorous lifestyle at these ages, and because activity-based bone remodeling happens over a relatively long period of times (years) it makes sense that the ratio begins to increase faster around the age of 70 which would be around when bony responses to a change in physical activity would occur (Tollison & Kreigel 1990; Weiping, Bauman, & Cardozo 2010). However, this potential explanation has its fair share of issues. It does not account for occupations that are not physically strenuous, such as office work, or consider activities that individuals may partake in after retirement. The 70-79 years age cohort has the highest amount of variation in shape based on the rho scores from the GPA for males and the lowest cortical bone area. This age cohort also has over double the amount of variation as any other age cohort regardless of sex indicating that there are significant changes in bone shape occurring from 70-79 years in males and that there may be some drastic changes in cortical bone area during this period. Incorporation of other variables

based on demographic information will be useful in future analyses to parse out what factors other than age are potentially causing these variations in shape.

The difference between cortical bone area in the four anatomical planes could be due to differential loading patterns. There are higher rates of compressive stress in the posterior and medial sides of the femur which may be causing higher rates of cortical bone retention in these areas in both males and females (Cowin 1983; Ruff & Hayes 1983; Brock & Ruff 1988; Feik et al. 2000; Mays 2015; Lerebours et al. 2016). The anterior side of the femur has the most uniform pattern of cortical bone remodeling as individuals age in both sexes. This reinforces the results of the linear regressions that the highest levels of correlation are seen in the A-P and M-L measures at midshaft. This pattern of remodeling could be due to the higher levels of tensional stress along this surface. However, these areas were also subject to varying levels and types of stress depending upon what types of activities in which the individual was regularly participating.

Some of the variation seen in the sum of squares scores (GSS) is likely caused by portions of the subtrochanteric area and the flaring of the distal end of the femur near the epiphyses being captured in the digital radiographs.

The remainder of the variation in the MV:BV at the cross sections of the diaphysis observed can most likely be attributed to a variety of confounding factors including stature, body mass, physical activity level, day to day activities, and genetics. Self-reported demographic data for the donated skeletal collection is available for a portion of the individuals and can be included in further multivariate tests to parse out how much residual variation can be attributed to these factors. However, since this data is

self-reported there are inconsistencies with how variables such as socio-economic status and physical activity levels are recorded or possibly may not have been recorded in some of the earlier donations.

Body mass is likely playing a role in the residual variation in the MV:BV. Larger individuals must compensate for increases in biomechanical loading forces or risk fracture. Previous studies have shown that body mass and increased bone dimensions are correlated (Ruff, Scott, & Liu 1991; Chevalier et al. 2018; Pomeroy et al. 2018). BMI (body mass index) and cadaveric body mass data are available for the donated collection and should be included in further studies involving this sample, a cursory look at the sample used in this study shows that the majority of individuals from 50 to 79 years have a BMI in the range of overweight, individuals over 80 years have lower BMIs, and individuals at 90+ have the lowest BMIs. Physical activity is also positively correlated with bone dimensions but without demographic data it may be impossible to tell from single elements whether an increase in size is due to higher body mass or higher levels of physical activity.

As discussed previously, smoking and drinking habits influence bone density (Hollenbach et al. 1993: Jin Kim et al. 2003; Hae Dong et al. 2017). A hidden impact on bone dimensions caused by smoking and drinking is their subsequent effect on daily activities. Heavy smokers and drinkers likely have lower levels of physical activity and lower levels of overall nutrition.

There is also the fact that the MV:BV can only get so high before the bone becomes structurally unsound and breaks. In other words, the cortical area of the bone likely reaches a critical mass where any additional bone loss would result in fracture. The

expansion of the diameter of the bone does not need to equal the amount of bone lost on the endosteal surface but, as is seen in the GPAs in the 80-89 and 90+ years age cohorts for both females and males, the rate of endosteal bone loss and appositional growth appears to equalize. However, these are also the age cohorts with the lowest number of individuals. The results of this and previous studies suggest that there are likely peak and valley periods of bone remodeling throughout an individual's life (Smith & Walker 1964; Feik et al.1997). The 90+ age cohort may be experiencing one of lulls in remodeling activity. There is also the possibility that bone remodeling processes mirror those of other biological processes, breaking down and losing efficiency as individuals progress to the older age cohorts.

The results of this study can be applied in both forensic and bioarchaeological contexts. In either forensic or archaeological settings, finding a complete skeleton is rare. Various taphonomic factors influence the completeness and condition of the remains. There may only be a handful of skeletal elements remaining and/or these elements could be fragmentary. The method presented in this thesis only requires the diaphysis of the femur and is non-destructive.

Forensically, this age estimation method can be applied as a secondary age estimation technique for females when an individual is confidently sexed as female and aged as older than 50 years by other aging methods such as pelvic indictors. It can also be used for males and individuals classified as indeterminate sex, but the age prediction should be looked at more critically in analyses of these individuals. This method can accurately age an individual in 10 year ranges up until 80+ years which is an improvement over macroscopic methods. The estimated age should be interpreted as a

highest likelihood age and the prediction interval should be used as the range of potential ages. The ability to accurately age individuals is vital when compiling a biological profile for an unidentified individual and reducing the potential missing persons pool to individuals in age cohorts of 50-59, 60-69, 70-79, and 80+ years improves the chances of a positive identification. Using radiographs allows other analyses to be conducted at the same time without needing physical access to the remains.

Bioarcheaologically, this age estimation method has several potential applications. In large samples, an accurate representation of the demography of past populations is possible. Average age-at-death in a population can be estimated more accurately and to some degree with more ease than with this method than previous ones. To some extent, the MV:BV and bone shape can also be used to estimate the biomechanical forces that acted upon past individuals. The benefits of this age estimation method over others are mainly that this method can be used with fragmentary material and that it is non-destructive. The femoral diaphysis usually preserves well and even if only a section of the diaphysis is present age can still be estimated. Archaeological material also may be subject to specific regulations (NAGPRA). As this is a non-destructive and non-invasive method, the ability to estimate the age of remains that have been culturally attributed is increased.

Generally, the results of the regression tests, prediction intervals, and Procrustes analysis agree and support the hypotheses presented in the introduction. There appears to be a consistent rate of cortical bone loss from 50 to around 80 years followed by sporadic periods of variable bone loss at different sites along the midshaft and proximal diaphysis. At 20% total length from the distal end, in both the anterior-posterior and medio-lateral

planes, the MV:BV was consistent throughout the aging process and showed little to no variation in shape.

VI. CONCLUSIONS

The results of this study show that there is a weak to moderate correlation with the MV:BV (medullary cavity volume: total bone volume ratio) and age in individuals over 50 years. This correlation is significantly stronger in women and has the highest correlation with age in the MV:BV measures at midshaft. The results also indicate that there are areas of the femoral diaphysis that are subject to higher rates of remodeling than others and that some of the resulting changes in shaft shape can be attributed to the aging process. In both the antero-posterior and medio-lateral planes the highest levels of resorption can be seen at and around the midshaft of the diaphysis. There is little variability at the distal end and an intermediate level of variability at the proximal end.

The findings of this study are consistent with previous research and show that a non-invasive method can be used to accurately estimate age in individuals up to 80 years. The prediction intervals do show higher errors with the older age cohorts, but within this sample it is possible to estimate age within a 10-year error through the 70-79 years age cohort. Inclusion of more individuals in the upper age ranges, and potentially individuals below 50 years, would help determine the full extent of how accurate this method is. I would expect the inclusion of younger individuals to reduce the accuracy somewhat because non-pathological bone loss does not begin until towards the end of the 4th decade of life (Stein et al. 1998). Individuals younger than 34 may reduce the level of correlation and be misclassified as older individuals based on the higher MV:BV and smaller bone dimensions. An evenly age distributed sample would be able to show the full extent of the changes in the MV:BV and diaphyseal shape with age. While the scans in this study were taken using a micro-CT system, any digital radiograph system can be used. The

results also show that if certain sections of the bone are missing i.e. the epiphyses or even portions of the shaft an age estimation can be made. However, it is always preferred to use multiple methods to estimate aspects of the biological profile.

It is possible, and would be greatly beneficial, to extend this study further by incorporating other variables that affect the measures and shape of the femur and to apply this method to other populations. Future studies incorporating stature, body mass, and occupation can be conducted on the data gathered from this population by incorporating self-reported demographic data from the donation paperwork that accompanies the individuals upon their admission into the body donation program through the Forensic Anthropology Center and Texas State University.

There is also the potential to extend this method for use in a longitudinal study. This non-invasive, non-destructive technique can be used on living individuals to analyze how cortical bone area and bone shape change throughout an individual's life in response to age as well as a variety of other factors.

This study is limited to a majority American white sample and therefore it is not appropriate to apply these findings to other populations without first testing the applicability of the method. There may be variation between regional populations and social classes that contributes to differences in femur measures and shape. It would also be beneficial to use an evenly sex distributed sample or look exclusively at one of the sexes.

APPENDIX SECTION

Section 1. *JMP Shapiro-Wilkes Test for Normalcy*

Distributions
Age-years

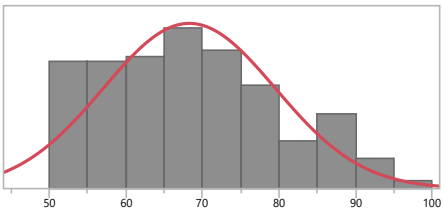

Normal (68.2866,11.2478)

Summary Statistics

Mean	68.286585
Std Dev	11.247776
Std Err Mean	0.8783037
Upper 95% Mean	70.020906
Lower 95% Mean	66.552265
N	164

Fitted Normal
Parameter Estimates

Type	Parameter	Estimate	Lower 95%	Upper 95%
Location	μ	68.286585	66.552265	70.020906
Dispersion	σ	11.247776	10.148038	12.616945

Measure	
-2*LogLikelihood	1258.2277
AICc	1262.3023
BIC	1268.4275

Goodness-of-Fit Test

Shapiro-Wilk W Test

W	Prob<W
0.963555	0.0003*

Note: Ho = The data is from the Normal distribution. Small p-values reject Ho.

Section 2. *JMP Linear Regressions for Averaged Measures*

Linear regressions for averaged measures, A-P and M-L measures, and summed measures are presented below. α=0.95 for confidence (curved line) and prediction (straight line) intervals.

Section 2a. With Outliers

Bivariate Fit of Age_yrs By Avg_Ratio_75 Sex=F

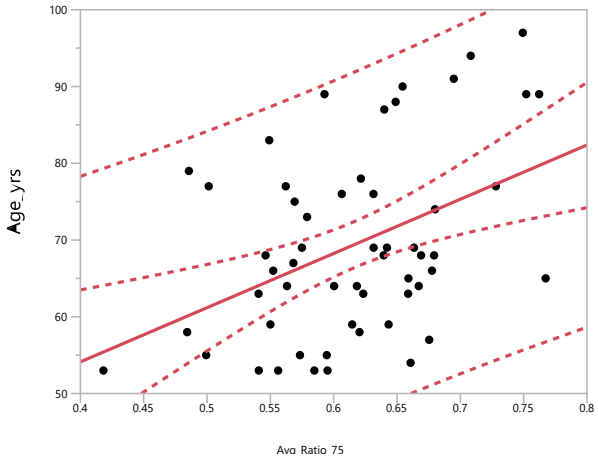

Linear Fit

Summary Statistics

	Value	Lower 95%	Upper 95%	Signif. Prob
Correlation	0.427463	0.182909	0.6222	0.0011*
Covariance	0.383276			
Count	55			

Variable	Mean	Std Dev
Avg_Ratio_75	0.615802	0.073662
Age_yrs	69.36364	12.17217

Linear Fit

Age_yrs = 25.866314 + 70.635291*Avg_Ratio_75

Summary of Fit

RSquare	0.182725
RSquare Adj	0.167305
Root Mean Square Error	11.10736
Mean of Response	69.36364
Observations (or Sum Wgts)	55

Analysis of Variance

Source	DF	Sum of Squares	Mean Square	F Ratio
Model	1	1461.9332	1461.93	11.8497
Error	53	6538.7941	123.37	Prob > F
C. Total	54	8000.7273		0.0011*

Parameter Estimates

Term	Estimate	Std Error	t Ratio	Prob>|t|
Intercept	25.866314	12.72445	2.03	0.0471*
Avg_Ratio_75	70.635291	20.5196	3.44	0.0011*

Section 2a cont.

Bivariate Fit of Age_yrs By Avg_Ratio_Mid Sex=F

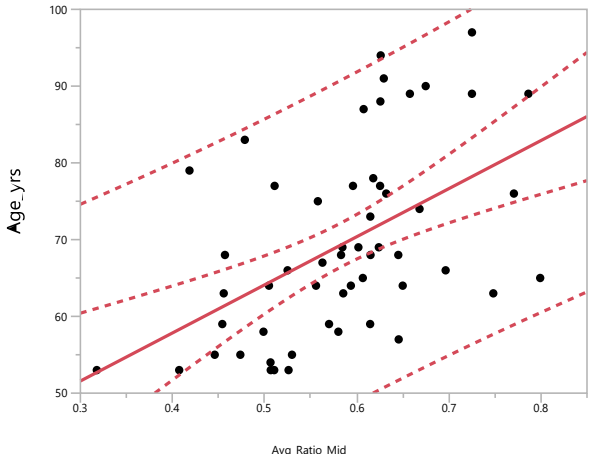

Summary Statistics

	Value	Lower 95%	Upper 95%	Signif. Prob
Correlation	0.505488	0.27739	0.679642	<.0001*
Covariance	0.604192			
Count	55			

Variable	Mean	Std Dev
Avg_Ratio_Mid	0.583877	0.098197
Age_yrs	69.36364	12.17217

Linear Fit

Age_yrs = 32.778611 + 62.658759*Avg_Ratio_Mid

Summary of Fit

RSquare	0.255518
RSquare Adj	0.241471
Root Mean Square Error	10.60117
Mean of Response	69.36364
Observations (or Sum Wgts)	55

Analysis of Variance

Source	DF	Sum of Squares	Mean Square	F Ratio
Model	1	2044.3286	2044.33	18.1904
Error	53	5956.3987	112.38	Prob > F
C. Total	54	8000.7273		<.0001*

Parameter Estimates

Term	Estimate	Std Error	t Ratio	Prob>|t|
Intercept	32.778611	8.696209	3.77	0.0004*
Avg_Ratio_Mid	62.658759	14.69131	4.27	<.0001*

Section 2a cont.

Bivariate Fit of Age_yrs By Avg_Ratio_20 Sex=F

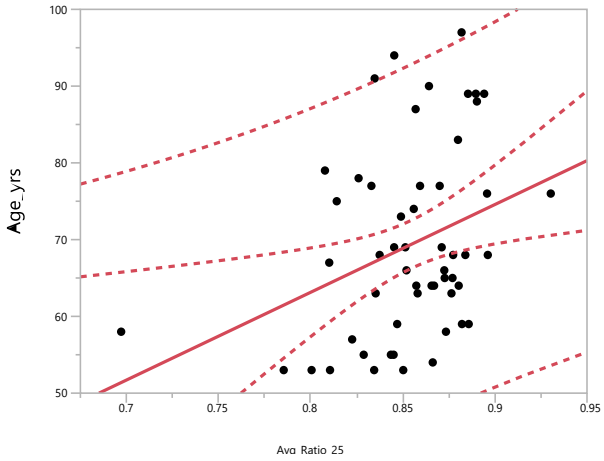

Summary Statistics

	Value	Lower 95%	Upper 95%	Signif. Prob
Correlation	0.333067	0.074339	0.549784	0.0130*
Covariance	0.143756			
Count	55			

Variable	Mean	Std Dev
Avg_Ratio_25	0.854458	0.035459
Age_yrs	69.36364	12.17217

Linear Fit

Age_yrs = -28.32959 + 114.33359*Avg_Ratio_25

Summary of Fit

RSquare	0.110934
RSquare Adj	0.094159
Root Mean Square Error	11.58494
Mean of Response	69.36364
Observations (or Sum Wgts)	55

Analysis of Variance

Source	DF	Sum of Squares	Mean Square	F Ratio
Model	1	887.5504	887.550	6.6131
Error	53	7113.1769	134.211	Prob > F
C. Total	54	8000.7273		0.0130*

Parameter Estimates

Term	Estimate	Std Error	t Ratio	Prob>|t|
Intercept	-28.32959	38.02145	-0.75	0.4595
Avg_Ratio_25	114.33359	44.46018	2.57	0.0130*

Section 2a cont.

Bivariate Fit of Age_yrs By Avg_Ratio_All Sex=F

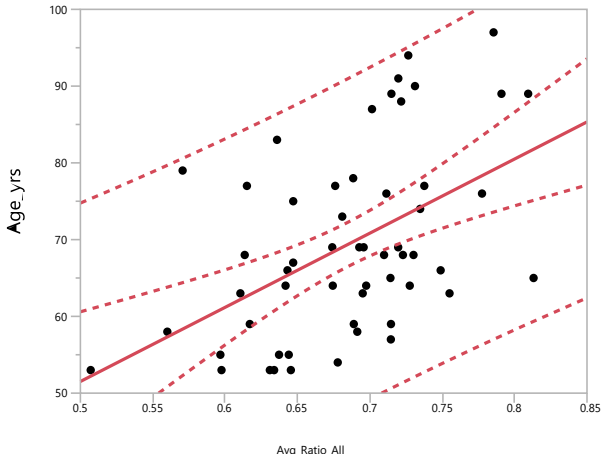

Linear Fit

Summary Statistics

	Value	Lower 95%	Upper 95%	Signif. Prob
Correlation	0.49589	0.265525	0.67269	0.0001*
Covariance	0.377075			
Count	55			

Variable	Mean	Std Dev
Avg_Ratio_All	0.684712	0.06247
Age_yrs	69.36364	12.17217

Linear Fit

Age_yrs = 3.2048842 + 96.622714*Avg_Ratio_All

Summary of Fit

RSquare	0.245907
RSquare Adj	0.231679
Root Mean Square Error	10.66938
Mean of Response	69.36364
Observations (or Sum Wgts)	55

Analysis of Variance

Source	DF	Sum of Squares	Mean Square	F Ratio
Model	1	1967.4355	1967.44	17.2831
Error	53	6033.2918	113.84	Prob > F
C. Total	54	8000.7273		0.0001*

Parameter Estimates

Term	Estimate	Std Error	t Ratio	Prob>|t|
Intercept	3.2048842	15.97878	0.20	0.8418
Avg_Ratio_All	96.622714	23.24172	4.16	0.0001*

Section 2a cont.

Bivariate Fit of Age_yrs By Avg_Ratio_75 Sex=M

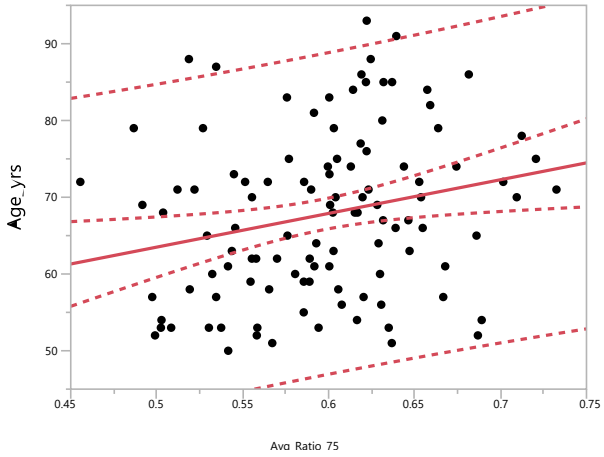

Summary Statistics

	Value	Lower 95%	Upper 95%	Signif. Prob
Correlation	0.233384	0.047362	0.403761	0.0146*
Covariance	0.143862			
Count	109			

Variable	Mean	Std Dev
Avg_Ratio_75	0.596627	0.05724
Age_yrs	67.74312	10.76896

Linear Fit

Age_yrs = 41.546506 + 43.907882*Avg_Ratio_75

Summary of Fit

RSquare	0.054468
RSquare Adj	0.045631
Root Mean Square Error	10.52039
Mean of Response	67.74312
Observations (or Sum Wgts)	109

Analysis of Variance

Source	DF	Sum of Squares	Mean Square	F Ratio
Model	1	682.203	682.203	6.1638
Error	107	11842.604	110.679	Prob > F
C. Total	108	12524.807		0.0146*

Parameter Estimates

Term	Estimate	Std Error	t Ratio	Prob>|t|
Intercept	41.546506	10.59965	3.92	0.0002*
Avg_Ratio_75	43.907882	17.6855	2.48	0.0146*

Section 2a cont.

Bivariate Fit of Age_yrs By Avg_Ratio_Mid Sex=M

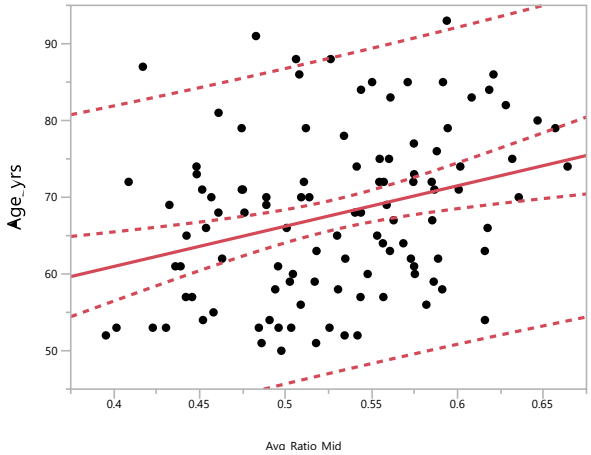

Summary Statistics

	Value	Lower 95%	Upper 95%	Signif. Prob
Correlation	0.304336	0.123292	0.465774	0.0013*
Covariance	0.204255			
Count	109			

Variable	Mean	Std Dev
Avg_Ratio_Mid	0.528677	0.062323
Age_yrs	67.74312	10.76896

Linear Fit

Age_yrs = 39.941397 + 52.587312*Avg_Ratio_Mid

Summary of Fit

RSquare	0.09262
RSquare Adj	0.08414
Root Mean Square Error	10.30595
Mean of Response	67.74312
Observations (or Sum Wgts)	109

Analysis of Variance

Source	DF	Sum of Squares	Mean Square	F Ratio
Model	1	1160.051	1160.05	10.9220
Error	107	11364.756	106.21	Prob > F
C. Total	108	12524.807		0.0013*

Parameter Estimates

Term	Estimate	Std Error	t Ratio	Prob>|t|
Intercept	39.941397	8.470145	4.72	<.0001*
Avg_Ratio_Mid	52.587312	15.91221	3.30	0.0013*

Section 2a cont.

Bivariate Fit of Age_yrs By Avg_Ratio_20 Sex=M

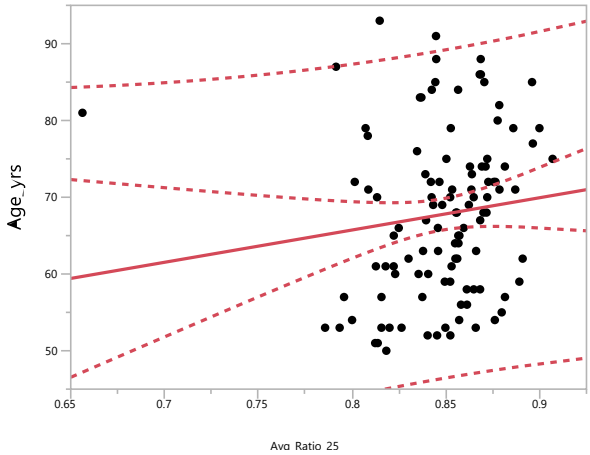

Summary Statistics

	Value	Lower 95%	Upper 95%	Signif. Prob
Correlation	0.124435	-0.06519	0.305388	0.1973
Covariance	0.042695			
Count	109			

Variable	Mean	Std Dev
Avg_Ratio_25	0.847864	0.031861
Age_yrs	67.74312	10.76896

Linear Fit

Age_yrs = 32.083071 + 42.058684*Avg_Ratio_25

Summary of Fit

RSquare	0.015484
RSquare Adj	0.006283
Root Mean Square Error	10.73507
Mean of Response	67.74312
Observations (or Sum Wgts)	109

Analysis of Variance

Source	DF	Sum of Squares	Mean Square	F Ratio
Model	1	193.934	193.934	1.6828
Error	107	12330.874	115.242	Prob > F
C. Total	108	12524.807		0.1973

Parameter Estimates

Term	Estimate	Std Error	t Ratio	Prob>|t|
Intercept	32.083071	27.50832	1.17	0.2461
Avg_Ratio_25	42.058684	32.42158	1.30	0.1973

Section 2a cont.

Bivariate Fit of Age_yrs By Avg_Ratio_All Sex=M

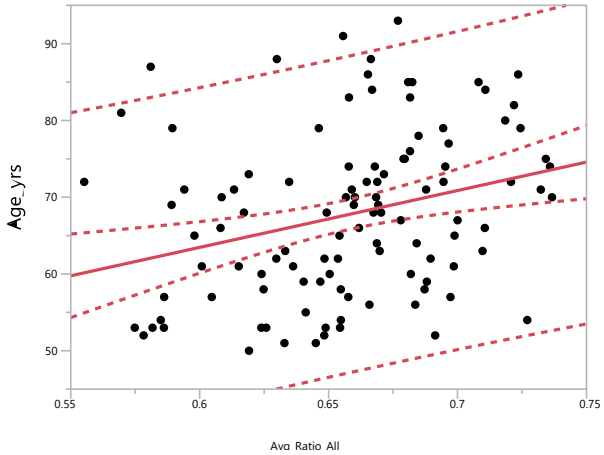

Summary Statistics

	Value	Lower 95%	Upper 95%	Signif. Prob
Correlation	0.28845	0.106106	0.452026	0.0024*
Covariance	0.130271			
Count	109			

Variable	Mean	Std Dev
Avg_Ratio_All	0.657723	0.041937
Age_yrs	67.74312	10.76896

Linear Fit

Age_yrs = 19.025546 + 74.070079*Avg_Ratio_All

Summary of Fit

RSquare	0.083204
RSquare Adj	0.074635
Root Mean Square Error	10.35929
Mean of Response	67.74312
Observations (or Sum Wgts)	109

Analysis of Variance

Source	DF	Sum of Squares	Mean Square	F Ratio
Model	1	1042.109	1042.11	9.7108
Error	107	11482.698	107.31	Prob > F
C. Total	108	12524.807		0.0024*

Parameter Estimates

Term	Estimate	Std Error	t Ratio	Prob>|t|
Intercept	19.025546	15.66506	1.21	0.2272
Avg_Ratio_All	74.070079	23.76929	3.12	0.0024*

Section 2b. Without Outliers

Bivariate Fit of Age_yrs By Avg_Ratio_75 Sex=F

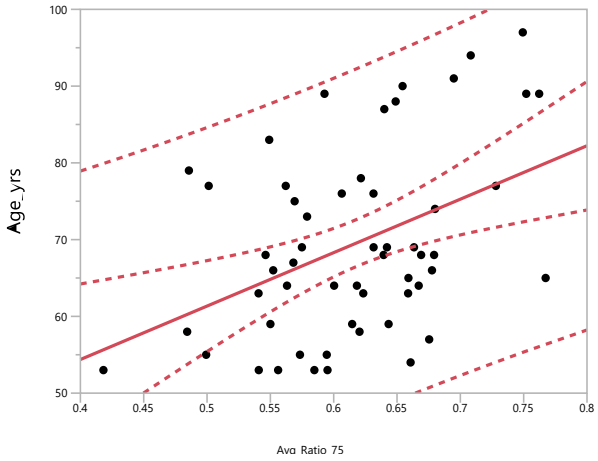

Linear Fit

Summary Statistics

	Value	Lower 95%	Upper 95%	Signif. Prob
Correlation	0.411896	0.162003	0.612144	0.0020*
Covariance	0.361792			
Count	54			

Variable	Mean	Std Dev
Avg_Ratio_75	0.618237	0.072085
Age_yrs	69.57407	12.18505

Linear Fit

Age_yrs = 26.528752 + 69.625963*Avg_Ratio_75

Summary of Fit

RSquare	0.169659
RSquare Adj	0.15369
Root Mean Square Error	11.20965
Mean of Response	69.57407
Observations (or Sum Wgts)	54

Analysis of Variance

Source	DF	Sum of Squares	Mean Square	F Ratio
Model	1	1335.0776	1335.08	10.6248
Error	52	6534.1261	125.66	Prob > F
C. Total	53	7869.2037		0.0020*

Parameter Estimates

Term	Estimate	Std Error	t Ratio	Prob>|t|
Intercept	26.528752	13.29361	2.00	0.0512
Avg_Ratio_75	69.625963	21.36043	3.26	0.0020*

Section 2b cont.

Bivariate Fit of Age_yrs By Avg_Ratio_Mid Sex=F

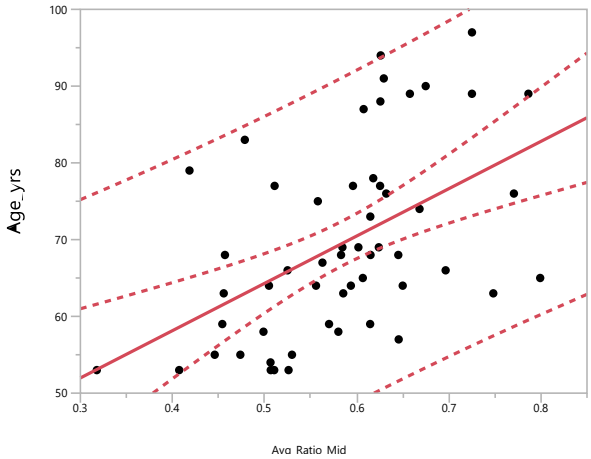

Summary Statistics

	Value	Lower 95%	Upper 95%	Signif. Prob
Correlation	0.497844	0.265471	0.675551	0.0001*
Covariance	0.597002			
Count	54			

Variable	Mean	Std Dev
Avg_Ratio_Mid	0.585454	0.098414
Age_yrs	69.57407	12.18505

Linear Fit

Age_yrs = 33.486533 + 61.640301*Avg_Ratio_Mid

Summary of Fit

RSquare	0.247848
RSquare Adj	0.233384
Root Mean Square Error	10.66882
Mean of Response	69.57407
Observations (or Sum Wgts)	54

Analysis of Variance

Source	DF	Sum of Squares	Mean Square	F Ratio
Model	1	1950.3682	1950.37	17.1350
Error	52	5918.8355	113.82	Prob > F
C. Total	53	7869.2037		0.0001*

Parameter Estimates

Term	Estimate	Std Error	t Ratio	Prob>|t|
Intercept	33.486533	8.838036	3.79	0.0004*
Avg_Ratio_Mid	61.640301	14.89097	4.14	0.0001*

Section 2b cont.

Bivariate Fit of Age_yrs By Avg_Ratio_20 Sex=F

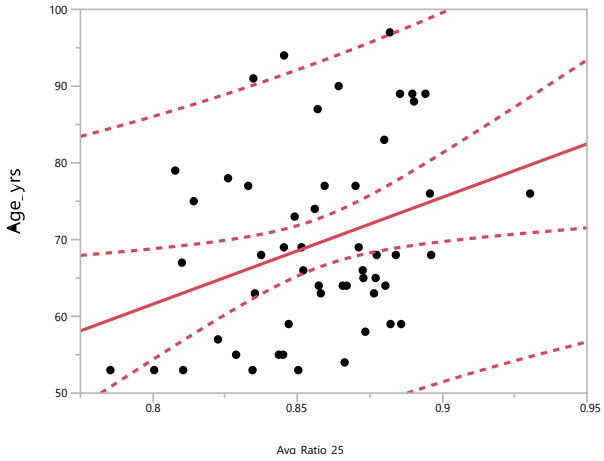

Summary Statistics

	Value	Lower 95%	Upper 95%	Signif. Prob
Correlation	0.324204	0.061809	0.544681	0.0168*
Covariance	0.112111			
Count	54			

Variable	Mean	Std Dev
Avg_Ratio_25	0.857371	0.028379
Age_yrs	69.57407	12.18505

Linear Fit

Age_yrs = -49.77278 + 139.2009*Avg_Ratio_25

Summary of Fit

RSquare	0.105108
RSquare Adj	0.087899
Root Mean Square Error	11.63721
Mean of Response	69.57407
Observations (or Sum Wgts)	54

Analysis of Variance

Source	DF	Sum of Squares	Mean Square	F Ratio
Model	1	827.1161	827.116	6.1076
Error	52	7042.0876	135.425	Prob > F
C. Total	53	7869.2037		0.0168*

Parameter Estimates

Term	Estimate	Std Error	t Ratio	Prob>|t|
Intercept	-49.77278	48.31813	-1.03	0.3077
Avg_Ratio_25	139.2009	56.32586	2.47	0.0168*

Section 2b cont.

Bivariate Fit of Age_yrs By Avg_Ratio_All Sex=F

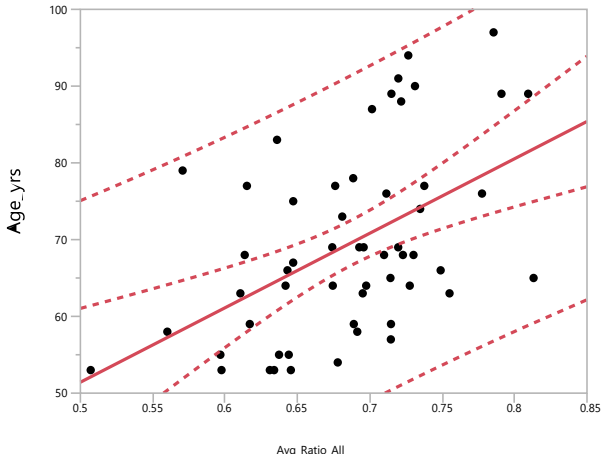

Linear Fit

Summary Statistics

	Value	Lower 95%	Upper 95%	Signif. Prob
Correlation	0.483082	0.247311	0.664845	0.0002*
Covariance	0.356969			
Count	54			

Variable	Mean	Std Dev
Avg_Ratio_All	0.687021	0.060643
Age_yrs	69.57407	12.18505

Linear Fit

Age_yrs = 2.8878288 + 97.065868*Avg_Ratio_All

Summary of Fit

RSquare	0.233368
RSquare Adj	0.218625
Root Mean Square Error	10.77103
Mean of Response	69.57407
Observations (or Sum Wgts)	54

Analysis of Variance

Source	DF	Sum of Squares	Mean Square	F Ratio
Model	1	1836.4217	1836.42	15.8292
Error	52	6032.7820	116.02	Prob > F
C. Total	53	7869.2037		0.0002*

Parameter Estimates

Term	Estimate	Std Error	t Ratio	Prob>|t|
Intercept	2.8878288	16.82525	0.17	0.8644
Avg_Ratio_All	97.065868	24.39706	3.98	0.0002*

Section 2b cont.

Bivariate Fit of Age_yrs By Avg_Ratio_75 Sex=M

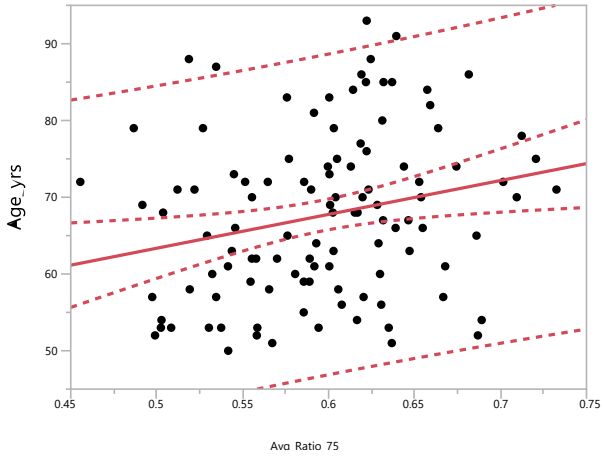

Summary Statistics

	Value	Lower 95%	Upper 95%	Signif. Prob
Correlation	0.236104	0.049331	0.406922	0.0139*
Covariance	0.14585			
Count	108			

Variable	Mean	Std Dev
Avg_Ratio_75	0.596674	0.057505
Age_yrs	67.62037	10.74228

Linear Fit

Age_yrs = 41.303728 + 44.105544*Avg_Ratio_75

Summary of Fit

RSquare	0.055745
RSquare Adj	0.046837
Root Mean Square Error	10.4877
Mean of Response	67.62037
Observations (or Sum Wgts)	108

Analysis of Variance

Source	DF	Sum of Squares	Mean Square	F Ratio
Model	1	688.307	688.307	6.2578
Error	106	11659.128	109.992	Prob > F
C. Total	107	12347.435		0.0139*

Parameter Estimates

Term	Estimate	Std Error	t Ratio	Prob>|t|
Intercept	41.303728	10.56838	3.91	0.0002*
Avg_Ratio_75	44.105544	17.63121	2.50	0.0139*

Section 2b cont.

Bivariate Fit of Age_yrs By Avg_Ratio_Mid Sex=M

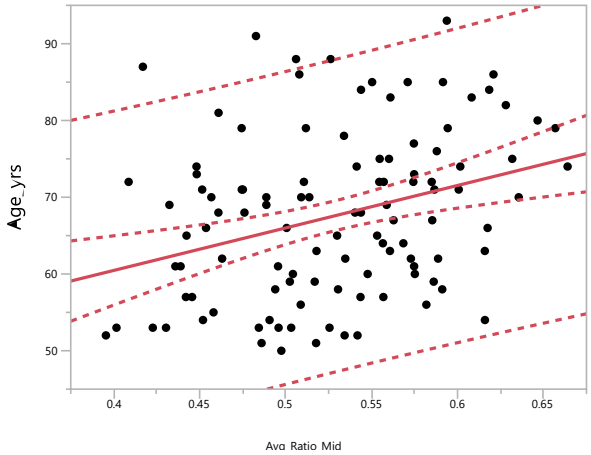

Summary Statistics

	Value	Lower 95%	Upper 95%	Signif. Prob
Correlation	0.320874	0.140414	0.480699	0.0007*
Covariance	0.214629			
Count	108			

Variable	Mean	Std Dev
Avg_Ratio_Mid	0.529304	0.062267
Age_yrs	67.62037	10.74228

Linear Fit

Age_yrs = 38.319692 + 55.356972*Avg_Ratio_Mid

Summary of Fit

RSquare	0.10296
RSquare Adj	0.094497
Root Mean Square Error	10.22213
Mean of Response	67.62037
Observations (or Sum Wgts)	108

Analysis of Variance

Source	DF	Sum of Squares	Mean Square	F Ratio
Model	1	1271.290	1271.29	12.1664
Error	106	11076.146	104.49	Prob > F
C. Total	107	12347.435		0.0007*

Parameter Estimates

Term	Estimate	Std Error	t Ratio	Prob>|t|
Intercept	38.319692	8.457731	4.53	<.0001*
Avg_Ratio_Mid	55.356972	15.87053	3.49	0.0007*

Section 2b cont.

Bivariate Fit of Age_yrs By Avg_Ratio_20 Sex=M

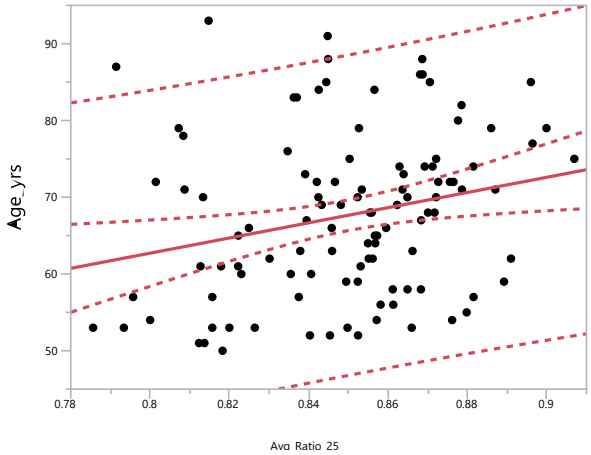

Summary Statistics

	Value	Lower 95%	Upper 95%	Signif. Prob
Correlation	0.239676	0.053108	0.410077	0.0125*
Covariance	0.067054			
Count	108			

Variable	Mean	Std Dev
Avg_Ratio_25	0.849638	0.026044
Age_yrs	67.62037	10.74228

Linear Fit

Age_yrs = -16.37422 + 98.859227*Avg_Ratio_25

Summary of Fit

RSquare	0.057445
RSquare Adj	0.048553
Root Mean Square Error	10.47825
Mean of Response	67.62037
Observations (or Sum Wgts)	108

Analysis of Variance

Source	DF	Sum of Squares	Mean Square	F Ratio
Model	1	709.295	709.295	6.4602
Error	106	11638.141	109.794	Prob > F
C. Total	107	12347.435		0.0125*

Parameter Estimates

Term	Estimate	Std Error	t Ratio	Prob>|t|
Intercept	-16.37422	33.06198	-0.50	0.6214
Avg_Ratio_25	98.859227	38.89491	2.54	0.0125*

Section 2b cont.

Bivariate Fit of Age_yrs By Avg_Ratio_All Sex=M

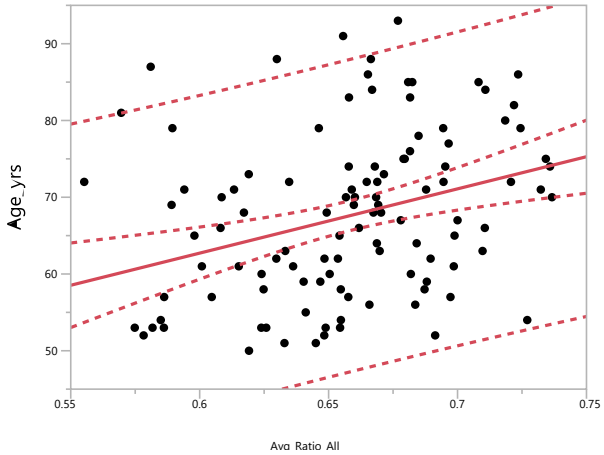

Summary Statistics

	Value	Lower 95%	Upper 95%	Signif. Prob
Correlation	0.321578	0.141184	0.481303	0.0007*
Covariance	0.142511			
Count	108			

Variable	Mean	Std Dev
Avg_Ratio_All	0.658539	0.041254
Age_yrs	67.62037	10.74228

Linear Fit

Age_yrs = 12.476372 + 83.736884*Avg_Ratio_All

Summary of Fit

RSquare	0.103412
RSquare Adj	0.094954
Root Mean Square Error	10.21955
Mean of Response	67.62037
Observations (or Sum Wgts)	108

Analysis of Variance

Source	DF	Sum of Squares	Mean Square	F Ratio
Model	1	1276.876	1276.88	12.2260
Error	106	11070.559	104.44	Prob > F
C. Total	107	12347.435		0.0007*

Parameter Estimates

Term	Estimate	Std Error	t Ratio	Prob>|t|
Intercept	12.476372	15.8015	0.79	0.4315
Avg_Ratio_All	83.736884	23.94828	3.50	0.0007*

Section 3. *JMP Linear Regressions for All Measures Separately*

Section 3a. With Outliers.

Bivariate Fit of Age_yrs By APRatio_75 Sex=F

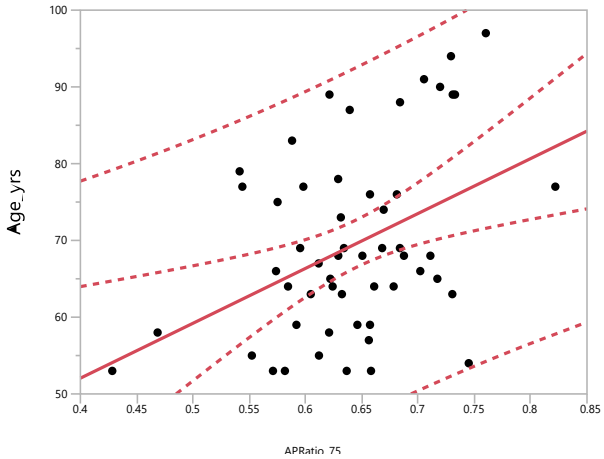

Linear Fit

Summary Statistics

	Value	Lower 95%	Upper 95%	Signif. Prob
Correlation	0.389748	0.136201	0.595375	0.0036*
Covariance	0.315288			
Count	54			

Variable	Mean	Std Dev
APRatio_75	0.644965	0.066389
Age_yrs	69.57407	12.18505

Linear Fit

Age_yrs = 23.436985 + 71.534251*APRatio_75

Summary of Fit

RSquare	0.151903
RSquare Adj	0.135594
Root Mean Square Error	11.32887
Mean of Response	69.57407
Observations (or Sum Wgts)	54

Analysis of Variance

Source	DF	Sum of Squares	Mean Square	F Ratio
Model	1	1195.3576	1195.36	9.3138
Error	52	6673.8461	128.34	Prob > F
C. Total	53	7869.2037		0.0036*

Parameter Estimates

Term	Estimate	Std Error	t Ratio	Prob>|t|
Intercept	23.436985	15.19617	1.54	0.1291
APRatio_75	71.534251	23.43967	3.05	0.0036*

Section 3a cont.

Bivariate Fit of Age_yrs By MLRatio_75 Sex=F

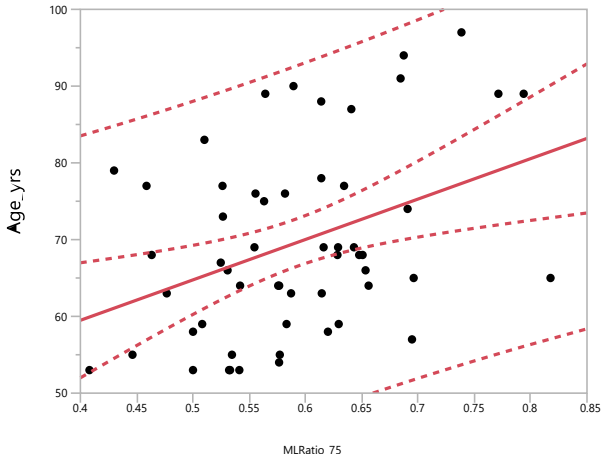

Linear Fit

Summary Statistics

	Value	Lower 95%	Upper 95%	Signif. Prob
Correlation	0.380544	0.125579	0.588354	0.0045*
Covariance	0.408296			
Count	54			

Variable	Mean	Std Dev
MLRatio_75	0.591508	0.088053
Age_yrs	69.57407	12.18505

Linear Fit

Age_yrs = 38.424722 + 52.660889*MLRatio_75

Summary of Fit

RSquare	0.144813
RSquare Adj	0.128368
Root Mean Square Error	11.37612
Mean of Response	69.57407
Observations (or Sum Wgts)	54

Analysis of Variance

Source	DF	Sum of Squares	Mean Square	F Ratio
Model	1	1139.5663	1139.57	8.8054
Error	52	6729.6374	129.42	Prob > F
C. Total	53	7869.2037		0.0045*

Parameter Estimates

Term	Estimate	Std Error	t Ratio	Prob>|t|
Intercept	38.424722	10.61074	3.62	0.0007*
MLRatio_75	52.660889	17.74649	2.97	0.0045*

Section 3a cont.

Bivariate Fit of Age_yrs By APRatio_Mid Sex=F

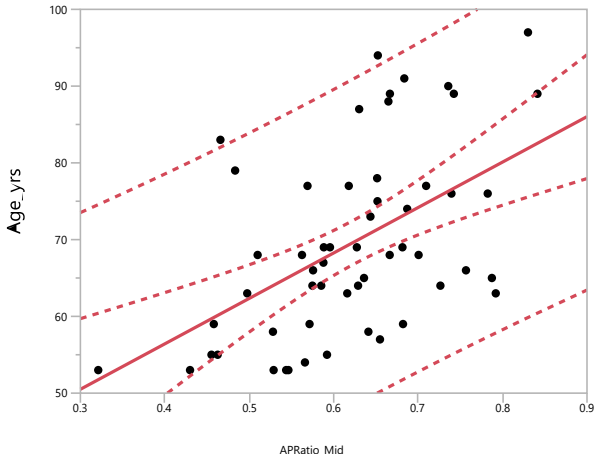

Summary Statistics

	Value	Lower 95%	Upper 95%	Signif. Prob
Correlation	0.519016	0.291809	0.690778	<.0001*
Covariance	0.67558			
Count	54			

Variable	Mean	Std Dev
APRatio_Mid	0.622174	0.106824
Age_yrs	69.57407	12.18505

Linear Fit

Age_yrs = 32.739804 + 59.202551*APRatio_Mid

Summary of Fit

RSquare	0.269378
RSquare Adj	0.255328
Root Mean Square Error	10.51502
Mean of Response	69.57407
Observations (or Sum Wgts)	54

Analysis of Variance

Source	DF	Sum of Squares	Mean Square	F Ratio
Model	1	2119.7911	2119.79	19.1722
Error	52	5749.4126	110.57	Prob > F
C. Total	53	7869.2037		<.0001*

Parameter Estimates

Term	Estimate	Std Error	t Ratio	Prob>|t|
Intercept	32.739804	8.533146	3.84	0.0003*
APRatio_Mid	59.202551	13.52085	4.38	<.0001*

Section 3a cont.

Bivariate Fit of Age_yrs By MLRatio_Mid Sex=F

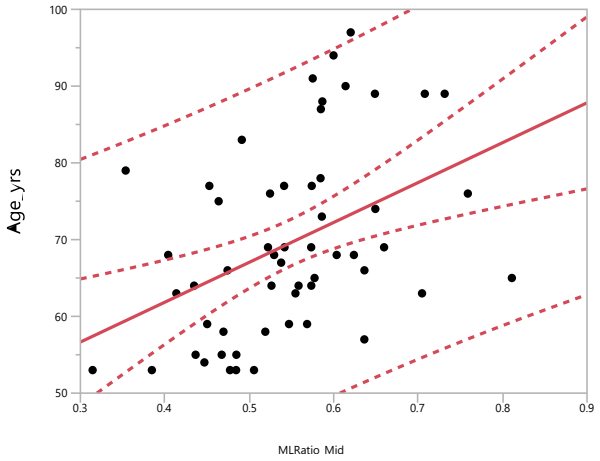

Summary Statistics

	Value	Lower 95%	Upper 95%	Signif. Prob
Correlation	0.42591	0.178506	0.622661	0.0013*
Covariance	0.518425			
Count	54			

Variable	Mean	Std Dev
MLRatio_Mid	0.548734	0.099894
Age_yrs	69.57407	12.18505

Linear Fit

Age_yrs = 41.066145 + 51.952215*MLRatio_Mid

Summary of Fit

RSquare	0.181399
RSquare Adj	0.165657
Root Mean Square Error	11.13012
Mean of Response	69.57407
Observations (or Sum Wgts)	54

Analysis of Variance

Source	DF	Sum of Squares	Mean Square	F Ratio
Model	1	1427.4652	1427.47	11.5230
Error	52	6441.7385	123.88	Prob > F
C. Total	53	7869.2037		0.0013*

Parameter Estimates

Term	Estimate	Std Error	t Ratio	Prob>|t|
Intercept	41.066145	8.533623	4.81	<.0001*
MLRatio_Mid	51.952215	15.30457	3.39	0.0013*

Section 3a cont.

Bivariate Fit of Age_yrs By APRatio_20 Sex=F

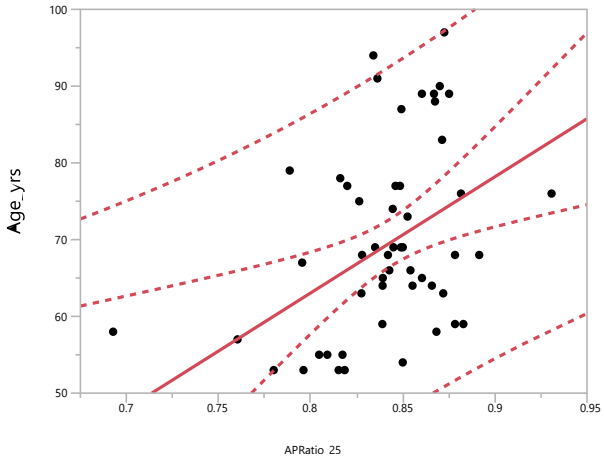

Summary Statistics

	Value	Lower 95%	Upper 95%	Signif. Prob
Correlation	0.385757	0.131589	0.592335	0.0040*
Covariance	0.146019			
Count	54			

Variable	Mean	Std Dev
APRatio_25	0.843095	0.031065
Age_yrs	69.57407	12.18505

Linear Fit

Age_yrs = -57.99642 + 151.31212*APRatio_20

Summary of Fit

RSquare	0.148809
RSquare Adj	0.13244
Root Mean Square Error	11.34952
Mean of Response	69.57407
Observations (or Sum Wgts)	54

Analysis of Variance

Source	DF	Sum of Squares	Mean Square	F Ratio
Model	1	1171.0054	1171.01	9.0908
Error	52	6698.1983	128.81	Prob > F
C. Total	53	7869.2037		0.0040*

Parameter Estimates

Term	Estimate	Std Error	t Ratio	Prob>|t|
Intercept	-57.99642	42.33867	-1.37	0.1766
APRatio_25	151.31212	50.18473	3.02	0.0040*

Section 3a cont.

Bivariate Fit of Age_yrs By MLRatio_20 Sex=F

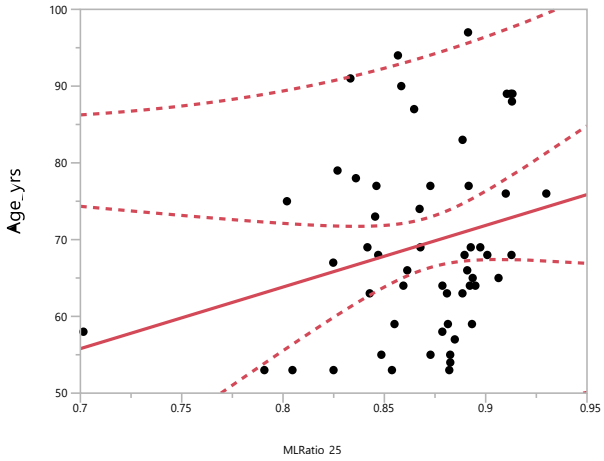

Summary Statistics

	Value	Lower 95%	Upper 95%	Signif. Prob
Correlation	0.205622	-0.06576	0.448679	0.1358
Covariance	0.078203			
Count	54			

Variable	Mean	Std Dev
MLRatio_25	0.871648	0.031212
Age_yrs	69.57407	12.18505

Linear Fit

Age_yrs = -0.395732 + 80.273044*MLRatio_20

Summary of Fit

RSquare	0.04228
RSquare Adj	0.023863
Root Mean Square Error	12.03879
Mean of Response	69.57407
Observations (or Sum Wgts)	54

Analysis of Variance

Source	DF	Sum of Squares	Mean Square	F Ratio
Model	1	332.7133	332.713	2.2956
Error	52	7536.4904	144.933	Prob > F
C. Total	53	7869.2037		0.1358

Parameter Estimates

Term	Estimate	Std Error	t Ratio	Prob>|t|
Intercept	-0.395732	46.20954	-0.01	0.9932
MLRatio_25	80.273044	52.98068	1.52	0.1358

Section 3a cont.

Bivariate Fit of Age_yrs By APRatio_75 Sex=M

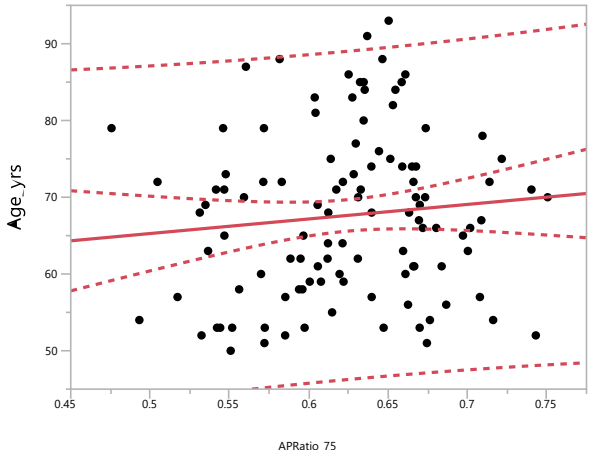

Summary Statistics

	Value	Lower 95%	Upper 95%	Signif. Prob
Correlation	0.101968	-0.08872	0.285441	0.2937
Covariance	0.063268			
Count	108			

Variable	Mean	Std Dev
APRatio_75	0.623858	0.05776
Age_yrs	67.62037	10.74228

Linear Fit

Age_yrs = 55.789519 + 18.964019*APRatio_75

Summary of Fit

RSquare	0.010397
RSquare Adj	0.001062
Root Mean Square Error	10.73658
Mean of Response	67.62037
Observations (or Sum Wgts)	108

Analysis of Variance

Source	DF	Sum of Squares	Mean Square	F Ratio
Model	1	128.381	128.381	1.1137
Error	106	12219.054	115.274	Prob > F
C. Total	107	12347.435		0.2937

Parameter Estimates

Term	Estimate	Std Error	t Ratio	Prob>|t|
Intercept	55.789519	11.25816	4.96	<.0001*
APRatio_75	18.964019	17.96989	1.06	0.2937

Section 3a cont.

Bivariate Fit of Age_yrs By MLRatio_75 Sex=M

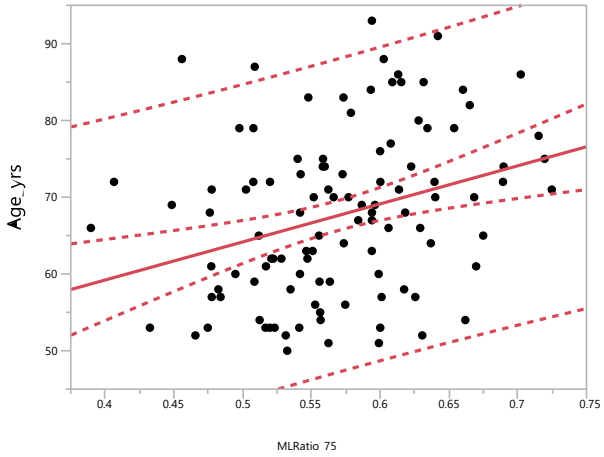

Summary Statistics

	Value	Lower 95%	Upper 95%	Signif. Prob
Correlation	0.313332	0.132185	0.474227	0.0010*
Covariance	0.228431			
Count	108			

Variable	Mean	Std Dev
MLRatio_75	0.569491	0.067866
Age_yrs	67.62037	10.74228

Linear Fit

Age_yrs = 39.375757 + 49.59627*MLRatio_75

Summary of Fit

RSquare	0.098177
RSquare Adj	0.089669
Root Mean Square Error	10.24934
Mean of Response	67.62037
Observations (or Sum Wgts)	108

Analysis of Variance

Source	DF	Sum of Squares	Mean Square	F Ratio
Model	1	1212.237	1212.24	11.5397
Error	106	11135.198	105.05	Prob > F
C. Total	107	12347.435		0.0010*

Parameter Estimates

Term	Estimate	Std Error	t Ratio	Prob>|t|
Intercept	39.375757	8.372821	4.70	<.0001*
MLRatio_75	49.59627	14.59995	3.40	0.0010*

Section 3a cont.

Bivariate Fit of Age_yrs By APRatio_Mid Sex=M

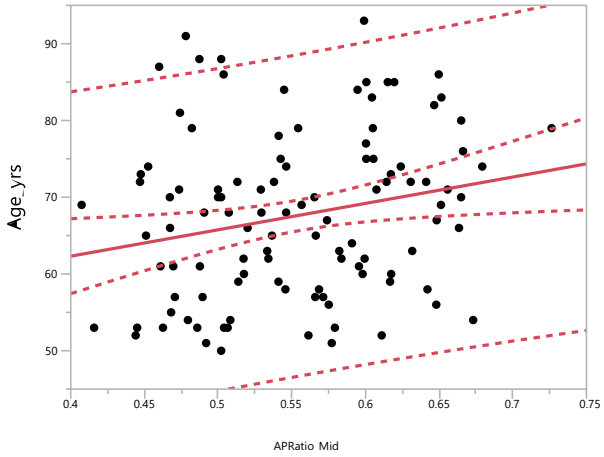

Summary Statistics

	Value	Lower 95%	Upper 95%	Signif. Prob
Correlation	0.223417	0.035961	0.395685	0.0201*
Covariance	0.167571			
Count	108			

Variable	Mean	Std Dev
APRatio_Mid	0.554197	0.069821
Age_yrs	67.62037	10.74228

Linear Fit

Age_yrs = 48.570665 + 34.373541*APRatio_Mid

Summary of Fit

RSquare	0.049915
RSquare Adj	0.040952
Root Mean Square Error	10.52002
Mean of Response	67.62037
Observations (or Sum Wgts)	108

Analysis of Variance

Source	DF	Sum of Squares	Mean Square	F Ratio
Model	1	616.323	616.323	5.5690
Error	106	11731.113	110.671	Prob > F
C. Total	107	12347.435		0.0201*

Parameter Estimates

Term	Estimate	Std Error	t Ratio	Prob>|t|
Intercept	48.570665	8.135591	5.97	<.0001*
APRatio_Mid	34.373541	14.56589	2.36	0.0201*

Section 3a cont.

Bivariate Fit of Age_yrs By MLRatio_Mid Sex=M

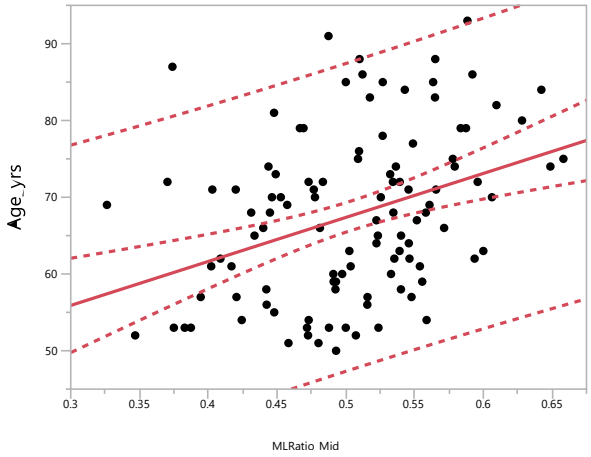

Summary Statistics

	Value	Lower 95%	Upper 95%	Signif. Prob
Correlation	0.360546	0.184117	0.514467	0.0001*
Covariance	0.261687			
Count	108			

Variable	Mean	Std Dev
MLRatio_Mid	0.504412	0.067565
Age_yrs	67.62037	10.74228

Linear Fit

Age_yrs = 38.705715 + 57.323527*MLRatio_Mid

Summary of Fit

RSquare	0.129993
RSquare Adj	0.121786
Root Mean Square Error	10.06692
Mean of Response	67.62037
Observations (or Sum Wgts)	108

Analysis of Variance

Source	DF	Sum of Squares	Mean Square	F Ratio
Model	1	1605.085	1605.09	15.8382
Error	106	10742.350	101.34	Prob > F
C. Total	107	12347.435		0.0001*

Parameter Estimates

Term	Estimate	Std Error	t Ratio	Prob>|t|
Intercept	38.705715	7.329795	5.28	<.0001*
MLRatio_Mid	57.323527	14.40392	3.98	0.0001*

Section 3a cont.

Bivariate Fit of Age_yrs By APRatio_20 Sex=M

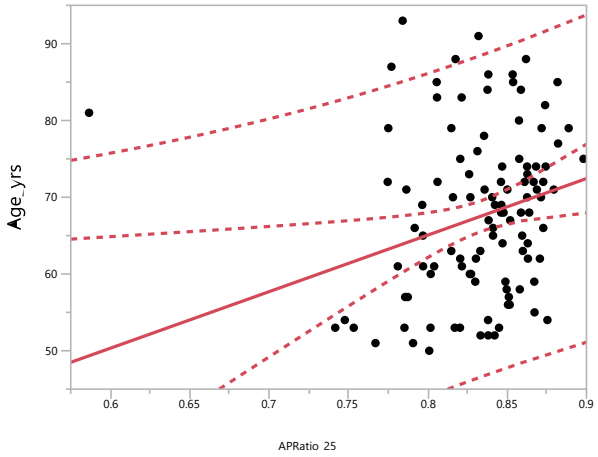

Summary Statistics

	Value	Lower 95%	Upper 95%	Signif. Prob
Correlation	0.225368	0.038013	0.397416	0.0190*
Covariance	0.079557			
Count	108			

Variable	Mean	Std Dev
APRatio_25	0.83467	0.032862
Age_yrs	67.62037	10.74228

Linear Fit

Age_yrs = 6.1291862 + 73.671234*APRatio_20

Summary of Fit

RSquare	0.050791
RSquare Adj	0.041836
Root Mean Square Error	10.51517
Mean of Response	67.62037
Observations (or Sum Wgts)	108

Analysis of Variance

Source	DF	Sum of Squares	Mean Square	F Ratio
Model	1	627.133	627.133	5.6719
Error	106	11720.302	110.569	Prob > F
C. Total	107	12347.435		0.0190*

Parameter Estimates

Term	Estimate	Std Error	t Ratio	Prob>|t|
Intercept	6.1291862	25.83942	0.24	0.8130
APRatio_25	73.671234	30.93389	2.38	0.0190*

Section 3a cont.

Bivariate Fit of Age_yrs By MLRatio_20 Sex=M

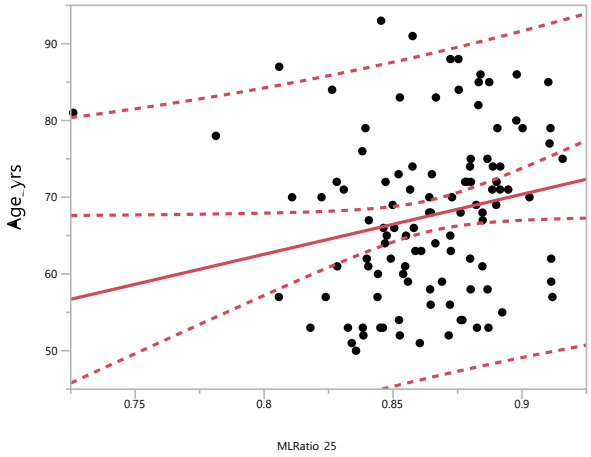

Summary Statistics

	Value	Lower 95%	Upper 95%	Signif. Prob
Correlation	0.192235	0.003384	0.367846	0.0462*
Covariance	0.054551			
Count	108			

Variable	Mean	Std Dev
MLRatio_25	0.864606	0.026417
Age_yrs	67.62037	10.74228

Linear Fit

Age_yrs = 0.0321477 + 78.172237*MLRatio_20

Summary of Fit

RSquare	0.036954
RSquare Adj	0.027869
Root Mean Square Error	10.59153
Mean of Response	67.62037
Observations (or Sum Wgts)	108

Analysis of Variance

Source	DF	Sum of Squares	Mean Square	F Ratio
Model	1	456.291	456.291	4.0675
Error	106	11891.144	112.181	Prob > F
C. Total	107	12347.435		0.0462*

Parameter Estimates

Term	Estimate	Std Error	t Ratio	Prob>|t|
Intercept	0.0321477	33.52815	0.00	0.9992
MLRatio_25	78.172237	38.76059	2.02	0.0462*

Section 3b. Without Outliers.

Bivariate Fit of Age_yrs By APRatio_75 Sex=F

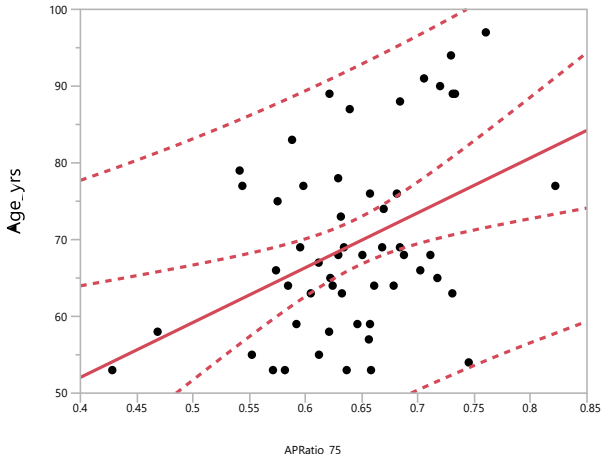

Linear Fit

Summary Statistics

	Value	Lower 95%	Upper 95%	Signif. Prob
Correlation	0.389748	0.136201	0.595375	0.0036*
Covariance	0.315288			
Count	54			

Variable	Mean	Std Dev
APRatio_75	0.644965	0.066389
Age_yrs	69.57407	12.18505

Linear Fit

Age_yrs = 23.436985 + 71.534251*APRatio_75

Summary of Fit

RSquare	0.151903
RSquare Adj	0.135594
Root Mean Square Error	11.32887
Mean of Response	69.57407
Observations (or Sum Wgts)	54

Analysis of Variance

Source	DF	Sum of Squares	Mean Square	F Ratio
Model	1	1195.3576	1195.36	9.3138
Error	52	6673.8461	128.34	Prob > F
C. Total	53	7869.2037		0.0036*

Parameter Estimates

Term	Estimate	Std Error	t Ratio	Prob>|t|
Intercept	23.436985	15.19617	1.54	0.1291
APRatio_75	71.534251	23.43967	3.05	0.0036*

Section 3b cont.

Bivariate Fit of Age_yrs By MLRatio_75 Sex=F

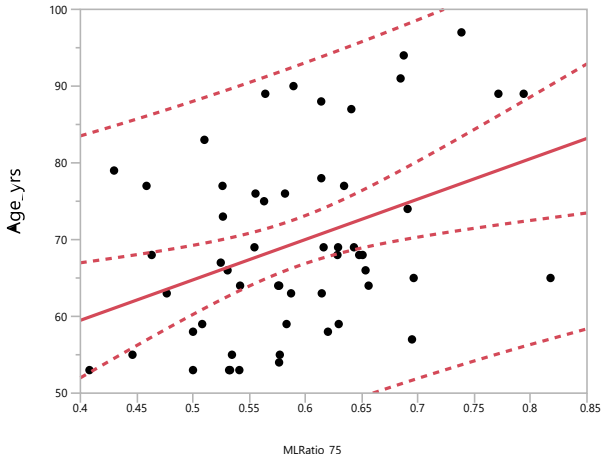

Linear Fit

Summary Statistics

	Value	Lower 95%	Upper 95%	Signif. Prob
Correlation	0.380544	0.125579	0.588354	0.0045*
Covariance	0.408296			
Count	54			

Variable	Mean	Std Dev
MLRatio_75	0.591508	0.088053
Age_yrs	69.57407	12.18505

Linear Fit

Age_yrs = 38.424722 + 52.660889*MLRatio_75

Summary of Fit

RSquare	0.144813
RSquare Adj	0.128368
Root Mean Square Error	11.37612
Mean of Response	69.57407
Observations (or Sum Wgts)	54

Analysis of Variance

Source	DF	Sum of Squares	Mean Square	F Ratio
Model	1	1139.5663	1139.57	8.8054
Error	52	6729.6374	129.42	Prob > F
C. Total	53	7869.2037		0.0045*

Parameter Estimates

Term	Estimate	Std Error	t Ratio	Prob>|t|
Intercept	38.424722	10.61074	3.62	0.0007*
MLRatio_75	52.660889	17.74649	2.97	0.0045*

Section 3b cont.

Bivariate Fit of Age_yrs By APRatio_Mid Sex=F

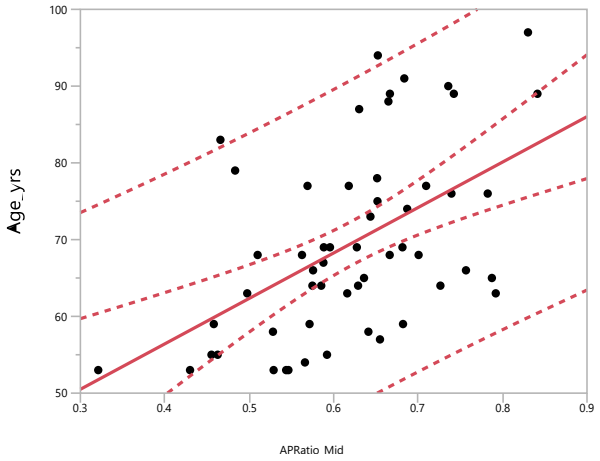

Summary Statistics

	Value	Lower 95%	Upper 95%	Signif. Prob
Correlation	0.519016	0.291809	0.690778	<.0001*
Covariance	0.67558			
Count	54			

Variable	Mean	Std Dev
APRatio_Mid	0.622174	0.106824
Age_yrs	69.57407	12.18505

Linear Fit

Age_yrs = 32.739804 + 59.202551*APRatio_Mid

Summary of Fit

RSquare	0.269378
RSquare Adj	0.255328
Root Mean Square Error	10.51502
Mean of Response	69.57407
Observations (or Sum Wgts)	54

Analysis of Variance

Source	DF	Sum of Squares	Mean Square	F Ratio
Model	1	2119.7911	2119.79	19.1722
Error	52	5749.4126	110.57	Prob > F
C. Total	53	7869.2037		<.0001*

Parameter Estimates

Term	Estimate	Std Error	t Ratio	Prob>|t|
Intercept	32.739804	8.533146	3.84	0.0003*
APRatio_Mid	59.202551	13.52085	4.38	<.0001*

Section 3b cont.

Bivariate Fit of Age_yrs By MLRatio_Mid Sex=F

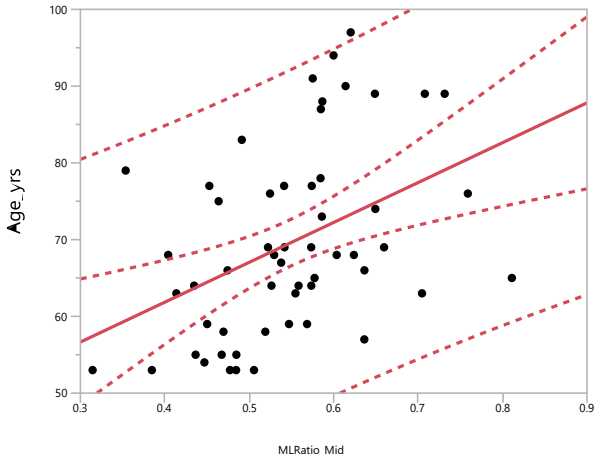

Summary Statistics

	Value	Lower 95%	Upper 95%	Signif. Prob
Correlation	0.42591	0.178506	0.622661	0.0013*
Covariance	0.518425			
Count	54			

Variable	Mean	Std Dev
MLRatio_Mid	0.548734	0.099894
Age_yrs	69.57407	12.18505

Linear Fit

Age_yrs = 41.066145 + 51.952215*MLRatio_Mid

Summary of Fit

RSquare	0.181399
RSquare Adj	0.165657
Root Mean Square Error	11.13012
Mean of Response	69.57407
Observations (or Sum Wgts)	54

Analysis of Variance

Source	DF	Sum of Squares	Mean Square	F Ratio
Model	1	1427.4652	1427.47	11.5230
Error	52	6441.7385	123.88	Prob > F
C. Total	53	7869.2037		0.0013*

Parameter Estimates

Term	Estimate	Std Error	t Ratio	Prob>|t|
Intercept	41.066145	8.533623	4.81	<.0001*
MLRatio_Mid	51.952215	15.30457	3.39	0.0013*

Section 3b cont.

Bivariate Fit of Age_yrs By APRatio_20 Sex=F

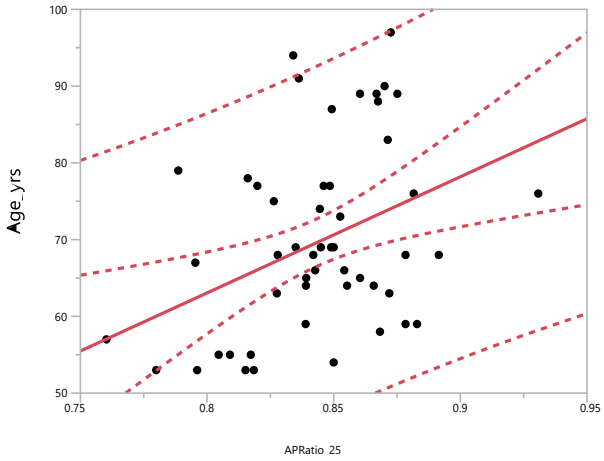

Summary Statistics

	Value	Lower 95%	Upper 95%	Signif. Prob
Correlation	0.385757	0.131589	0.592335	0.0040*
Covariance	0.146019			
Count	54			

Variable	Mean	Std Dev
APRatio_25	0.843095	0.031065
Age_yrs	69.57407	12.18505

Linear Fit

Age_yrs = -57.99642 + 151.31212*APRatio_25

Summary of Fit

RSquare	0.148809
RSquare Adj	0.13244
Root Mean Square Error	11.34952
Mean of Response	69.57407
Observations (or Sum Wgts)	54

Analysis of Variance

Source	DF	Sum of Squares	Mean Square	F Ratio
Model	1	1171.0054	1171.01	9.0908
Error	52	6698.1983	128.81	Prob > F
C. Total	53	7869.2037		0.0040*

Parameter Estimates

Term	Estimate	Std Error	t Ratio	Prob>|t|
Intercept	-57.99642	42.33867	-1.37	0.1766
APRatio_25	151.31212	50.18473	3.02	0.0040*

Section 3b cont.

Bivariate Fit of Age_yrs By MLRatio_20 Sex=F

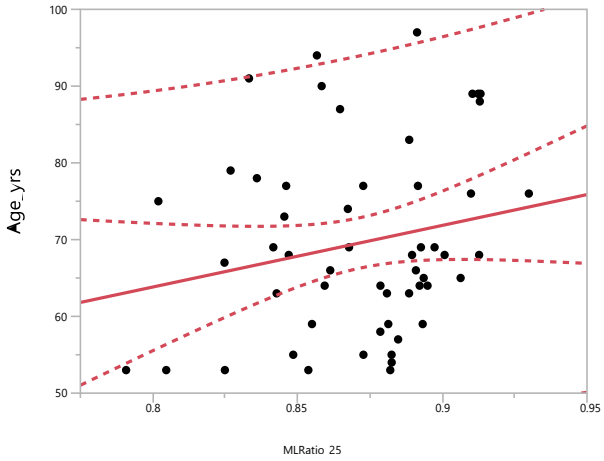

Summary Statistics

	Value	Lower 95%	Upper 95%	Signif. Prob
Correlation	0.205622	-0.06576	0.448679	0.1358
Covariance	0.078203			
Count	54			

Variable	Mean	Std Dev
MLRatio_25	0.871648	0.031212
Age_yrs	69.57407	12.18505

Linear Fit

Age_yrs = -0.395732 + 80.273044*MLRatio_25

Summary of Fit

RSquare	0.04228
RSquare Adj	0.023863
Root Mean Square Error	12.03879
Mean of Response	69.57407
Observations (or Sum Wgts)	54

Analysis of Variance

Source	DF	Sum of Squares	Mean Square	F Ratio
Model	1	332.7133	332.713	2.2956
Error	52	7536.4904	144.933	Prob > F
C. Total	53	7869.2037		0.1358

Parameter Estimates

Term	Estimate	Std Error	t Ratio	Prob>|t|
Intercept	-0.395732	46.20954	-0.01	0.9932
MLRatio_25	80.273044	52.98068	1.52	0.1358

Section 3b cont.

Bivariate Fit of Age_yrs By APRatio_75 Sex=M

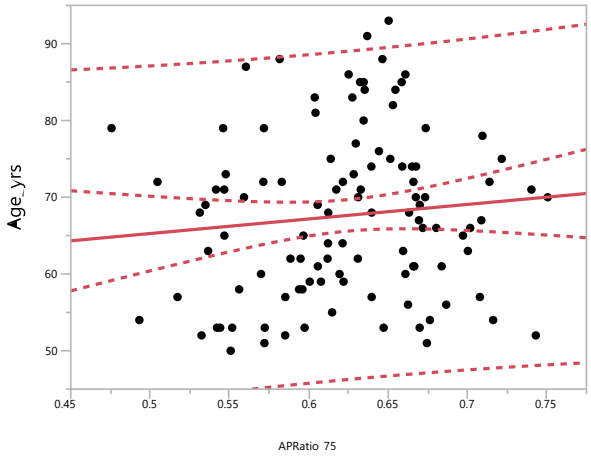

Summary Statistics

	Value	Lower 95%	Upper 95%	Signif. Prob
Correlation	0.101968	-0.08872	0.285441	0.2937
Covariance	0.063268			
Count	108			

Variable	Mean	Std Dev
APRatio_75	0.623858	0.05776
Age_yrs	67.62037	10.74228

Linear Fit

Age_yrs = 55.789519 + 18.964019*APRatio_75

Summary of Fit

RSquare	0.010397
RSquare Adj	0.001062
Root Mean Square Error	10.73658
Mean of Response	67.62037
Observations (or Sum Wgts)	108

Analysis of Variance

Source	DF	Sum of Squares	Mean Square	F Ratio
Model	1	128.381	128.381	1.1137
Error	106	12219.054	115.274	Prob > F
C. Total	107	12347.435		0.2937

Parameter Estimates

Term	Estimate	Std Error	t Ratio	Prob>|t|
Intercept	55.789519	11.25816	4.96	<.0001*
APRatio_75	18.964019	17.96989	1.06	0.2937

Section 3b cont.

Bivariate Fit of Age_yrs By MLRatio_75 Sex=M

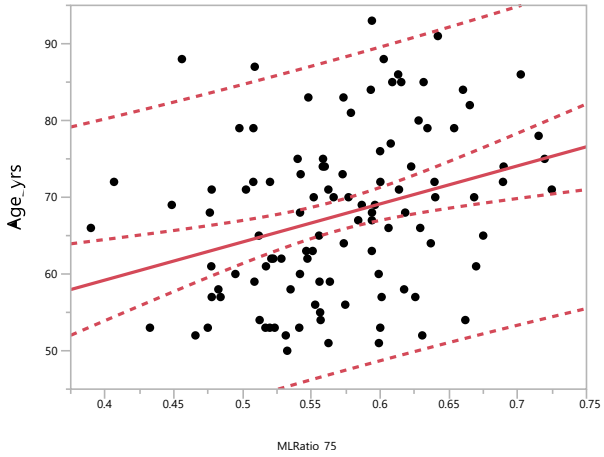

Summary Statistics

	Value	Lower 95%	Upper 95%	Signif. Prob
Correlation	0.313332	0.132185	0.474227	0.0010*
Covariance	0.228431			
Count	108			

Variable	Mean	Std Dev
MLRatio_75	0.569491	0.067866
Age_yrs	67.62037	10.74228

Linear Fit

Age_yrs = 39.375757 + 49.59627*MLRatio_75

Summary of Fit

RSquare	0.098177
RSquare Adj	0.089669
Root Mean Square Error	10.24934
Mean of Response	67.62037
Observations (or Sum Wgts)	108

Analysis of Variance

Source	DF	Sum of Squares	Mean Square	F Ratio
Model	1	1212.237	1212.24	11.5397
Error	106	11135.198	105.05	Prob > F
C. Total	107	12347.435		0.0010*

Parameter Estimates

Term	Estimate	Std Error	t Ratio	Prob>|t|
Intercept	39.375757	8.372821	4.70	<.0001*
MLRatio_75	49.59627	14.59995	3.40	0.0010*

Section 3b cont.

Bivariate Fit of Age_yrs By APRatio_Mid Sex=M

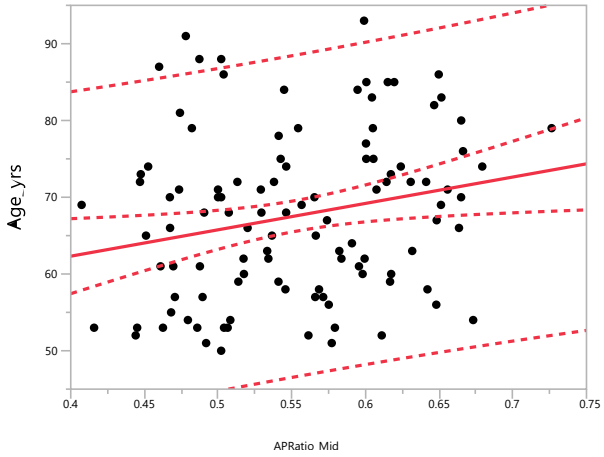

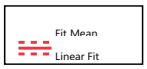

Summary Statistics

	Value	Lower 95%	Upper 95%	Signif. Prob
Correlation	0.223417	0.035961	0.395685	0.0201*
Covariance	0.167571			
Count	108			

Variable	Mean	Std Dev
APRatio_Mid	0.554197	0.069821
Age_yrs	67.62037	10.74228

Linear Fit

Age_yrs = 48.570665 + 34.373541*APRatio_Mid

Summary of Fit

RSquare	0.049915
RSquare Adj	0.040952
Root Mean Square Error	10.52002
Mean of Response	67.62037
Observations (or Sum Wgts)	108

Analysis of Variance

Source	DF	Sum of Squares	Mean Square	F Ratio
Model	1	616.323	616.323	5.5690
Error	106	11731.113	110.671	Prob > F
C. Total	107	12347.435		0.0201*

Parameter Estimates

Term	Estimate	Std Error	t Ratio	Prob>|t|
Intercept	48.570665	8.135591	5.97	<.0001*
APRatio_Mid	34.373541	14.56589	2.36	0.0201*

Section 3b cont.

Bivariate Fit of Age_yrs By MLRatio_Mid Sex=M

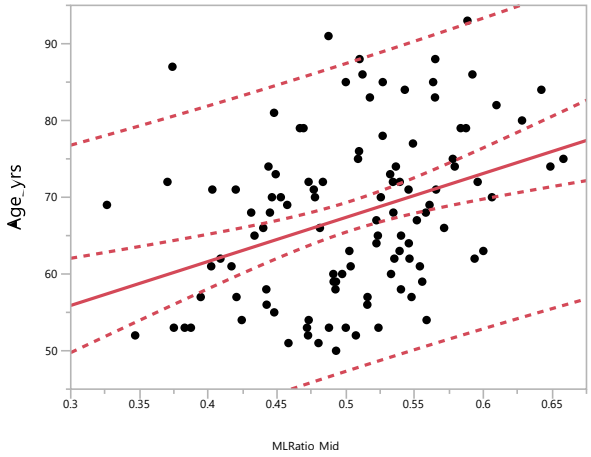

Summary Statistics

	Value	Lower 95%	Upper 95%	Signif. Prob
Correlation	0.360546	0.184117	0.514467	0.0001*
Covariance	0.261687			
Count	108			

Variable	Mean	Std Dev
MLRatio_Mid	0.504412	0.067565
Age_yrs	67.62037	10.74228

Linear Fit

Age_yrs = 38.705715 + 57.323527*MLRatio_Mid

Summary of Fit

RSquare	0.129993
RSquare Adj	0.121786
Root Mean Square Error	10.06692
Mean of Response	67.62037
Observations (or Sum Wgts)	108

Analysis of Variance

Source	DF	Sum of Squares	Mean Square	F Ratio
Model	1	1605.085	1605.09	15.8382
Error	106	10742.350	101.34	Prob > F
C. Total	107	12347.435		0.0001*

Parameter Estimates

Term	Estimate	Std Error	t Ratio	Prob>|t|
Intercept	38.705715	7.329795	5.28	<.0001*
MLRatio_Mid	57.323527	14.40392	3.98	0.0001*

Section 3b cont.

Bivariate Fit of Age_yrs By APRatio_20 Sex=M

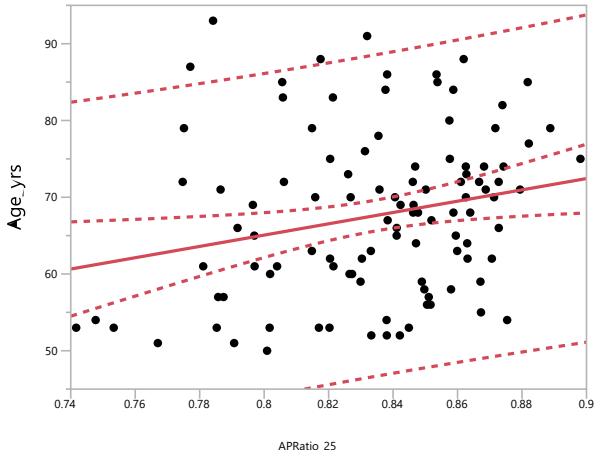

Summary Statistics

	Value	Lower 95%	Upper 95%	Signif. Prob
Correlation	0.225368	0.038013	0.397416	0.0190*
Covariance	0.079557			
Count	108			

Variable	Mean	Std Dev
APRatio_25	0.83467	0.032862
Age_yrs	67.62037	10.74228

Linear Fit

Age_yrs = 6.1291862 + 73.671234*APRatio_25

Summary of Fit

RSquare	0.050791
RSquare Adj	0.041836
Root Mean Square Error	10.51517
Mean of Response	67.62037
Observations (or Sum Wgts)	108

Analysis of Variance

Source	DF	Sum of Squares	Mean Square	F Ratio
Model	1	627.133	627.133	5.6719
Error	106	11720.302	110.569	Prob > F
C. Total	107	12347.435		0.0190*

Parameter Estimates

Term	Estimate	Std Error	t Ratio	Prob>|t|
Intercept	6.1291862	25.83942	0.24	0.8130
APRatio_25	73.671234	30.93389	2.38	0.0190*

Section 3b cont.

Bivariate Fit of Age_yrs By MLRatio_20 Sex=M

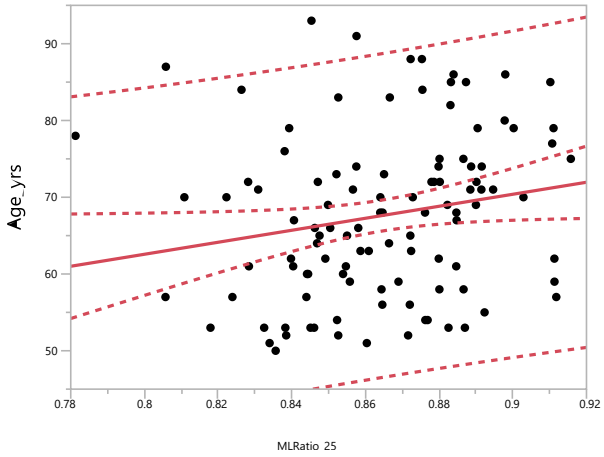

Summary Statistics

	Value	Lower 95%	Upper 95%	Signif. Prob
Correlation	0.192235	0.003384	0.367846	0.0462*
Covariance	0.054551			
Count	108			

Variable	Mean	Std Dev
MLRatio_25	0.864606	0.026417
Age_yrs	67.62037	10.74228

Linear Fit

Age_yrs = 0.0321477 + 78.172237*MLRatio_25

Summary of Fit

RSquare	0.036954
RSquare Adj	0.027869
Root Mean Square Error	10.59153
Mean of Response	67.62037
Observations (or Sum Wgts)	108

Analysis of Variance

Source	DF	Sum of Squares	Mean Square	F Ratio
Model	1	456.291	456.291	4.0675
Error	106	11891.144	112.181	Prob > F
C. Total	107	12347.435		0.0462*

Parameter Estimates

Term	Estimate	Std Error	t Ratio	Prob>|t|
Intercept	0.0321477	33.52815	0.00	0.9992
MLRatio_25	78.172237	38.76059	2.02	0.0462*

Section 4. *JMP Linear Regressions for Summed Measures.*

Section 4a. With Outliers.

Bivariate Fit of Age_yrs By Sum_Ratio_75 Sex=F

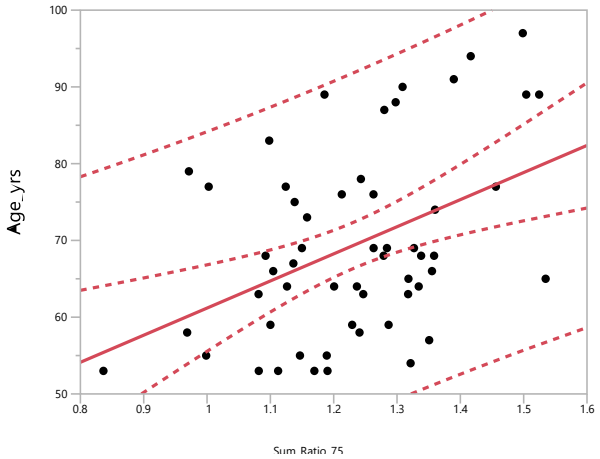

Linear Fit

Summary Statistics

	Value	Lower 95%	Upper 95%	Signif. Prob
Correlation	0.427463	0.182909	0.6222	0.0011*
Covariance	0.766553			
Count	55			

Variable	Mean	Std Dev
Sum_Ratio_75	1.231603	0.147325
Age_yrs	69.36364	12.17217

Linear Fit

Age_yrs = 25.866314 + 35.317646*Sum_Ratio_75

Summary of Fit

RSquare	0.182725
RSquare Adj	0.167305
Root Mean Square Error	11.10736
Mean of Response	69.36364
Observations (or Sum Wgts)	55

Analysis of Variance

Source	DF	Sum of Squares	Mean Square	F Ratio
Model	1	1461.9332	1461.93	11.8497
Error	53	6538.7941	123.37	Prob > F
C. Total	54	8000.7273		0.0011*

Parameter Estimates

Term	Estimate	Std Error	t Ratio	Prob>|t|
Intercept	25.866314	12.72445	2.03	0.0471*
Sum_Ratio_75	35.317646	10.2598	3.44	0.0011*

Section 4a cont.

Bivariate Fit of Age_yrs By Sum_Ratio_Mid Sex=F

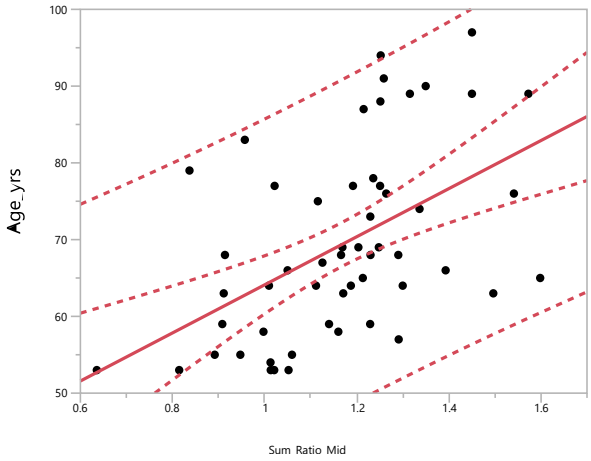

Linear Fit

Summary Statistics

	Value	Lower 95%	Upper 95%	Signif. Prob
Correlation	0.505488	0.27739	0.679642	<.0001*
Covariance	1.208385			
Count	55			

Variable	Mean	Std Dev
Sum_Ratio_Mid	1.167755	0.196393
Age_yrs	69.36364	12.17217

Linear Fit

Age_yrs = 32.778611 + 31.32938*Sum_Ratio_Mid

Summary of Fit

RSquare	0.255518
RSquare Adj	0.241471
Root Mean Square Error	10.60117
Mean of Response	69.36364
Observations (or Sum Wgts)	55

Analysis of Variance

Source	DF	Sum of Squares	Mean Square	F Ratio
Model	1	2044.3286	2044.33	18.1904
Error	53	5956.3987	112.38	Prob > F
C. Total	54	8000.7273		<.0001*

Parameter Estimates

Term	Estimate	Std Error	t Ratio	Prob>|t|
Intercept	32.778611	8.696209	3.77	0.0004*
Sum_Ratio_Mid	31.32938	7.345653	4.27	<.0001*

Section 4a cont.

Bivariate Fit of Age_yrs By Sum_Ratio_20 Sex=F

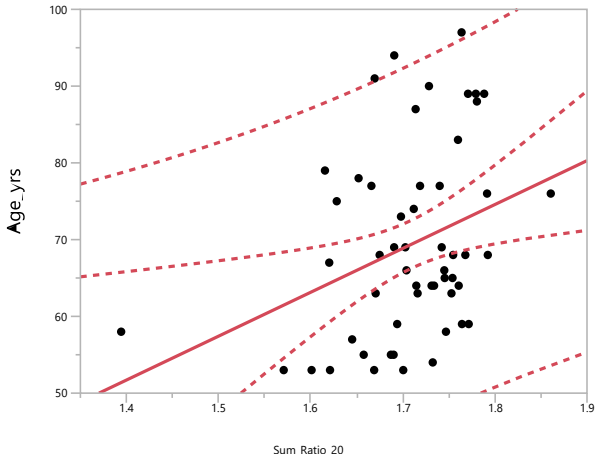

Summary Statistics

	Value	Lower 95%	Upper 95%	Signif. Prob
Correlation	0.333067	0.074339	0.549784	0.0130*
Covariance	0.287512			
Count	55			

Variable	Mean	Std Dev
Sum_Ratio_20	1.708916	0.070918
Age_yrs	69.36364	12.17217

Linear Fit

Age_yrs = -28.3296 + 57.166797*Sum_Ratio_20

Summary of Fit

RSquare	0.110934
RSquare Adj	0.094159
Root Mean Square Error	11.58494
Mean of Response	69.36364
Observations (or Sum Wgts)	55

Analysis of Variance

Source	DF	Sum of Squares	Mean Square	F Ratio
Model	1	887.5504	887.550	6.6131
Error	53	7113.1769	134.211	Prob > F
C. Total	54	8000.7273		0.0130*

Parameter Estimates

Term	Estimate	Std Error	t Ratio	Prob>|t|
Intercept	-28.3296	38.02145	-0.75	0.4595
Sum_Ratio_20	57.166797	22.23009	2.57	0.0130*

Section 4a cont.

Bivariate Fit of Age_yrs By Sum_Ratio_All Sex=F

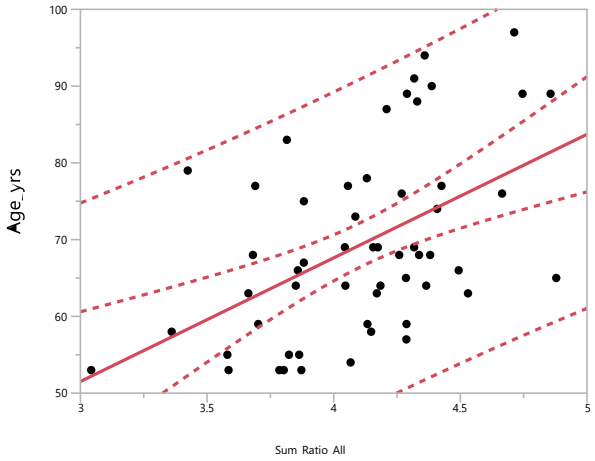

Linear Fit

Summary Statistics

	Value	Lower 95%	Upper 95%	Signif. Prob
Correlation	0.49589	0.265525	0.67269	0.0001*
Covariance	2.262449			
Count	55			

Variable	Mean	Std Dev
Sum_Ratio_All	4.108273	0.374822
Age_yrs	69.36364	12.17217

Linear Fit

Age_yrs = 3.2048841 + 16.103786*Sum_Ratio_All

Summary of Fit

RSquare	0.245907
RSquare Adj	0.231679
Root Mean Square Error	10.66938
Mean of Response	69.36364
Observations (or Sum Wgts)	55

Analysis of Variance

Source	DF	Sum of Squares	Mean Square	F Ratio
Model	1	1967.4355	1967.44	17.2831
Error	53	6033.2918	113.84	Prob > F
C. Total	54	8000.7273		0.0001*

Parameter Estimates

Term	Estimate	Std Error	t Ratio	Prob>|t|
Intercept	3.2048841	15.97878	0.20	0.8418
Sum_Ratio_All	16.103786	3.873619	4.16	0.0001*

Section 4a cont.

Bivariate Fit of Age_yrs By Sum_Ratio_75 Sex=M

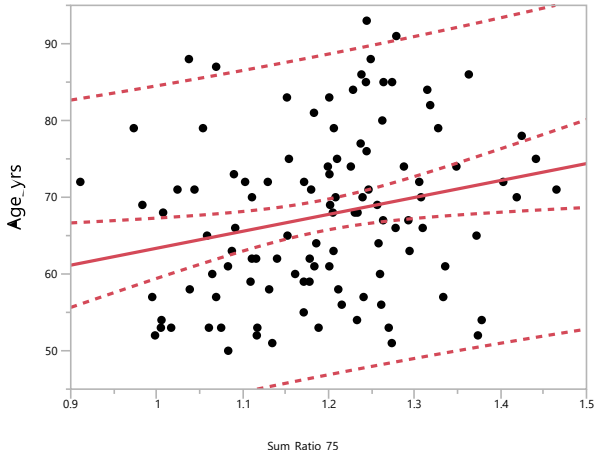

Summary Statistics

	Value	Lower 95%	Upper 95%	Signif. Prob
Correlation	0.236104	0.049331	0.406922	0.0139*
Covariance	0.291699			
Count	108			

Variable	Mean	Std Dev
Sum_Ratio_75	1.193349	0.11501
Age_yrs	67.62037	10.74228

Linear Fit

Age_yrs = 41.303728 + 22.052772*Sum_Ratio_75

Summary of Fit

RSquare	0.055745
RSquare Adj	0.046837
Root Mean Square Error	10.4877
Mean of Response	67.62037
Observations (or Sum Wgts)	108

Analysis of Variance

Source	DF	Sum of Squares	Mean Square	F Ratio
Model	1	688.307	688.307	6.2578
Error	106	11659.128	109.992	Prob > F
C. Total	107	12347.435		0.0139*

Parameter Estimates

Term	Estimate	Std Error	t Ratio	Prob>|t|
Intercept	41.303728	10.56838	3.91	0.0002*
Sum_Ratio_75	22.052772	8.815603	2.50	0.0139*

Section 4a cont.

Bivariate Fit of Age_yrs By Sum_Ratio_Mid Sex=M

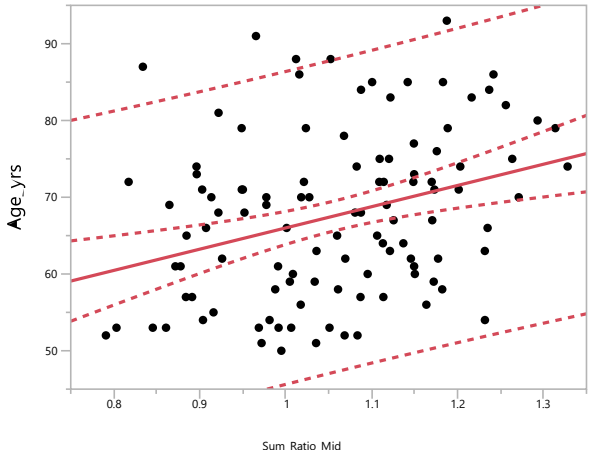

Summary Statistics

	Value	Lower 95%	Upper 95%	Signif. Prob
Correlation	0.320874	0.140414	0.480699	0.0007*
Covariance	0.429258			
Count	108			

Variable	Mean	Std Dev
Sum_Ratio_Mid	1.058608	0.124534
Age_yrs	67.62037	10.74228

Linear Fit

Age_yrs = 38.319692 + 27.678486*Sum_Ratio_Mid

Summary of Fit

RSquare	0.10296
RSquare Adj	0.094497
Root Mean Square Error	10.22213
Mean of Response	67.62037
Observations (or Sum Wgts)	108

Analysis of Variance

Source	DF	Sum of Squares	Mean Square	F Ratio
Model	1	1271.290	1271.29	12.1664
Error	106	11076.146	104.49	Prob > F
C. Total	107	12347.435		0.0007*

Parameter Estimates

Term	Estimate	Std Error	t Ratio	Prob>|t|
Intercept	38.319692	8.457731	4.53	<.0001*
Sum_Ratio_Mid	27.678486	7.935266	3.49	0.0007*

Section 4a cont.

Bivariate Fit of Age_yrs By Sum_Ratio_20 Sex=M

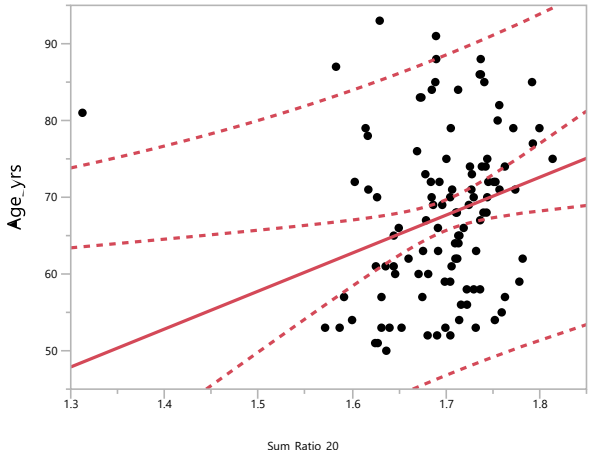

Summary Statistics

	Value	Lower 95%	Upper 95%	Signif. Prob
Correlation	0.239676	0.053108	0.410077	0.0125*
Covariance	0.134108			
Count	108			

Variable	Mean	Std Dev
Sum_Ratio_20	1.699277	0.052088
Age_yrs	67.62037	10.74228

Linear Fit

Age_yrs = -16.37422 + 49.429614*Sum_Ratio_20

Summary of Fit

RSquare	0.057445
RSquare Adj	0.048553
Root Mean Square Error	10.47825
Mean of Response	67.62037
Observations (or Sum Wgts)	108

Analysis of Variance

Source	DF	Sum of Squares	Mean Square	F Ratio
Model	1	709.295	709.295	6.4602
Error	106	11638.141	109.794	Prob > F
C. Total	107	12347.435		0.0125*

Parameter Estimates

Term	Estimate	Std Error	t Ratio	Prob>|t|
Intercept	-16.37422	33.06198	-0.50	0.6214
Sum_Ratio_20	49.429614	19.44745	2.54	0.0125*

Section 4a cont.

Bivariate Fit of Age_yrs By Sum_Ratio_All Sex=M

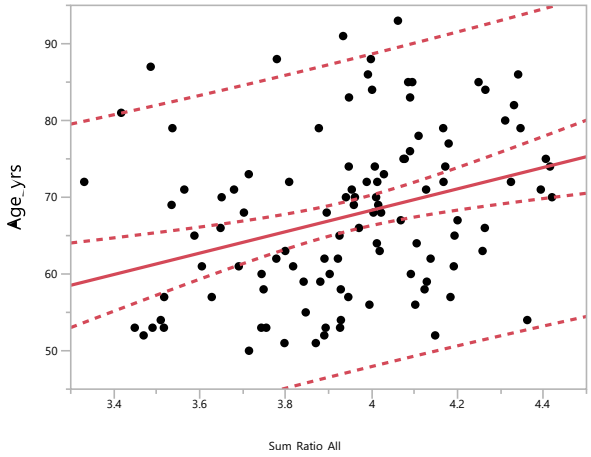

Summary Statistics

	Value	Lower 95%	Upper 95%	Signif. Prob
Correlation	0.321578	0.141184	0.481303	0.0007*
Covariance	0.855066			
Count	108			

Variable	Mean	Std Dev
Sum_Ratio_All	3.951234	0.247524
Age_yrs	67.62037	10.74228

Linear Fit

Age_yrs = 12.476372 + 13.956147*Sum_Ratio_All

Summary of Fit

RSquare	0.103412
RSquare Adj	0.094954
Root Mean Square Error	10.21955
Mean of Response	67.62037
Observations (or Sum Wgts)	108

Analysis of Variance

Source	DF	Sum of Squares	Mean Square	F Ratio
Model	1	1276.876	1276.88	12.2260
Error	106	11070.559	104.44	Prob > F
C. Total	107	12347.435		0.0007*

Parameter Estimates

Term	Estimate	Std Error	t Ratio	Prob>|t|
Intercept	12.476372	15.8015	0.79	0.4315
Sum_Ratio_All	13.956147	3.991379	3.50	0.0007*

Section 4b. Without Outliers.

Bivariate Fit of Age_yrs By Sum_Ratio_75 Sex=F

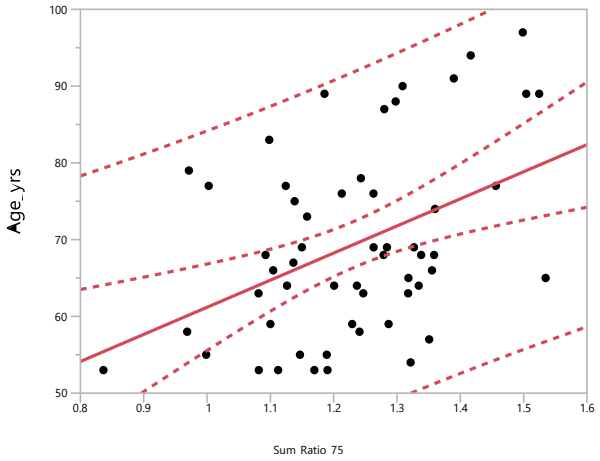

Linear Fit

Summary Statistics

	Value	Lower 95%	Upper 95%	Signif. Prob
Correlation	0.427463	0.182909	0.6222	0.0011*
Covariance	0.766553			
Count	55			

Variable	Mean	Std Dev
Sum_Ratio_75	1.231603	0.147325
Age_yrs	69.36364	12.17217

Linear Fit

Age_yrs = 25.866314 + 35.317646*Sum_Ratio_75

Summary of Fit

RSquare	0.182725
RSquare Adj	0.167305
Root Mean Square Error	11.10736
Mean of Response	69.36364
Observations (or Sum Wgts)	55

Analysis of Variance

Source	DF	Sum of Squares	Mean Square	F Ratio
Model	1	1461.9332	1461.93	11.8497
Error	53	6538.7941	123.37	Prob > F
C. Total	54	8000.7273		0.0011*

Parameter Estimates

Term	Estimate	Std Error	t Ratio	Prob>|t|
Intercept	25.866314	12.72445	2.03	0.0471*
Sum_Ratio_75	35.317646	10.2598	3.44	0.0011*

Section 4b cont.

Bivariate Fit of Age_yrs By Sum_Ratio_Mid Sex=F

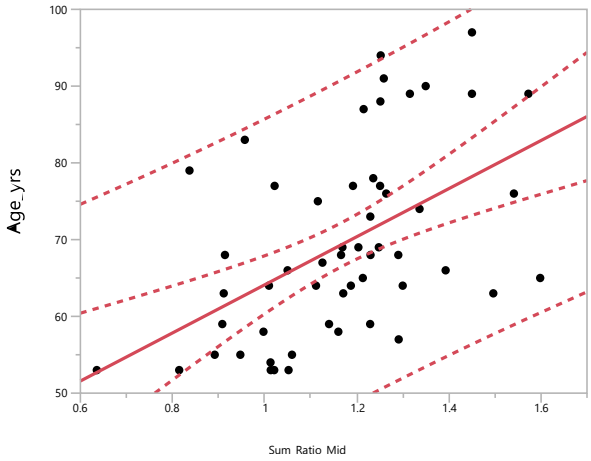

Summary Statistics

	Value	Lower 95%	Upper 95%	Signif. Prob
Correlation	0.505488	0.27739	0.679642	<.0001*
Covariance	1.208385			
Count	55			

Variable	Mean	Std Dev
Sum_Ratio_Mid	1.167755	0.196393
Age_yrs	69.36364	12.17217

Linear Fit

Age_yrs = 32.778611 + 31.32938*Sum_Ratio_Mid

Summary of Fit

RSquare	0.255518
RSquare Adj	0.241471
Root Mean Square Error	10.60117
Mean of Response	69.36364
Observations (or Sum Wgts)	55

Analysis of Variance

Source	DF	Sum of Squares	Mean Square	F Ratio
Model	1	2044.3286	2044.33	18.1904
Error	53	5956.3987	112.38	Prob > F
C. Total	54	8000.7273		<.0001*

Parameter Estimates

Term	Estimate	Std Error	t Ratio	Prob>|t|
Intercept	32.778611	8.696209	3.77	0.0004*
Sum_Ratio_Mid	31.32938	7.345653	4.27	<.0001*

Section 4b cont.

Bivariate Fit of Age_yrs By Sum_Ratio_20 Sex=F

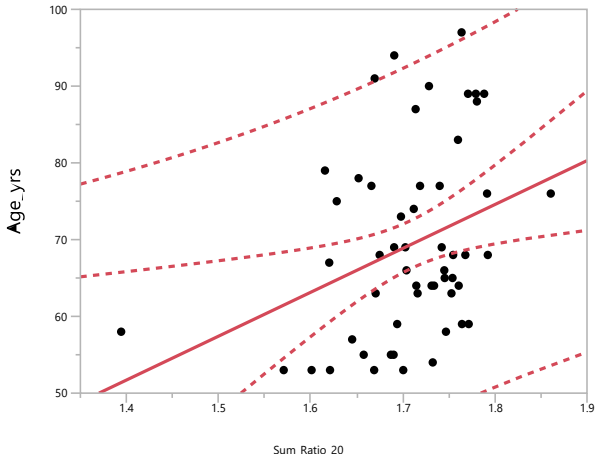

Summary Statistics

	Value	Lower 95%	Upper 95%	Signif. Prob
Correlation	0.333067	0.074339	0.549784	0.0130*
Covariance	0.287512			
Count	55			

Variable	Mean	Std Dev
Sum_Ratio_20	1.708916	0.070918
Age_yrs	69.36364	12.17217

Linear Fit

Age_yrs = -28.3296 + 57.166797*Sum_Ratio_20

Summary of Fit

RSquare	0.110934
RSquare Adj	0.094159
Root Mean Square Error	11.58494
Mean of Response	69.36364
Observations (or Sum Wgts)	55

Analysis of Varianc

Source	DF	Sum of Squares	Mean Square	F Ratio
Model	1	887.5504	887.550	6.6131
Error	53	7113.1769	134.211	Prob > F
C. Total	54	8000.7273		0.0130*

Parameter Estimates

Term	Estimate	Std Error	t Ratio	Prob>|t|
Intercept	-28.3296	38.02145	-0.75	0.4595
Sum_Ratio_20	57.166797	22.23009	2.57	0.0130*

Section 4b cont.

Bivariate Fit of Age_yrs By Sum_Ratio_All Sex=F

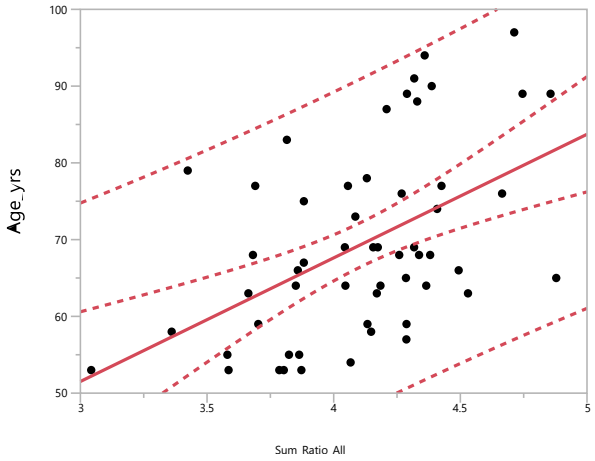

Linear Fit

Summary Statistics

	Value	Lower 95%	Upper 95%	Signif. Prob
Correlation	0.49589	0.265525	0.67269	0.0001*
Covariance	2.262449			
Count	55			

Variable	Mean	Std Dev
Sum_Ratio_All	4.108273	0.374822
Age_yrs	69.36364	12.17217

Linear Fit

Age_yrs = 3.2048841 + 16.103786*Sum_Ratio_All

Summary of Fit

RSquare	0.245907
RSquare Adj	0.231679
Root Mean Square Error	10.66938
Mean of Response	69.36364
Observations (or Sum Wgts)	55

Analysis of Variance

Source	DF	Sum of Squares	Mean Square	F Ratio
Model	1	1967.4355	1967.44	17.2831
Error	53	6033.2918	113.84	Prob > F
C. Total	54	8000.7273		0.0001*

Parameter Estimates

Term	Estimate	Std Error	t Ratio	Prob>|t|
Intercept	3.2048841	15.97878	0.20	0.8418
Sum_Ratio_All	16.103786	3.873619	4.16	0.0001*

Section 4b cont.

Bivariate Fit of Age_yrs By Sum_Ratio_75 Sex=M

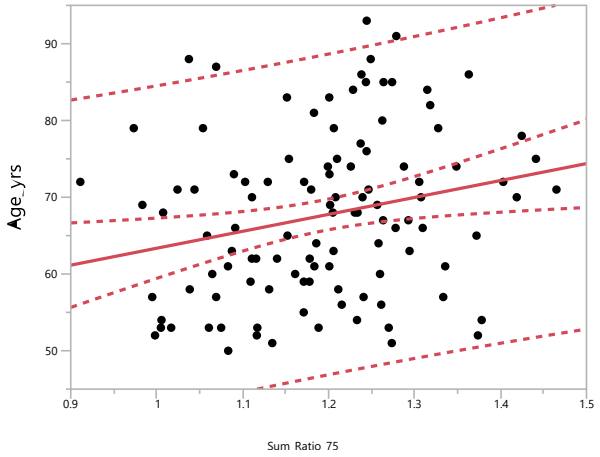

Summary Statistics

	Value	Lower 95%	Upper 95%	Signif. Prob
Correlation	0.236104	0.049331	0.406922	0.0139*
Covariance	0.291699			
Count	108			

Variable	Mean	Std Dev
Sum_Ratio_75	1.193349	0.11501
Age_yrs	67.62037	10.74228

Linear Fit

Age_yrs = 41.303728 + 22.052772*Sum_Ratio_75

Summary of Fit

RSquare	0.055745
RSquare Adj	0.046837
Root Mean Square Error	10.4877
Mean of Response	67.62037
Observations (or Sum Wgts)	108

Analysis of Variance

Source	DF	Sum of Squares	Mean Square	F Ratio
Model	1	688.307	688.307	6.2578
Error	106	11659.128	109.992	Prob > F
C. Total	107	12347.435		0.0139*

Parameter Estimates

Term	Estimate	Std Error	t Ratio	Prob>|t|
Intercept	41.303728	10.56838	3.91	0.0002*
Sum_Ratio_75	22.052772	8.815603	2.50	0.0139*

Section 4b cont.

Bivariate Fit of Age_yrs By Sum_Ratio_Mid Sex=M

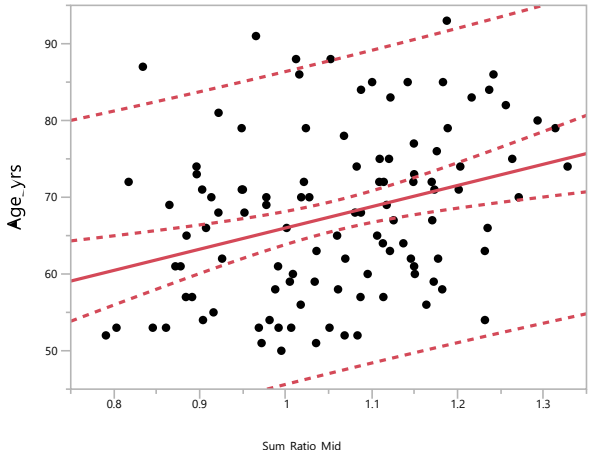

Summary Statistics

	Value	Lower 95%	Upper 95%	Signif. Prob
Correlation	0.320874	0.140414	0.480699	0.0007*
Covariance	0.429258			
Count	108			

Variable	Mean	Std Dev
Sum_Ratio_Mid	1.058608	0.124534
Age_yrs	67.62037	10.74228

Linear Fit

Age_yrs = 38.319692 + 27.678486*Sum_Ratio_Mid

Summary of Fit

RSquare	0.10296
RSquare Adj	0.094497
Root Mean Square Error	10.22213
Mean of Response	67.62037
Observations (or Sum Wgts)	108

Analysis of Variance

Source	DF	Sum of Squares	Mean Square	F Ratio
Model	1	1271.290	1271.29	12.1664
Error	106	11076.146	104.49	Prob > F
C. Total	107	12347.435		0.0007*

Parameter Estimates

Term	Estimate	Std Error	t Ratio	Prob>|t|
Intercept	38.319692	8.457731	4.53	<.0001*
Sum_Ratio_Mid	27.678486	7.935266	3.49	0.0007*

Section 4b cont.

Bivariate Fit of Age_yrs By Sum_Ratio_20 Sex=M

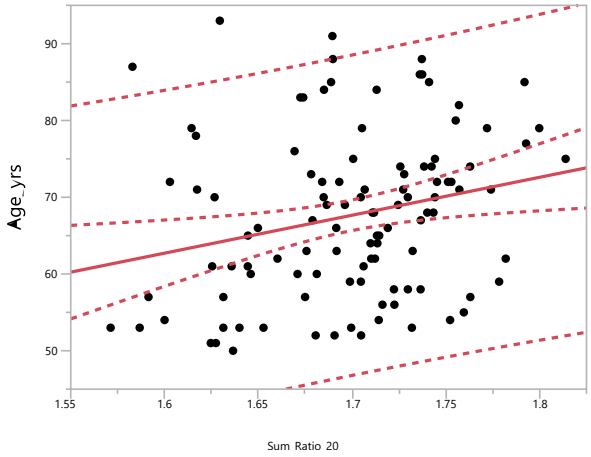

Summary Statistics

	Value	Lower 95%	Upper 95%	Signif. Prob
Correlation	0.239676	0.053108	0.410077	0.0125*
Covariance	0.134108			
Count	108			

Variable	Mean	Std Dev
Sum_Ratio_20	1.699277	0.052088
Age_yrs	67.62037	10.74228

Linear Fit

Age_yrs = -16.37422 + 49.429614*Sum_Ratio_20

Summary of Fit

RSquare	0.057445
RSquare Adj	0.048553
Root Mean Square Error	10.47825
Mean of Response	67.62037
Observations (or Sum Wgts)	108

Analysis of Variance

Source	DF	Sum of Squares	Mean Square	F Ratio
Model	1	709.295	709.295	6.4602
Error	106	11638.141	109.794	Prob > F
C. Total	107	12347.435		0.0125*

Parameter Estimates

Term	Estimate	Std Error	t Ratio	Prob>|t|
Intercept	-16.37422	33.06198	-0.50	0.6214
Sum_Ratio_20	49.429614	19.44745	2.54	0.0125*

Section 4b cont.

Bivariate Fit of Age_yrs By Sum_Ratio_All Sex=M

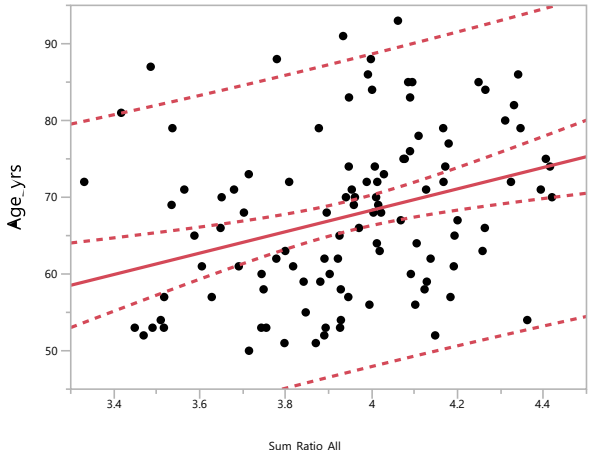

Summary Statistics

	Value	Lower 95%	Upper 95%	Signif. Prob
Correlation	0.321578	0.141184	0.481303	0.0007*
Covariance	0.855066			
Count	108			

Variable	Mean	Std Dev
Sum_Ratio_All	3.951234	0.247524
Age_yrs	67.62037	10.74228

Linear Fit

Age_yrs = 12.476372 + 13.956147*Sum_Ratio_All

Summary of Fit

RSquare	0.103412
RSquare Adj	0.094954
Root Mean Square Error	10.21955
Mean of Response	67.62037
Observations (or Sum Wgts)	108

Analysis of Variance

Source	DF	Sum of Squares	Mean Square	F Ratio
Model	1	1276.876	1276.88	12.2260
Error	106	11070.559	104.44	Prob > F
C. Total	107	12347.435		0.0007*

Parameter Estimates

Term	Estimate	Std Error	t Ratio	Prob>|t|
Intercept	12.476372	15.8015	0.79	0.4315
Sum_Ratio_All	13.956147	3.991379	3.50	0.0007*

Section 5. *LOESS Regression with Outliers for All, Averaged, and Summed Measures*

Bivariate Fit of Age_yrs By APRatio_75 Sex=F

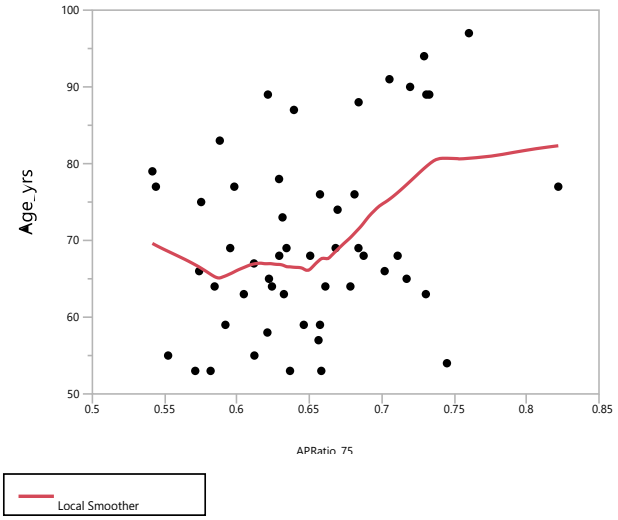

Bivariate Fit of Age_yrs By MLRatio_75 Sex=F

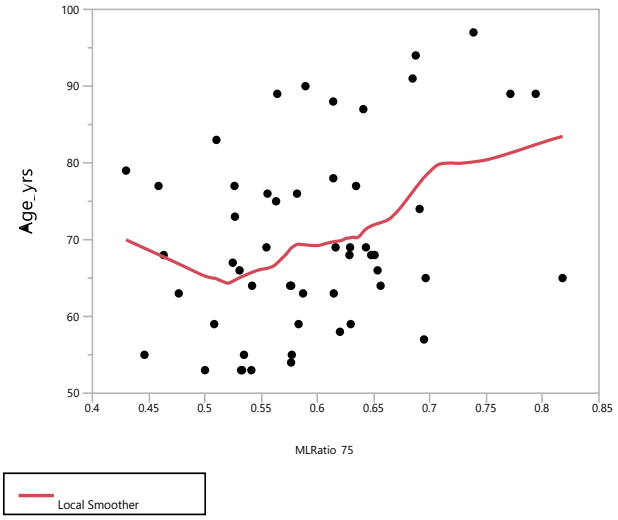

Bivariate Fit of Age_yrs By APRatio_Mid Sex=F

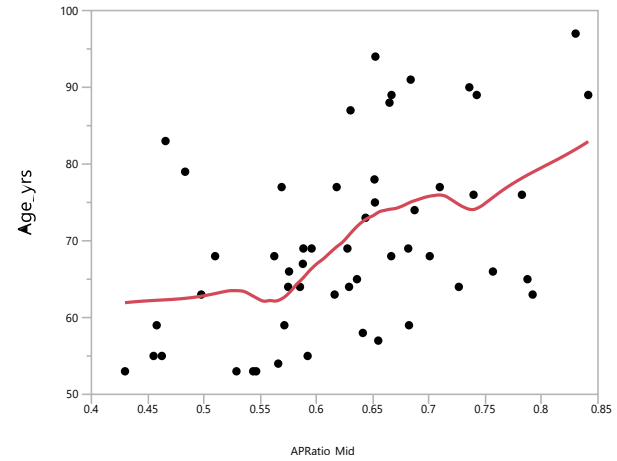

Bivariate Fit of Age_yrs By MLRatio_Mid Sex=F

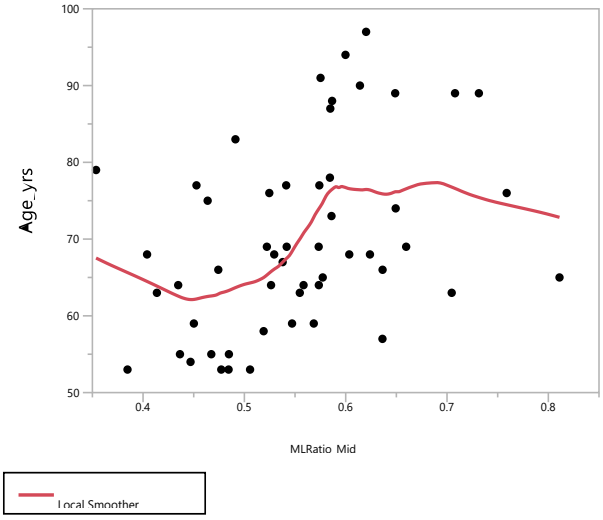

Bivariate Fit of Age_yrs By APRatio_20 Sex=F

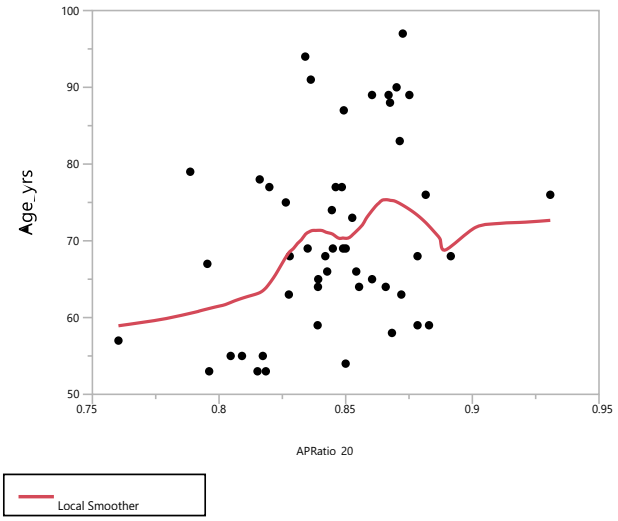

Bivariate Fit of Age_yrs By MLRatio_20 Sex=F

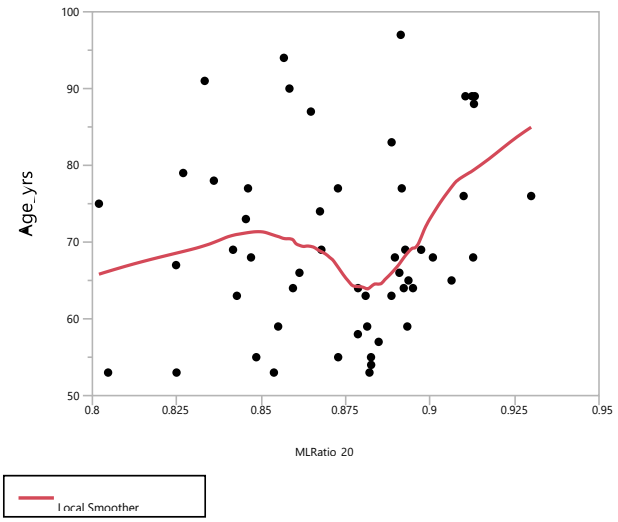

Bivariate Fit of Age_yrs By Sum_Ratio_75 Sex=F

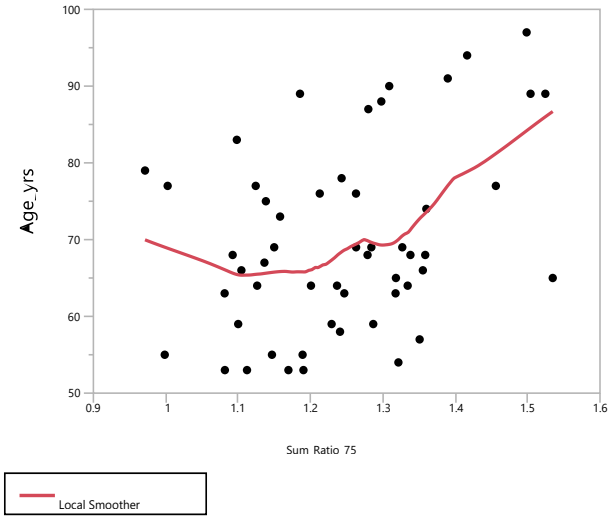

Bivariate Fit of Age_yrs By Sum_Ratio_Mid Sex=F

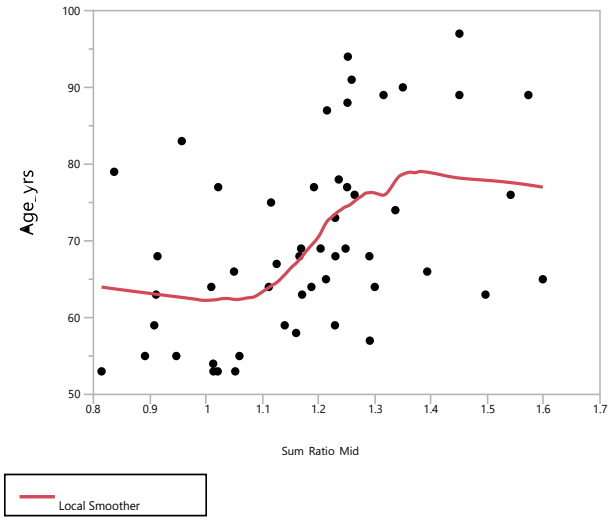

Bivariate Fit of Age_yrs By Sum_Ratio_20 Sex=F

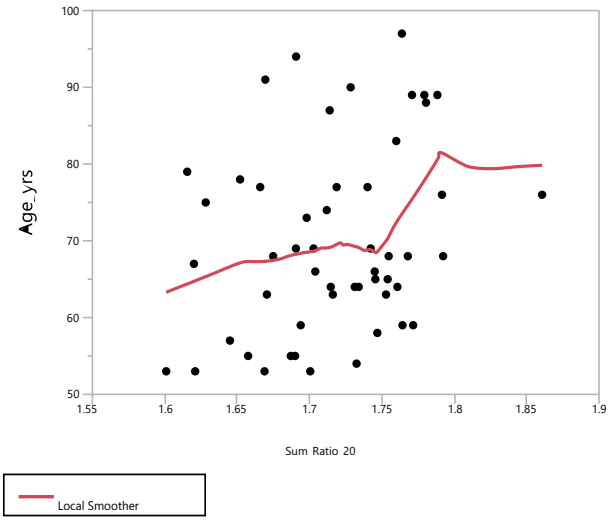

Bivariate Fit of Age_yrs By Sum_Ratio_All Sex=F

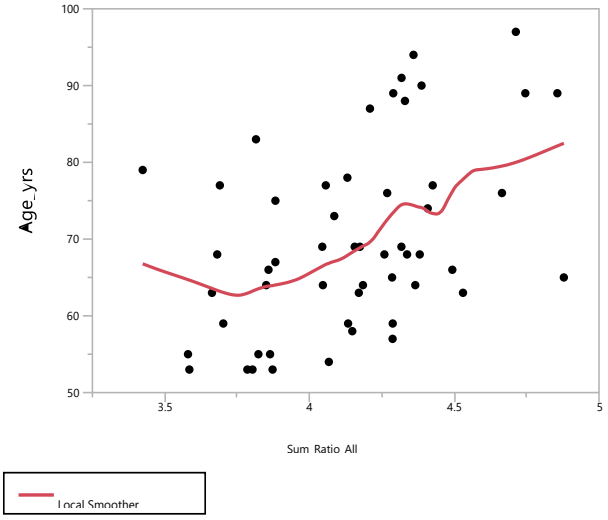

Bivariate Fit of Age_yrs By APRatio_75 Sex=M

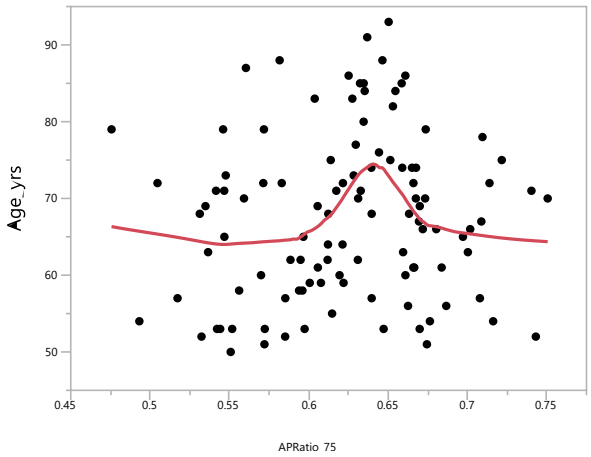

Bivariate Fit of Age_yrs By MLRatio_75 Sex=M

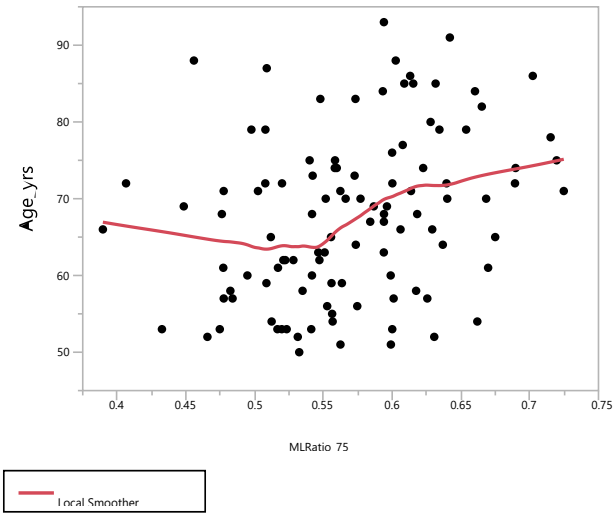

Bivariate Fit of Age_yrs By APRatio_Mid Sex=M

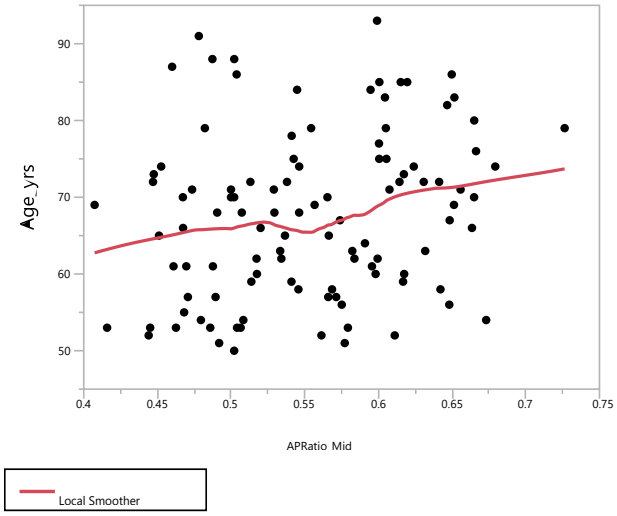

Bivariate Fit of Age_yrs By MLRatio_Mid Sex=M

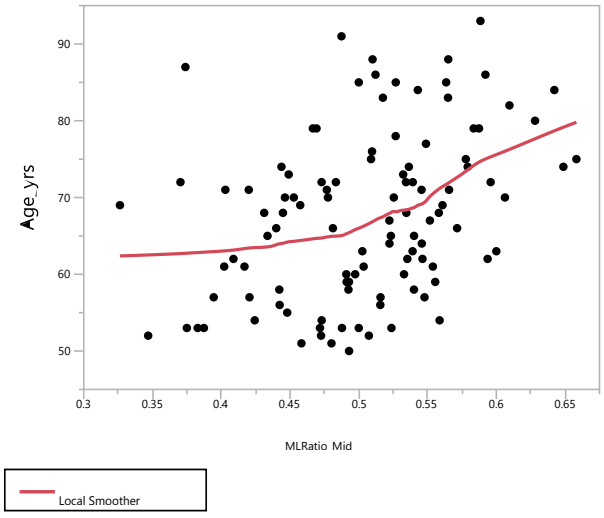

Bivariate Fit of Age_yrs By APRatio_20 Sex=M

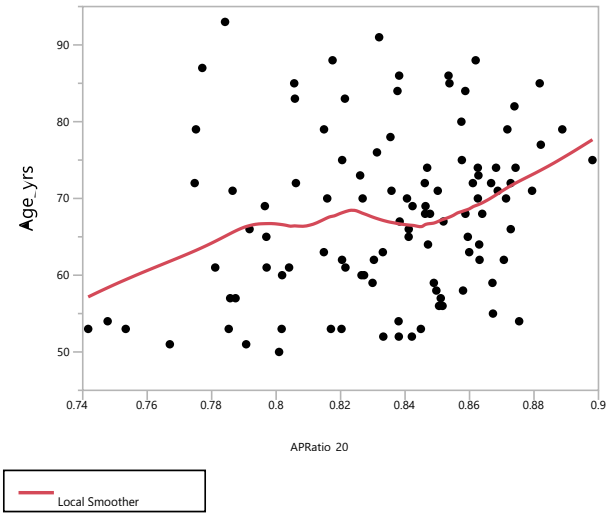

Bivariate Fit of Age_yrs By MLRatio_20 Sex=M

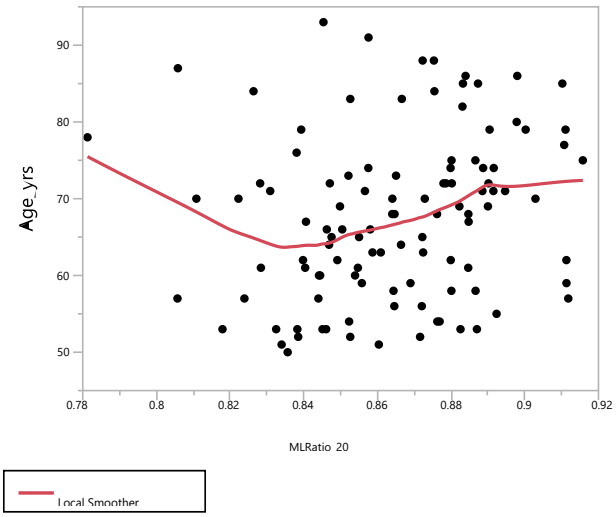

Bivariate Fit of Age_yrs By Sum_Ratio_75 Sex=M

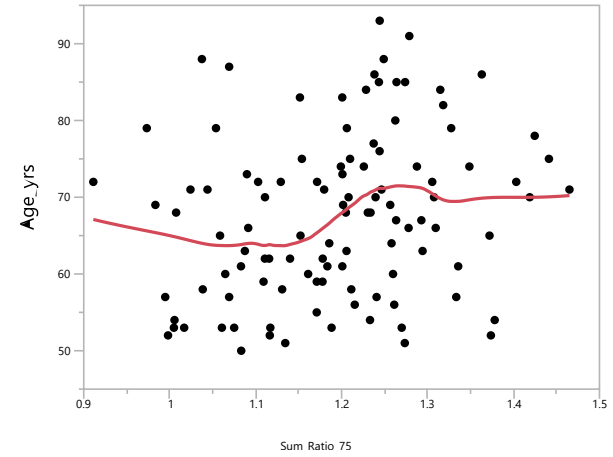

Bivariate Fit of Age_yrs By Sum_Ratio_Mid Sex=M

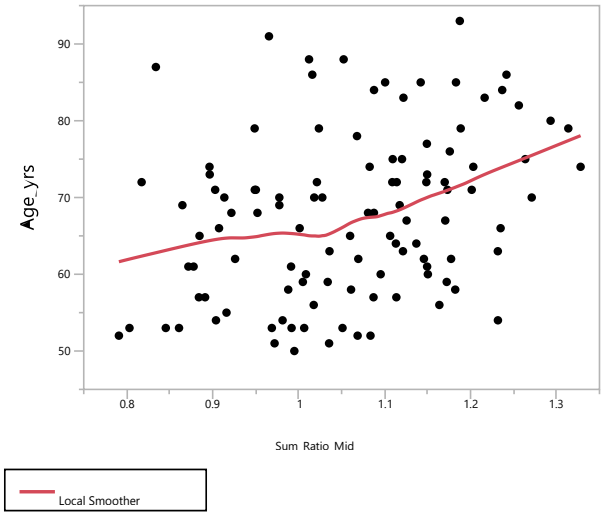

Bivariate Fit of Age_yrs By Sum_Ratio_20 Sex=M

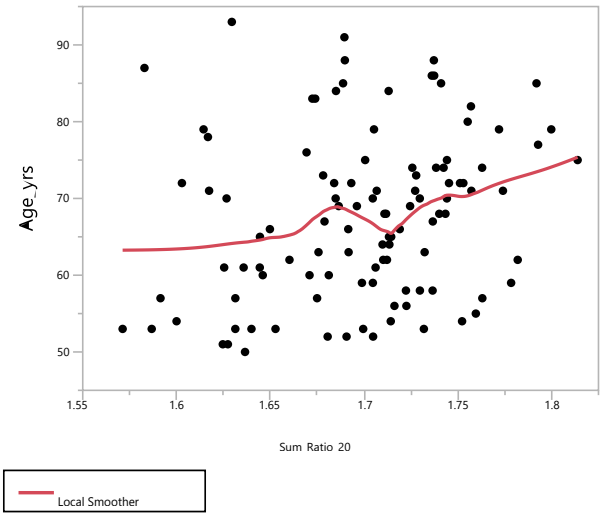

Bivariate Fit of Age_yrs By Sum_Ratio_All Sex=M

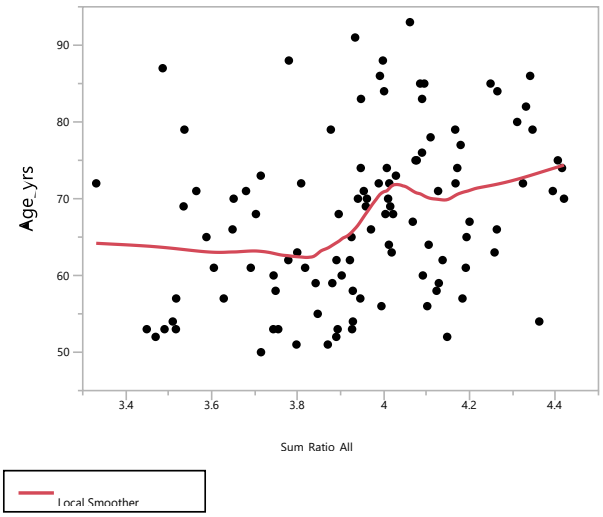

REFERENCES CITED

Atkinson PJ, Weatherfell JA. 1967. Variation in the density of the femoral diaphysis with age. J Bone Joint Surg Am 49(4):781-788.

Brock SL, Ruff CB. 1988. Diachronic patterns of changes in structural properties of the femur in the Prehistoric American Southwest. Am J Phys Anthropol 75:113-127.

Cardadeiro G, Baptista F, Zymbal V, Rodrigues LA, Sardinha LB. 2010. Ward's Area location, physical activity, and body composition in 8- and 9-year-old boys and girls. J Bone and Min Research 25(11):2304–2312.

Carlson DS, Armelagos GT, Van Gerven DP. 1976. Patterns of age-related cortical bone loss (osteoporosis) with the femoral diaphysis. Hum Biol 48(2):295-314.

Chevalier T, Clarys JP, Lefévre P, Beauthier JP, Louryan S, Cattrysse E. 2018. Body mass prediction from femoral volume and sixteen other femoral variables in the elderly: BMI and adipose tissue effects. Am J Phys Anthropol 166(1):26-42.

Cleveland WS. 1979. Robust locally body massed regression and smoothing scatterplots. Journal of the American Statistical Association 74:829-836.

Cleveland WS, Devlin SJ. 1988. Locally body massed regression: An approach to regression analysis by local fitting. J Am Stat Assc 83:596-610.

Cooper DM, Thomas CD, Clement JG, Turinsky AL, Sensen CW, Hallgrímsson B. 2007. Age-dependent change in the 3D structure of cortical porosity at the human femoral midshaft. Bone 40(4):957-965.

Cerezo-Román JI, Espinoza POH. 2014. Estimating age-at-death using the sternal end of the fourth ribs from Mexican males. Forensic Sci Int 236:196e.1-196.e6.

Cowin SC. 1983. The mechanical and stress adaptive properties of bone. Ann Biomed Eng 11:263-295.

Cowin SC. 2004. Tissue growth and remodeling. Annu Rev Biomed Eng 6(1):77-107.

Crowder C, Pfieffer S. 2010. The application of cortical bone histomorphometry to estimate age-at-death. In: Latham KE, Finnegan M, editors. Age estimation of the human skeleton. Illinois: Charles C Thomas. P193-215.

Curate F, Albuquerque A, Cunha EM. 2013. Age-at-death estimation using bone densitometry: Testing the Fernández Castillo and López Ruis method in two documented skeletal samples from Portugal. Forensic Sci Int 226:296.e1-296.e6.

Curate F, Cunha EM. 2017. Femoral cortical bone in a Portuguese reference skeletal collection. Antropologia Portuguesa 34: 91-109.

Disjkterhuis GB, Gower JC. 1992. The interpretation of General Procrustes Analysis and allied methods. Food Quality and Preference 3:67-87.

Dryden, I. L. (2018). shapes package. R Foundation for Statistical Computing, Vienna, Austria. Contributed package. Version 1.2.4. http://www.R-project.org.

Esri. 2017. ArcGIS Desktop, version 10.6.0.8321. Esri Inc.

Feik SA, Thomas CDL, Clement JG. 1997. Age-related changes in cortical porosity of the midshaft of the human femur. J Anat 191:407-416.

Feik SA, Thomas CDL, Bruns R, Clement JG. 2000. Regional variations in cortical modeling in the femoral mid-shaft: Sex and age differences. Am J Phys Anthropol 112:191-205.

Fox J, Weisberg S. 2018. Nonparametric regression in R: An appendix to An R companion to applied regression 3rd edition. Sage Publications Thousand Oaks, California.

Frost HM, Ferretti JL, Jee WSS. 1998. Perspectives: Some roles of mechanical usage, muscle strength, and the mechanostat in skeletal physiology, disease, and research. Calcif Tissue Int 62: 1-7.

Garn SM, Rohman CG, Béhor M, Viteri F, Guzman A. 1964. Compact bone deficiency in protein-calorie malnutrition. Science 145 (3639):1444-1445.

Garn SM, Rohmann, CG, Wagner B. 1967. Bone loss as a general phenomenon in man. FASEB 26(6):1729-1736.

Garn SM, Wagner B, Rohman CG, Ascoli W. 1968. Further evidence for continuing bone expansion. Am J Phys Anthropol 28:219-222.

Garn SM, Rohmann CG, Wagner B, Ascoli W. 1968. Continuing bone growth throughout life: A general phenomenon. Am J Phys Anthropol 28:313-318.

Garn SM, Solomon MA, Friedl J. 1981. Calcium intake and bone quality in the Elderly. Ecol Food Nutr 10:131-133.

Garn SM, Hawthorne VM, Larkin FA, Sullivan TVE, Decker SA. 1991. Long term continuity of bone cortical area. N Engl J Med 324:850.

Geske NL. 2013. An evaluation of three sternal rib end estimation techniques. Am J Phys Anthropol 150:129.

Goodall C. 1991. Procrustes methods in the statistical analysis of shape. J R Statist Soc B 53(2):285-339.

Gower JC. 1975. Generalized Procrustes Analysis. Psychometrika 40(1):33-51.

Hae-Dong J, Jae-Young H, Kyungdo H, Jae Chul L, Byung-Joon S, Sung-Woo C, Seung-Woo S, Jae-Hyuk Y, Si-Young P, Chungwon B. (2017). Relationship between Bone Mineral Density and Alcohol Intake: A Nationwide Health Survey Analysis of Postmenopausal Women. Public Library of Science Online: June 29, doi: 10.1371.

Hollenbach K. A., Barrett-Connor E., Edelstein S. L., Holbrook T. (1993). Cigarette Smoking and Bone Mineral Density in Older Men and Women. Am J Public Health 83 (9): 1265-1270.

Iscan MY, Loth SR, Wright RK. 1984. Age estimation from the rib by phase analysis: White males. J Forensic Sci 29(4):1094-1104.

Iscan MY, Loth SR, Wright RK. 1985. Age estimation from the rib by phase analysis: White females. J Forensic Sci 30(3):853-863.

Jin Kim M, Suk Shim M, Kyu Kim M, Lee Y, Goo Shin Y, Hee Chung C, Ok Kwon S. (2003). Effect of Chronic Alcohol Ingestion on Bone Mineral Density in Males without Liver Cirrhosis. Korean J Intern Med 18 (3): 174-180.

JMP®, Version 14. SAS Institute Inc., Cary, NC, 1989-2019.

Karakaş HM, Harma A. 2008. Femoral shaft bowing with age: A digital radiological study of Anatolian Caucasian adults. Diagn Interv Radiol 14:29-32.

Kaur H, Jit I. 1990. Age estimation from cortical index of the human clavicle in Northeast Indians. Am J Phys Anthropol 83:297-305.

Khan I, Jamil MMA, Nor FM. 2017. Evaluation and reliability of bone histological age estimation methods. J Fun and App Sci 9:663-680.

Langley NR, Jantz LM, Ousley SD, Jantz RL, Milner G. 2016. Data collection procedures for forensic skeletal material 2.0. Forensic Anthropology Center at The University of Tennessee. Knoxville TN.

Lerebours C, Buenzli PR, Scheiner S, Pivonka P. 2016. A multiscale mechanobiological model of bone remodeling predicts site-specific bone loss in the femur during osteoporosis and mechanical disuse. Biomech Model Mechanobiol 15:43-67.

Lovejoy CO, Meindl RS, Mensforth RP, Barton TJ. 1985. Multifactorial determination of skeletal age-at-death: A method and blind test of its accuracy. Am J Phys Anthropol 68:1-14.

Lovejoy CO, McCollum, PL Reno, Rosenman BA. 2003. Developmental biology and human evolution. Annu Rev Anthropol 32:85-109.

Martille L, Ubelaker D, Cattaneo C, Seguret F, Tremblay M, Baccino E. 2007. Comparison of four skeletal methods for the estimation of age-at-death on White and Black adults. J Forensic Sci 52:302-307.

Martin RB, Atkinson PJ. 1977. Age and sex related changes in the structure and strength of the human femoral shaft. J Biomech 10:223-231.

Mays SA. 1996. Age-dependent cortical loss in a Medieval population. Int J Osteoarchaeol 6:144-154.

Mays SA. 2006. Age-related cortical bone loss in women from a 3rd-4th century AD population from England. Am J Phys Anthropol 129:518-528.

Mays SM. 2014. A test of a recently devised method of estimating skeletal age-at-death using features of the adult acetabulum. J Forensic Sci 59(1):184-187.

Mays SM. 2015. Age-associated reduction in cortical bone in males, trends from the Third Century AD to the present day. Calcif Tissue Int 96:370-371.

Mays SM. 2015. The effect of factors other than age upon skeletal age indicators in the adult. Annals of Hum Biol 42(4): 330-339.

Mays SM. 2016. Estimation of stature in archaeological human skeletal remains from Britain. Am J Phys Anthropol 161(4):646-655.

MircroImages Inc. Wallis Filter Locally Adaptive Contrast Enhancement. TNTgis - Advanced Software for Geospatial Analysis https://www.microimages.com/documentation/TechGuides/55Wallis.pdf.

Moore MK, DiGangi EA. 2012. Research methods in human skeletal biology. Massachusetts: Associated Press.

Newport, F. (2018, May 10). Snapshot: Average American Predicts Retirement Age of 66. Retrieved November 15, 2018, from https://news.gallup.com/poll/234302/snapshot-americans-project-average-retirement-age.aspx.

Pawson IG. 1974 Radiographic determination of excessive bone loss in Alaskan Eskimos. Hum Biol 46(3):369-380.

Pfeiffer S. 1980. Age changes in the external dimensions of adult bone. Am J Phys Anthropol 52:529-532.

Pomeroy E, Wells JCK, Cole TJ, Stock JT. 2018. Relationship between body mass, lean mass, fat mass, and limb bone cross-sectional geometry: Implications for estimating body mass and physique from the skeleton. Am J Phys Anthropol 166(1):56-69.

R Core Team (2013). R: A language and environment for statistical computing. R Foundation for Statistical Computing, Vienna, Austria. http://www.R-project.org/.

RStudio Team. 2016. RStudio: Integrated development environment for R version 1.1.463. Rstudio, Inc. Boston, MA.

Ruff CB, Hayes W. 1983. Subperiosteal expansion and cortical remodeling of the human femur and tibia with aging. Science 217(4563):945-948.

Ruff CB, Hayes W. 1983. Cross-Sectional geometry of Pecos Pueblo femora and tibiae—A biomechanical investigation: I method and general patterns of variation. Am J Phys Anthropol 60:359-381.

Ruff CB. 1984. Allometry between length and cross-sectional dimensions of the femur and tibia in *Homo sapiens sapiens.* Am J Phys Anthropol 65:347-358.

Ruff CB, Hayes W. 1984. Age changes in geometry and mineral content of the lower limb bones. Ann Biomed Eng. 12:573-584.

Ruff CB, Scott WW, Liu AY. 1991. Articular and diaphyseal remodeling of the proximal femur with changes in body mass in adults. Am J Phys Anthropol 86(3):397-413.

Russo CR, Lauretani F, Seeman E, Bartali B, Bandinelli S, Di Iorio A, Guralnik J, Ferrucci L. 2005 Structural adaptations to bone loss in aging men and women. Bone 38:112-118.

Schindelin J, Arganda-Carreras I, Frise E, Kaynig V, Longair M, Pietzsch T, Preibisch S, Rueden C, Saalfeld S, Schmid B, Jean-Yves T, White DJ, Hartenstein V, Eliceiri K, Tomancak P, Cardona A. 2012. Fiji: an open-source platform for biological-image analysis. Nature Methods 9:676–682.

Schneider CA, Rasband WS, Eliceiri KW. 2012. NIH Image to ImageJ: 25 years of image analysis. Nature Methods 9(7):671-675.

Smith Jr. RW, Walker R. 1964. Femoral expansion in aging women: Implications for osteoporosis and fractures. Science 145(3628):156-157.

Stein MS, Thomas CDL, Feik SA, Ward JD, Clement JG. 1998. Bone size and mechanics at the femoral diaphysis across age and sex. J Biomech 31:1101-1110.

Taghizadeh E, Chandran U, Reyes M, Zysset P, Büchler P. 2017. Statistical analysis of the inter-individual variations of the bone shape, volume fraction and fabric and their correlations in the proximal femur. Bone 103:252-261.

Thomas CDL, Stein MS, Feik SA, Ward JD, Clement JG. 2000. Determination of age-at-death using combined morphology and histology of the femur. J Anat 196:463-471.

Tollison CD, Kriegel ML. 1990. Bone loss and physical inactivity: Can exercise prevent osteoporosis? Journal of South Carolina Medical Association 86(3):138-140.

Umbelino C, Curate F, Perinha A, Ferreira T, Cunha E, Bicho N. 2019. Cortical bone loss in a sample of human skeletons from the Muge Shell Middens. Arch Anth Sci 11(2):455-467.

Van Gerven DP, Armelagos GJ. 1970. Cortical Involution in Prehistoric Mississippian femora. Journal of Gerontology 25(1-4):20-22.

Walker RA, Lovejoy CO. 1985 Radiographic changes in the clavicle and proximal femur and their use in the determination of skeletal age-at-death. Am J Phys Anthropol 68:67-78.

Weiping Q, Bauman WA, Cardozo C. 2010. Bone and muscle loss after spinal cord injury: organ interactions bone and muscle after SCI. Annals of the New York Academy of Sciences 1211(1):66-84.

White TD, Black MT, Folkens PA. 2012. Human osteology third edition. Massachusetts: Elsevier Academic Press.

Zanetti EM, Crupi V, Bignardi C, Calderale PM. 2005. Radiograph-based femur morphing method. Med Biol Eng Comput 43:181-188.